DOE/NASA/0323-2
NASA CR-175114

SOLID LUBRICATION DESIGN METHODOLOGY

PHASE II - FINAL REPORT

R. A. PALLINI
L. D. WEDEVEN
M. A. RAGEN
B. B. AGGARWAL*

SKF INDUSTRIES, INC.
* Currently with Mechanical Technology, Inc.

February, 1986

Prepared for
NATIONAL AERONAUTICS AND SPACE ADMINISTRATION
Lewis Research Center
Under Contract DEN3-323

for

U.S. DEPARTMENT OF ENERGY

Conservation and Renewable Energy

Office of Vehicle and Engine R&D

DOE/NASA/0323-2
NASA CR-175114

SOLID LUBRICATION DESIGN METHODOLOGY
PHASE II - FINAL REPORT

R. A. PALLINI
L. D. WEDEVEN
M. A. RAGEN
B. B. AGGARWAL*

SKF INDUSTRIES, INC.
* Currently with Mechanical Technology, Inc.

February, 1986

Prepared for
NATIONAL AERONAUTICS AND SPACE ADMINISTRATION
Lewis Research Center
Under Contract DEN3-323

for

U.S. DEPARTMENT OF ENERGY
Conservation and Renewable Energy
Office of Vehicle and Engine R&D

1. Report No.	2. Government Accession No.	3. Recipient's Catalog No.
NASA CR- 175114		

4. Title and Subtitle	5. Report Date
Solid Lubrication Design Methodology Phase II - Final Report	February 1986
	6. Performing Organization Code

7. Author(s)	8. Performing Organization Report No.
R. A. Pallini L. D. Wedeven M. A. Ragen B. B. Aggarwal	AT86D002
	10. Work Unit No.

9. Performing Organization Name and Address	11. Contract or Grant No.
SKF Industries, Inc. 1100 First Avenue King of Prussia, PA 19406-1352	DEN3-323
	13. Type of Report and Period Covered
	Contractor Report

12. Sponsoring Agency Name and Address	14. Sponsoring Agency Code Report No.
U. S. Department of Energy Office of Vehicle and Engine R&D Washington, D.C. 20585	DOE/NASA/0323-2

15. Supplementary Notes

Final Report. Prepared under Contract Number DEN3-323. Project Manager, James C. Wood, Propulsion System Division, NASA Lewis Research Center, Cleveland, Ohio 44135.

16. Abstract

The high temperature performance of solid lubricated rolling elements was conducted with a specially designed traction (friction) test apparatus. Graphite lubricants containing three additives (silver, phosphate glass and zinc orthophosphate) were evaluated from room temperature to 540°C. Two hard coats were also evaluated.

The evaluation of these lubricants, using a burnishing method of application, shows a reasonable transfer of lubricant and wear protection for short duration testing except in the 200°C temperature range. The graphite lubricants containing silver and zinc orthophosphate additives were more effective than the phosphate glass material over the test conditions examined. Traction coefficients ranged from a low of 0.07 to a high of 0.6.

By curve fitting the traction data, empirical equations for slope and maximum traction coefficient as a function of contact pressure (P), rolling speed (U), and temperature (T) can be developed for each lubricant. A solid lubricant traction model was incorporated into an advanced bearing analysis code (SHABERTH). For comparison purposes, preliminary heat generation calculations were made for both oil and solid lubricated bearing operation. A preliminary analysis indicated a significantly higher heat generation for a solid lubricated ball bearing in a deep groove configuration. An analysis of a cylindrical roller bearing configuration showed a potential for a low friction solid lubricated bearing.

17. Key Words (Suggested by Author(s))	18. Distribution Statement
Adiabatic Diesel Engine Traction Slide/Roll Ratio Silicon Nitride, Graphite, Armoloy	Unclassified - Unlimited STAR Category 85 DOE Category UC-96

19. Security Classif. (of this report)	20. Security Classif. (of this page)	21. No. of pages	22. Price*
Unclassified	Unclassified	121	A08

*For sale by the National Technical Information Service, Springfield, Virginia 22161

FOREWORD

The work described in this report was performed under NASA Contract DEN3-323 for the U.S. Department of Energy. DOE sponsorship was under the guidance of Mr. S. Goguen and Mr. J. Fairbanks. Project Managers at NASA Lewis Research Center were Mr. G. Proc and Mr. J. Wood. Special thanks go out to Mr. Ditmar Hahn and Mr. Richard Bovenkerk at SKF Industries for their tremendous help in the SEM examinations and testing, respectively. Thanks is also extended to Prof. James Lauer and Mr. Peter Vogel of Rensselaer Polytechnic Institute for their fine I.R. spectroscopy work.

TABLE OF CONTENTS

	PAGE
FOREWORD	ii
1.0 INTRODUCTION	1
2.0 SUMMARY OF PHASE I RESULTS	4
3.0 TEST APPARATUS AND TEST PROCEDURE	8
3.1 Test Apparatus	8
3.2 Contact Traction Measurement	15
3.3 Test Specimens	20
3.3.1 Disk Specimens	20
3.3.2 Ball Specimens	20
3.3.3 Lubricant Specimens	23
3.4 Test Procedure	25
3.5 Test Matrix	26
4.0 SOLID LUBRICANT TRACTION TESTS	30
4.1 Initial Testing	30
4.2 Graphite Lubricants at High Temperature	30
4.2.1 P3310	35
4.2.2 P03Ag	45
4.2.3 P2003	55
4.3 "ARMOLOY" Coated M50 Steel	63
4.4 Titanium Nitride Coated M50 Steel	70
4.5 Discussion of Traction Results	79
4.6 Surface Analysis of Test Specimens	85
5.0 ANALYTICAL MODELLING	98
5.1 Traction Model Development	98
5.2 Parametric Studies	102
6.0 CONCLUSIONS & RECOMMENDATIONS	106
6.1 Conclusions	106
6.2 Design Criteria	106
6.3 Recommendations for Future Analysis	110
7.0 REFERENCES	112

LIST OF FIGURES

		PAGE
3.1	SCHEMATIC OF HIGH TEMPERATURE TRACTION TEST APPARATUS	9
3.2	BALL AND DISK ARRANGMENT IN TEST APPARATUS	10
3.3	HEATER AND TEST CHAMBER ENCLOSURE	11
3.4	ENTIRE OPERATING TEST RIG	14
3.5	DISK BURNISHING MECHANISM	16
3.6	VARIATION OF DISK SURFACE VELOCITY ACROSS THE CONTACT	17
3.7	CONTACT GEOMETRY FOR TRACTION FORCE AND SLIDE/ROLL RATIO MEASUREMENTS	19
3.8	DRAWING OF DISK SPECIMEN	21
3.9	DRAWING OF BALL SPECIMEN	22
4.1	TYPICAL TRACTION TEST RESULTS - TRACTION FORCE VS. SLIP CURVE	33
4.2	SILICON NITRIDE TEST BALL - P3310 T=270°C, CONTACT STRESS = 1378 MPa ROLLING SPEED = 6.35 m/s	36
4.3	LOCATION OF EDGES AND CENTER OF WEAR TRACK IN SEM PHOTOMICROGRAPHS	37
4.4	UNRUN SILICON NITRIDE BALL SURFACE	38
4.5	SILICON NITRIDE TEST BALL - P3310 T=370°C, CONTACT STRESS = 2068 MPa ROLLING SPEED = 3.8 m/s	40
4.6	SILICON NITRIDE TEST BALL - P3310 T=370°C, CONTACT STRESS = 1723 MPa ROLLING SPEED = 6.35 m/s	41
4.7	SILICON NITRIDE TEST BALL - P3310 T=540°C, CONTACT STRESS = 2068 MPa ROLLING SPEED = 6.35 m/s	42
4.8	SILICON NITRIDE TEST BALL - P3310 T=540°C, CONTACT STRESS = 1378 MPa ROLLING SPEED = 3.8 m/s	43

LIST OF FIGURES (CONTD)

		PAGE
4.9	SILICON NITRIDE TEST BALL - P3310 T=540°C, CONTACT STRESS = 1723 MPa ROLLING SPEED = 3.8 m/s	44
4.10	SILICON NITRIDE TEST BALL - P03Ag T=370°C, CONTACT STRESS = 1378 MPa ROLLING SPEED = 3.8 m/s	46
4.11	SILICON NITRIDE TEST BALL - P03Ag T=370°C, CONTACT STRESS = 1723 MPa ROLLING SPEED = 3.8 m/s	47
4.12	SILICON NITRIDE TEST BALL - P03Ag T=370°C, CONTACT STRESS = 2068 MPa ROLLING SPEED = 6.35 m/s	50
4.13	SILICON NITRIDE TEST BALL - P03Ag T=540°C, CONTACT STRESS = 1723 MPa ROLLING SPEED = 6.35 m/s	51
4.14	SILICON NITRIDE TEST BALL - P03Ag T=540°C, CONTACT STRESS = 1378 MPa ROLLING SPEED = 6.35 m/s	53
4.15	SILICON NITRIDE TEST BALL - P03Ag T=540°C, CONTACT STRESS = 1378 MPa ROLLING SPEED = 3.8 m/s	54
4.16	SILICON NITRIDE TEST BALL - P2003 T=370°C, CONTACT STRESS = 1723 MPa ROLLING SPEED = 3.8 m/s	56
4.17	SILICON NITRIDE TEST BALL - P2003 T=370°C, CONTACT STRESS = 2068 MPa ROLLING SPEED = 3.8 m/s	57
4.18	SILICON NITRIDE TEST BALL - P2003 T=540°C, CONTACT STRESS = 2068 MPa ROLLING SPEED = 3.8 m/s	58
4.19	SILICON NITRIDE TEST BALL - P2003 T=540°C, CONTACT STRESS = 2068 MPa ROLLING SPEED = 6.35 m/s	59

LIST OF FIGURES (CONTD)

		PAGE
4.20	SILICON NITRIDE TEST BALL - P2003 T=540°C, CONTACT STRESS = 1378 MPa ROLLING SPEED = 6.35 m/s	60
4.21	SILICON NITRIDE TEST BALL - ARMOLOY T=200°C, CONTACT STRESS = 2068 MPa ROLLING SPEED = 6.35 m/s	66
4.22	SILICON NITRIDE TEST BALL - ARMOLOY T=315°C, CONTACT STRESS = 1723 MPa ROLLING SPEED = 6.35 m/s	68
4.23	TEST SPECIMENS Si_3N_4/ARMOLOY/P03Ag T=200°C, CONTACT STRESS = 2068 MPa ROLLING SPEED = 6.35 m/s	69
4.24	TEST SPECIMENS Si_3N_4/ARMOLOY/P03Ag T=315°C, CONTACT STRESS = 1723 MPa ROLLING SPEED = 6.35 m/s	71
4.25	M50 TEST BALL - TiN COATED DISK ROOM TEMPERATURE CONTACT STRESS = 1378 MPa	74
4.26	M50 TEST BALL - TiN COATED DISK ROOM TEMPERATURE CONTACT STRESS = 1723 MPa	75
4.27	TiN COATED DISK TRACTION TEST CONTACT PATHS	77
4.28	TiN COATED DISK CONTACT PATH FOR 2068 MPa TEST	78
4.29	TRACTION TEST RESULTS P3310 LUBRICANT	80
4.30	TRACTION TEST RESULTS P03Ag LUBRICANT	81
4.31	TRACTION TEST RESULTS P2003 LUBRICANT	82

LIST OF FIGURES (CONTD)

		PAGE
4.32	TRACTION TEST RESULTS Si_3N_4 BALL ON ARMOLOY/M50 DISK	84
4.33	IR SPECTRUM BALL #3	87
4.34	IR SPECTRUM BALL #6	88
4.35	RATIOED SPECTRUM BALL #3	89
4.36	RATIOED SPECTRUM BALL #6	90
4.37	IR SPECTRUM BALL #4	92
4.38	IR SPECTRUM BALL #14	93
4.39	IR SPECTRUM BALL #16	94
4.40	THEORETICAL IR SPECTRUM OF PURE SILICON NITRIDE BALL	95
4.41	RATIOED SPECTRUM OF BALL #4	96
5.1	SOLID LUBRICATION TRACTION ANALYTICAL MODEL	99
5.2	SOLID AND LIQUID LUBRICATION HEAT GENERATION FOR A DEEP GROOVE BALL BEARING	103
5.3	SOLID AND LIQUID LUBRICATION HEAT GENERATION FOR A CYLINDRICAL ROLLER BEARING	104

LIST OF TABLES

		PAGE
3.1	AVERAGE PHYSICAL PROPERTIES OF GRAPHITE LUBRICANTS	24
3.2	HIGH TEMPERATURE GRAPHITE LUBRICATION TEST MATRIX	27
3.3	ARMOLOY COATED M50 STEEL DISK TEST MATRIX	29
4.1	HIGH TEMPERATURE GRAPHITE LUBRICATION TEST MATRIX	31
4.2	MEASURED TEST RESULTS FOR HIGH TEMPERATURE GRAPHITE LUBRICANTS	34
4.3	ARMOLOY COATED M50 STEEL DISK TEST MATRIX	64
4.4	MEASURED TEST RESULTS FOR ARMOLOY COATED M50 STEEL	65
4.5	TEST RESULTS FOR TiN COATED M50 STEEL DISK	73
5.1	SUMMARY OF REGRESSION ANALYSIS RESULTS	101

1.0 INTRODUCTION

The U.S. Department of Energy (DOE) in conjunction with the National Aeronautical and Space Administration (NASA) initiated a program in 1981 for the development of technologies applicable to the advanced low heat rejection diesel engine. The program titled Heavy Duty Transport Technology Program (HDTT) has the following stated goal [1]:

> "To provide the necessary technology base for use by industry in developing advanced heavy duty transport engines to permit a significant reduction of petroleum consumption per vehicle ton-mile."

The initial step identified by the program in an effort to realize the stated goal is to develop key technologies needed to overcome the major technical barriers of a low heat rejection engine (LHR Diesel). The key problem areas have been identified as follows [2]:

- Exhaust gas heat recovery
- Thermal insulation
- Adequate piston seals
- Emission standards
- Engine friction and wear

Part of the technology base building to attack the final item of the above list is the subject of this final report. The LHR

diesel engine is designed to achieve high engine efficiency and low fuel consumption through the combined effects of higher operating temperatures, reduced heat losses, lighter weight, and higher exhaust energy recovery. The higher operating temperatures, however, pose difficult structural, material and lubrication problems. Bearings and other load carrying contacts are required to operate over a temperature range that exceeds the capability of conventional lubricants.

A solution that offers potential is the use of solid lubricated rolling and sliding contacts. Unfortunately, there is very little design data available to aid in the design of solid lubricated rolling and sliding contacts. Testing of solid lubricated concentrated contacts has traditionally been done with pure sliding conditions. Consequently, the data has limited applicability to the technology required for contacts involving rolling or rolling with some sliding. These are the types of contacts that would occur in solid lubricated rolling element bearings for the lower engine areas of a LHR diesel engine.

The Solid Lubrication Design Methodology program sponsored by DOE and monitored by NASA-Lewis Research Center was a two-phase program at SKF Industries, Inc. to evaluate solid lubricants and bearing materials in combination under controlled test conditions representative of projected bearing requirements in LHR engines.

The aim was to develop quantitative and qualitative guidelines for use in the design of solid lubricated bearings, gears, and other load carrying components. In Phase I [3], the candidate lubricant and material combinations were evaluated at room temperature to select the most promising combinations for high temperature testing. Analytical models and design guidelines were developed based on these room temperature test results. Phase II was conducted with the selected combinations at high temperatures (up to 540°C) using a specially designed high temperature rolling contact test rig. The Phase II test data was used to refine the analytical models and guidelines to include the effects of high temperature.

This report describes the work done in Phase II of the program. The Phase I results are reviewed in Section 2.0. The test apparatus and test procedure are described in Section 3.0. All test results are presented and discussed in Section 4.0. The analytical models constructed with the traction force measurements collected are described and demonstrated in Section 5.0. Finally, Section 6.0 presents conclusions formulated upon the results of the entire program.

2.0 SUMMARY OF PHASE I RESULTS

During Phase I, an existing high speed, room temperature traction rig with a ball-on-disk configuration was used to obtain traction data as a function of contact slip. Most of the experiments were run with M50 tool steel ball and disk materials. Preliminary experimentation was conducted with silicon nitride and partially stabilized zirconia. The solid lubricants tested included a series of graphite lubricants and composite lubricant compacts. The graphite lubricants differed only by their additive packages. They were

- P03Ag (silver additive)
- P2003 (phosphate glass additive)
- P3310 (zinc orthophosphate additive)

The composite compact (Hughes Compact) consisted of a polyimide resin reinforced with a 3-D weave of carbon fibers and impregnated with a solid lubricant. The test results allowed the following observations:

1. The form of the traction vs. contact slip curve were similar to that found for oil lubrication. They differ in two important respects. With solid lubrication the rate at which traction increased with contact slip as well as the maximum level of the traction force was significantly higher.

2. For the short term testing conducted, it was possible to transfer adequate lubrication to the disk by burnishing.

3. Wear performance was found to be especially sensitive to contact slip and contact stress.

4. The best wear protection was provided by one of the composite solid lubricants (HAC2A/T50F4) followed by the graphites in the order of P2003, P3310, P03Ag.

5. Adequate transfer of solid lubricant was observed with M50 steel and silicon nitride disks. Burnishing of the partially stabilized zirconia did not provide adequate lubricant coatings and extensive wear resulted.

6. The material combination of M50 steel against silicon nitride gave superior wear performance over that of M50 steel against M50 steel.

Based on the results summarized above, several generalized design guidelines were formulated. Three main causes of the limited service life of solid lubricated rolling bearings are:

- excessive wear at rolling element/raceway contacts
- loss of clearance due to excessive heat generation
- cage or separator failures

The bearing geometry must be selected to promote formation of a durable lubricant film and to minimize heat generation at the contacts. The bearing and housing design should maximize the flow of heat away from the bearing. The following design criteria were suggested:

Reduce Contact Stress - This can be achieved by using a larger number or larger sized rolling element. Lower contact stress will enhance the maintenance of a lubricant film and reduce heat generation by lowering traction forces at the contact.

Reduce Sliding at the Contact - Heathcote slip at the contact can be reduced by lowering the conformity of rolling element raceway contacts. Lubricant film is depleted rapidly by sliding at the contact. Reducing conformity will, however, increase the contact stress. The selection of bearing geometry and materials must therefore involve a tradeoff.

Wear Resistant Bearing Materials - Use of silicon nitride disks reduced the wear of contact surfaces. Wear resistance can also be provided by coatings such as Armoloy and Titanium Nitride. The coatings can also be used to promote the formation and retention of solid lubricant films.

Heat Dissipation - The bearing and housing design must provide means of dissipating the heat generated at the element/raceway contacts.

At the end of Phase I, SKF decided to design and construct a new test apparatus optimized for testing high temperature, solid lubricated contacts. This rig would enable the continued testing of the more promising lubricants at temperatures up to 540°C and the refinement of the analytical traction models to include temperature effects.

3.0 TEST APPARATUS AND TEST PROCEDURE

3.1 Test Apparatus

To conduct the Phase II evaluations, SKF Industries designed and built a unique high temperature traction test rig. This facility studies the traction force generated between a single ball and a flat disk as a function of speed, contact stress, temperature, lubricant and material. A schematic of the test apparatus is shown in Figure 3.1. The ball and disk configuration is shown in the photograph of Figure 3.2.

The ball and disk are enclosed in a high temperature oven. The oven is made of walls consisting of exterior panels of 304 stainless steel (3mm thick) and interior panels of 310 stainless steel (2.3mm thick) with high temperature foam insulation between the panels. Openings for the heater inlet, ball and disk spindle extensions and the exhaust port are lined with 304 stainless steel tubing. Figure 3.3 is a photograph showing the heater and test chamber enclosure.

The test chamber is heated by passing ambient air over electric resistive heaters through stainless steel pipe to the chamber heater port. Current flow to the heaters is regulated by a controller which monitors the oven temperature via a thermocouple. A second controller shuts off the current if the

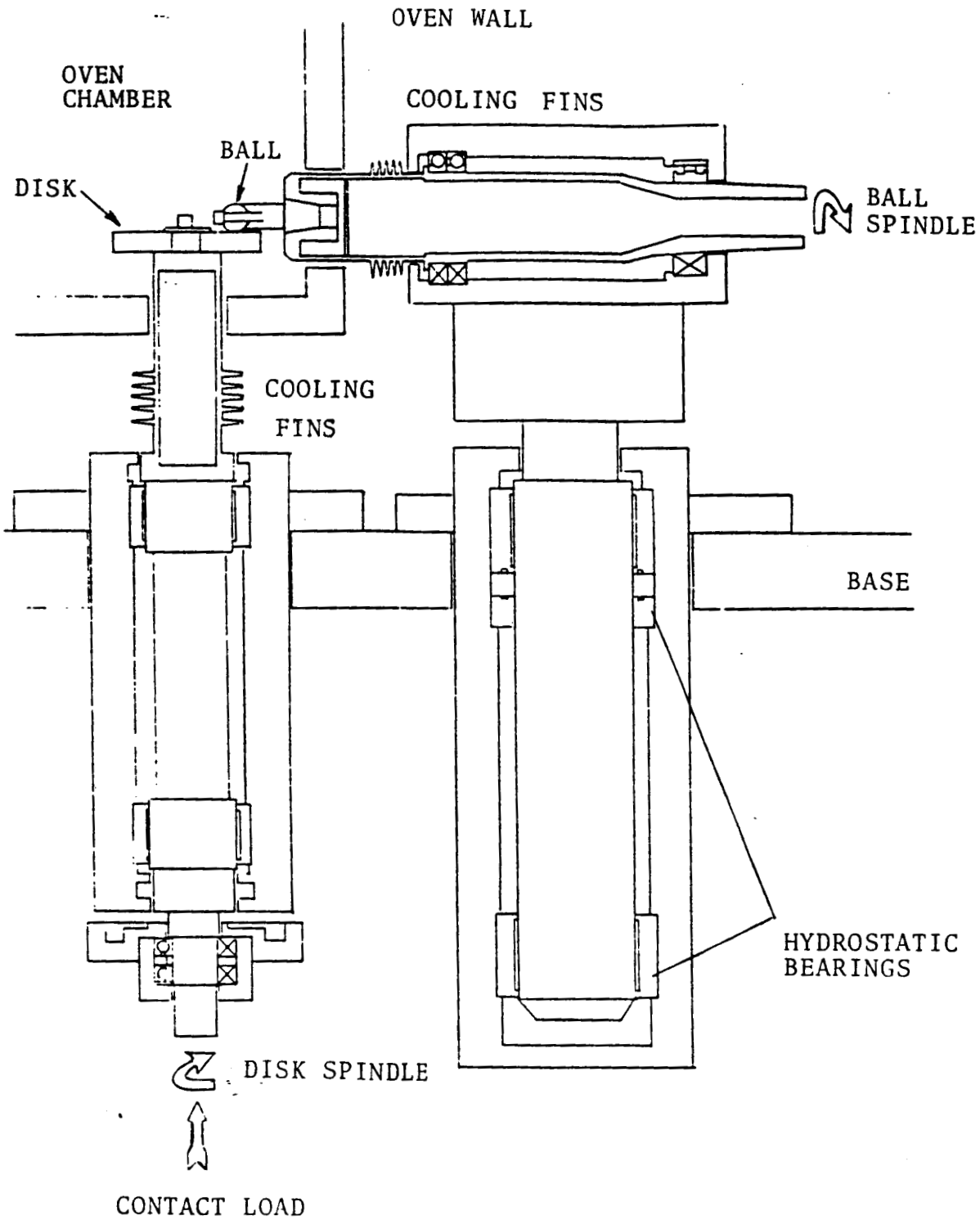

Figure 3.1 Schematic of High Temperature Traction Test Apparatus

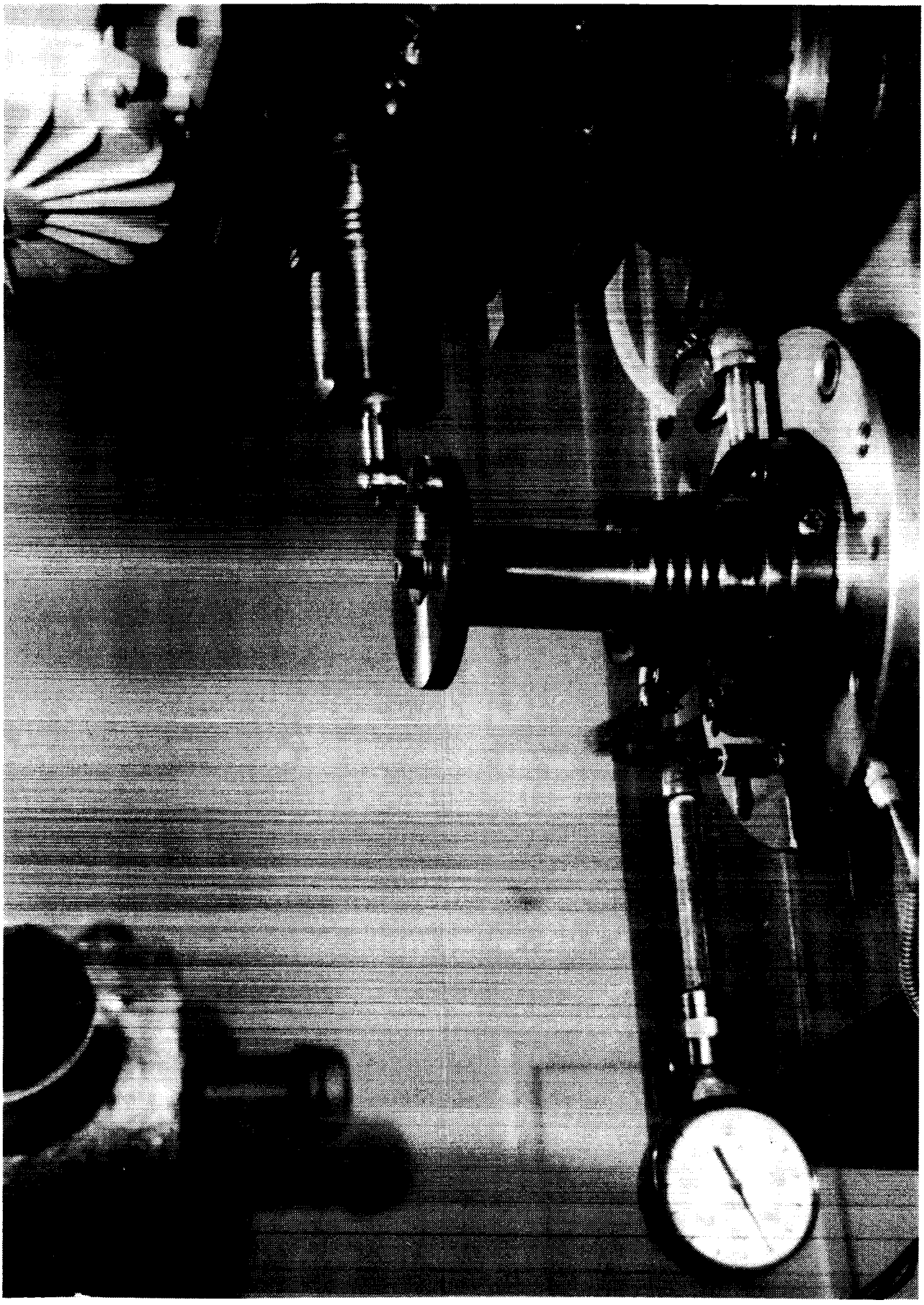

Figure 3.2 Ball and Disk Arrangement in Test Apparatus

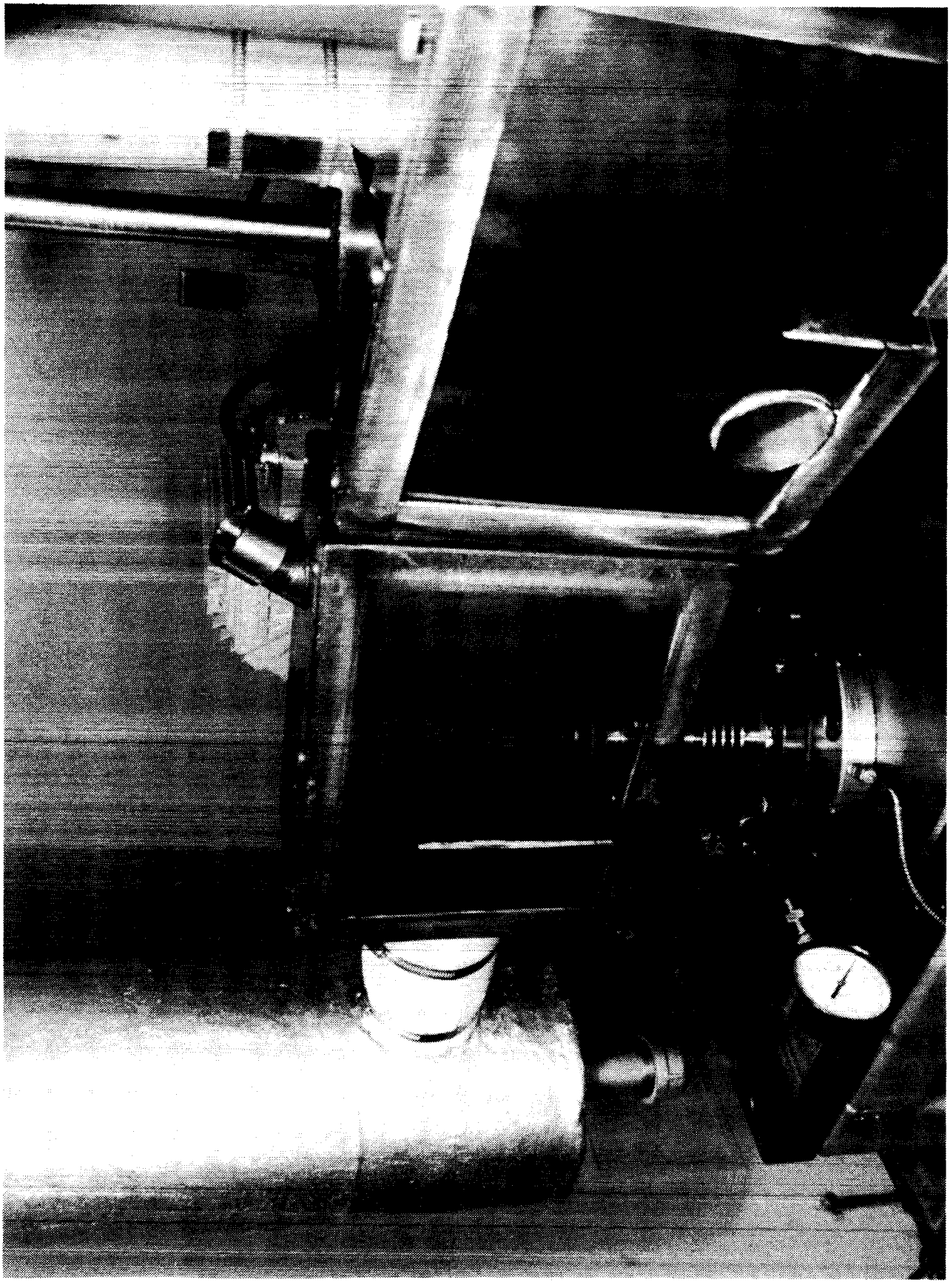

Figure 3.3 Heater and Test Chamber Enclosure

heating elements exceed specified temperature limits. The ambient air is supplied to the heater by an electrically driven oiless blower.

The test ball is adapted to a two-piece shaft assembly. A high temperature section is made from Inconel 625 and a low temperature section is made of AISI 8620 hot rolled steel. The two sections are welded together to form an integral unit. The shaft is hollow to allow passage of cooling air through the shaft. The shaft is supported by duplex angular contact ball bearings and a cylindrical roller bearing. The entire shaft and housing assembly is mounted on a slide to allow lateral movement and changes to the ball-to-disk contact location. The slide is mounted on a vertical shaft supported by radial and thrust hydrostatic bearings. Traction forces acting on the ball attempt to rotate the shaft about an axis perpendicular to its centerline. The rotation is restrained by a semiconductor load cell. The reactive force measured by the load cell is used to obtain the traction force at the ball/disk contact. The disk shaft is also a two-piece unit with high and low temperature sections. The disk shaft is radially supported by hydrostatic bearings. The contact load is supplied through the disk shaft using a dead weight loading device.

The disk and ball shafts are driven by independent motors. The ball shaft is driven by a 1491 watt (2 HP) synchronous AC motor

allowing a ball shaft speed up to 7200 rpm. The disk shaft is directly coupled to a 2237 watt (3 HP) synchronous AC motor providing a rotating speed of up to 3600 rpm. The shaft speeds are measured by speed sensors whose output is fed into an electrical circuit which provides a signal that is proportional to the slide/roll ratio (ratio in speeds if one shaft is varied from pure rolling conditions). The slide/roll ratio signal and the traction load cell output are fed to an X-Y plotter as the X and Y axes, respectively. In this manner, the traction force vs. slide/roll ratio curve, for a given test, is obtained directly. Figure 3.4 is a photograph of the entire test apparatus.

Contact lubrication is provided by burnishing the ball and disk surfaces. The ball is burnished only prior to the traction test while the disk is burnished both before and during the traction test. To burnish the ball, the load cell is replaced with a spring mechanism which causes the ball spindle to rotate about the vertical hydrostatic spindle until the ball bears against a lubricant specimen. The moment caused by the spring is then balanced by the moment created by the force generated at the lubricant/ball contact.

The disk is burnished by squeezing a lubricant specimen on both sides while it is rotating. The top lubricant specimen is housed in an arm which is supported by a rod. A similar arm supported by

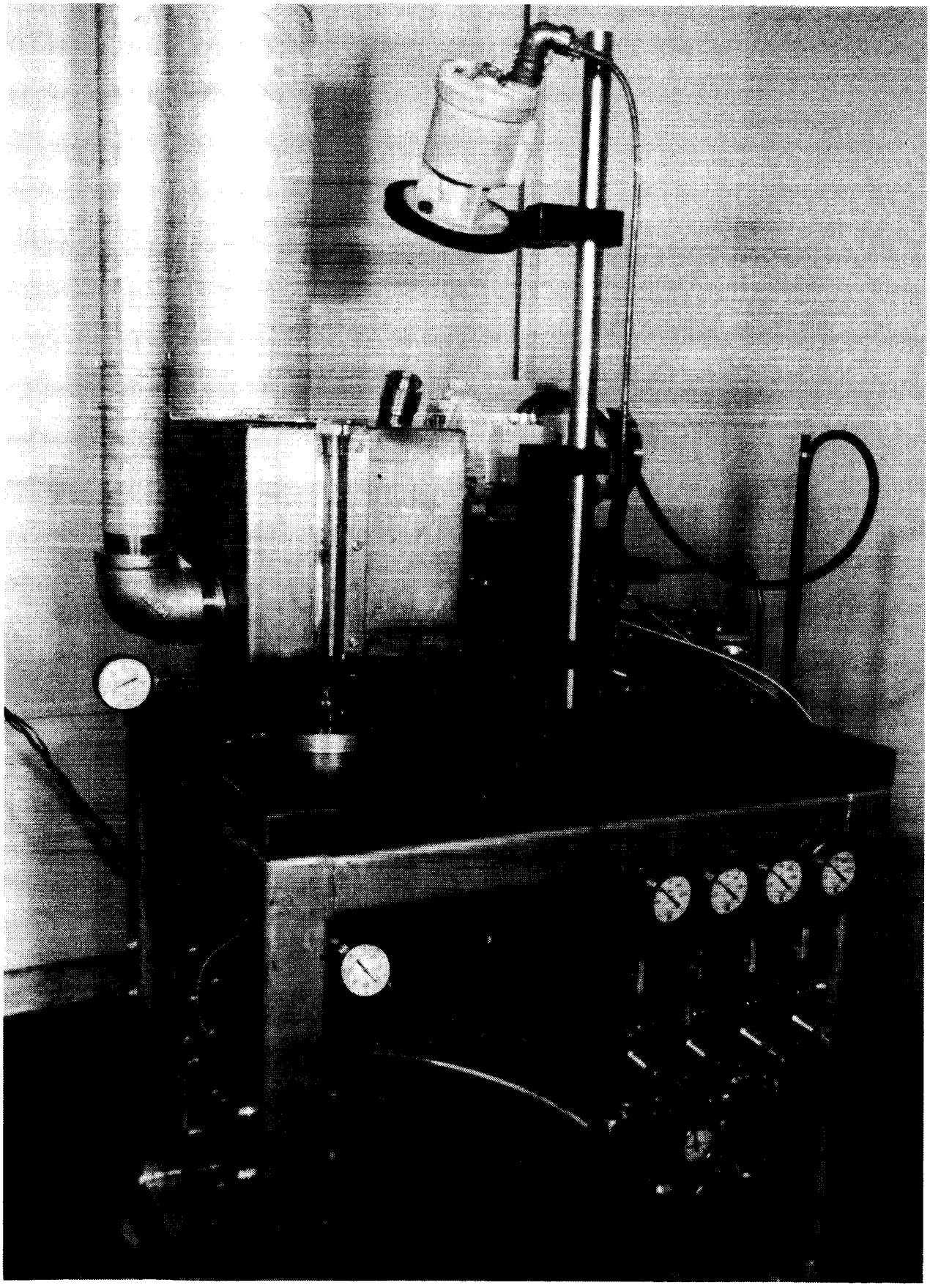

Figure 3.4 Entire Operating Test Rig

a tube supports the lower lubricant specimen. The rod is mounted in linear bearings inside the tube which itself is mounted on another set of linear bearings. A spring loaded plunger forces the lubricant specimens onto the disk surfaces. Figure 3.5 is a schematic of this device. This arrangement minimizes the effect of burnishing load on the contact load applied through the disk shaft.

3.2 Contact Traction Measurement

The individual ball and disk spindle speeds are varied during the test run to provide a controlled amount of differential slip between the two contacting surfaces. The degree of slip (S) is represented as a slide-to-roll ratio defined by

$$S = 2(U_D - U_B)/(U_D + U_B)$$

where U_D is the surface speed of the disk at the contact circle and U_B is the surface speed of the ball. The slide/roll ratio represents the average differential slip within the contact as shown in Figure 3.6. The slide/roll ratio is positive when the disk surface is faster than the ball surface and negative when the disk surface is slower than the ball surface.

The magnitude of the velocity variation, as depicted in Figure 3.6 is a function of contact size and radial position, R, of the ball on the disk surface. Much of the microslip variation within

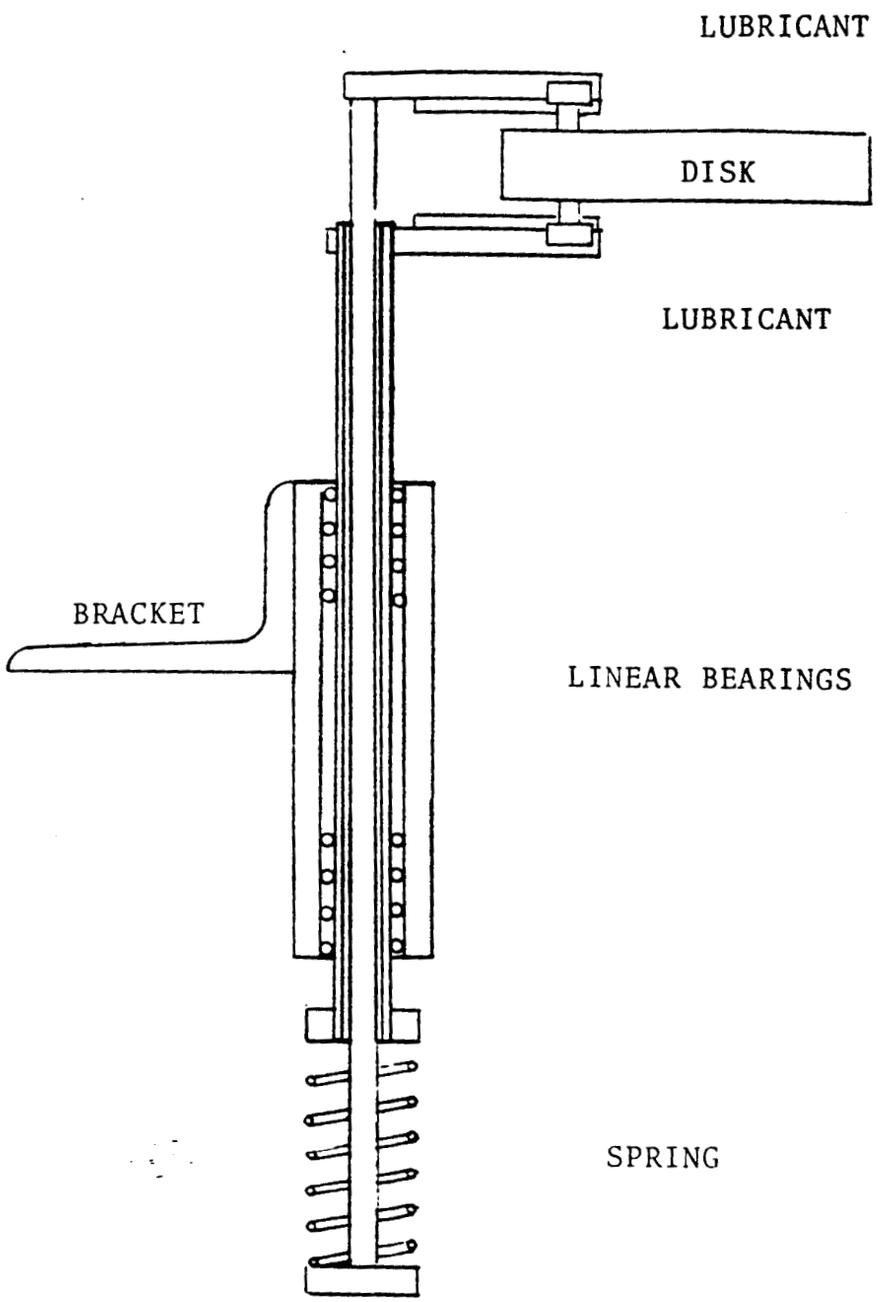

Figure 3.5 Disk Burnishing Mechanism

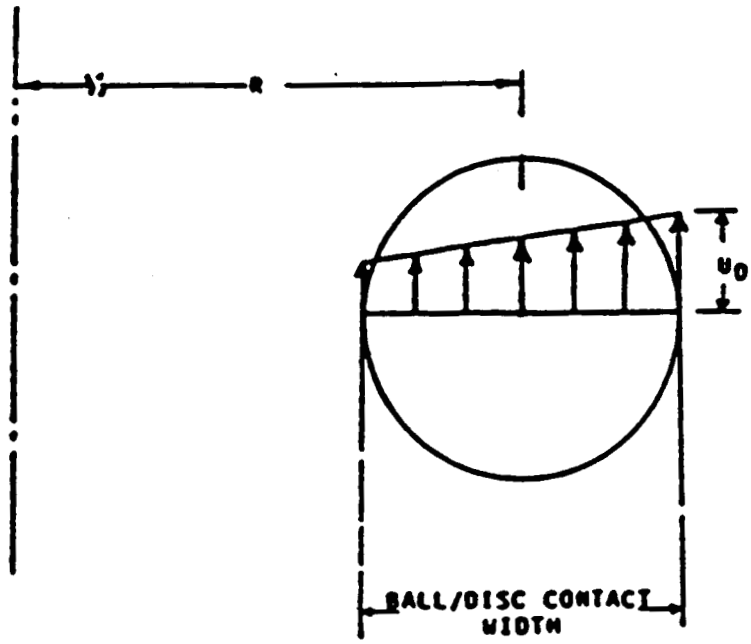

R - RADIAL POSITION OF THE BALL/DISC CONTACT ON THE SURFACE OF THE DISC

Figure 3.6 Variation of Disk Surface Velocity Across the Contact

the contact can be eliminated by operating the ball spindle at an angle with respect to the disk spindle. For the tests presented in this report, the rig was operated in the standard arrangement of a perpendicular axis.

The disk spindle has a toothed pulley for speed measurement. A proximity probe is placed near the pulley to generate a digital pulse train. The high speed ball spindle has direct digital speed output. The two outputs are fed into an electronic circuit of SKF design to give directly the slide/roll ratio defined above. This signal drives the X-axis of an X-Y pen plotter. The individual speeds of the drives are read from electronic counters. The output from the traction load cell is fed to the Y-axis of the plotter. Thus, the traction force versus slide/roll ratio curves can be obtained directly from the test rig. However, the traction force measured by the load cell is not the traction force at the contact. The traction force at the contact, T_c, is calculated from the traction load cell reading, T_L, using the relationship

$$T_c = T_L \, \ell_2/(\ell_1-0.5d)$$

where ℓ_2 is the lever arm for the load cell and ℓ_1 is the distance between the centerline of the disk shaft and the centerline of the axis of rotation of the ball/spindle assembly. This is illustrated in Figure 3.7. The calculation of the traction force at the contact is incorporated into the load cell calibration.

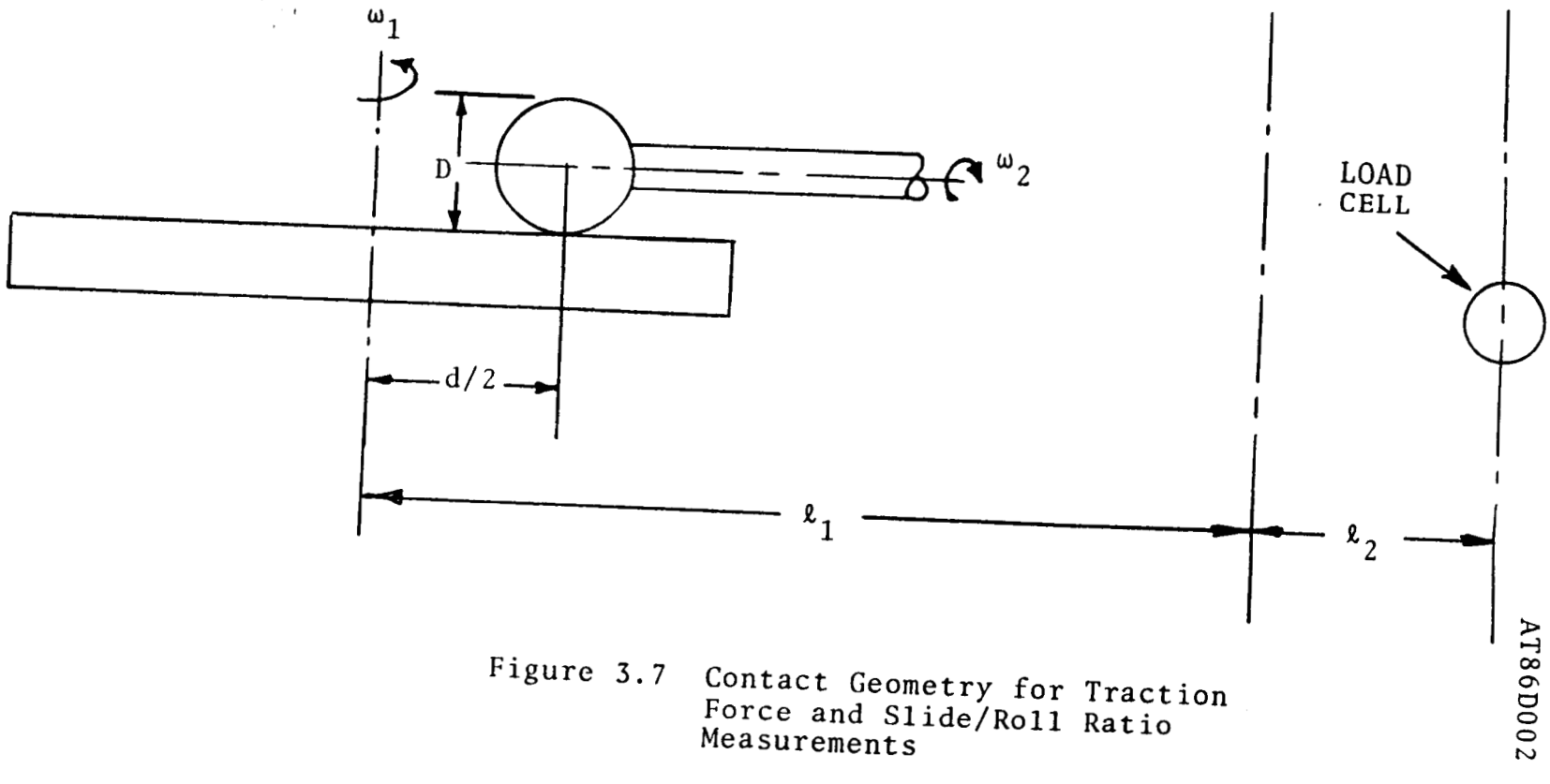

Figure 3.7 Contact Geometry for Traction Force and Slide/Roll Ratio Measurements

3.3 Test Specimens

3.3.1 Disk Specimens

Dimensions of disk specimens are shown in Figure 3.8. The disk materials used in Phase II testing were Norton NC132 hot pressed silicon nitride, Armoloy (electrodeposited thin dense chrome) coated M50 steel, and TiN (titanium nitride) coated M50 steel. The disk surfaces were ground such that the lay of surface roughness was circumferential. However, a ground silicon nitride surface does not have a significant topographical "lay" resulting from the grinding direction. The disks were ground to an RMS surface roughness of 0.06 μm to 0.075 μm (2.5 - 3.0 μinch).

3.3.2 Ball Specimens

Dimensions of the ball specimens are shown in Figure 3.9. The ball materials used in the Phase II testing were Norton NC132 hot pressed silicon nitride (Si_3N_4) and M50 steel. The ball specimens were standard 17.46mm (0.6875 inch) diameter bearing quality balls (AFBMA Anti-Friction Bearing Manufacturers Association Grade 10) modified as shown in Figure 3.9. A new ball was used for each test. The balls were attached to the drive spindle using a bolt and spring washer assembly.

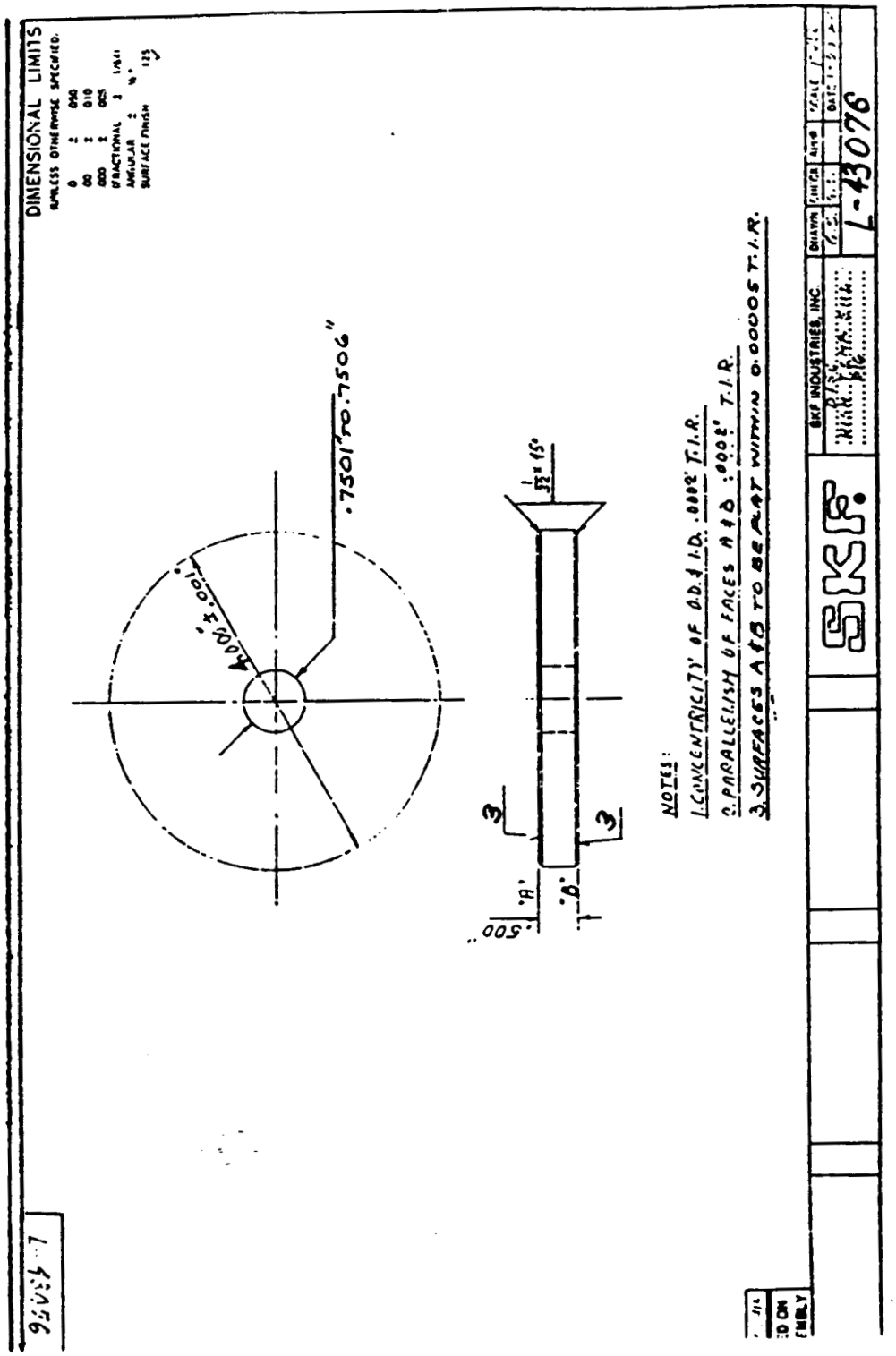

Figure 3.8 Drawing of Disk Specimen

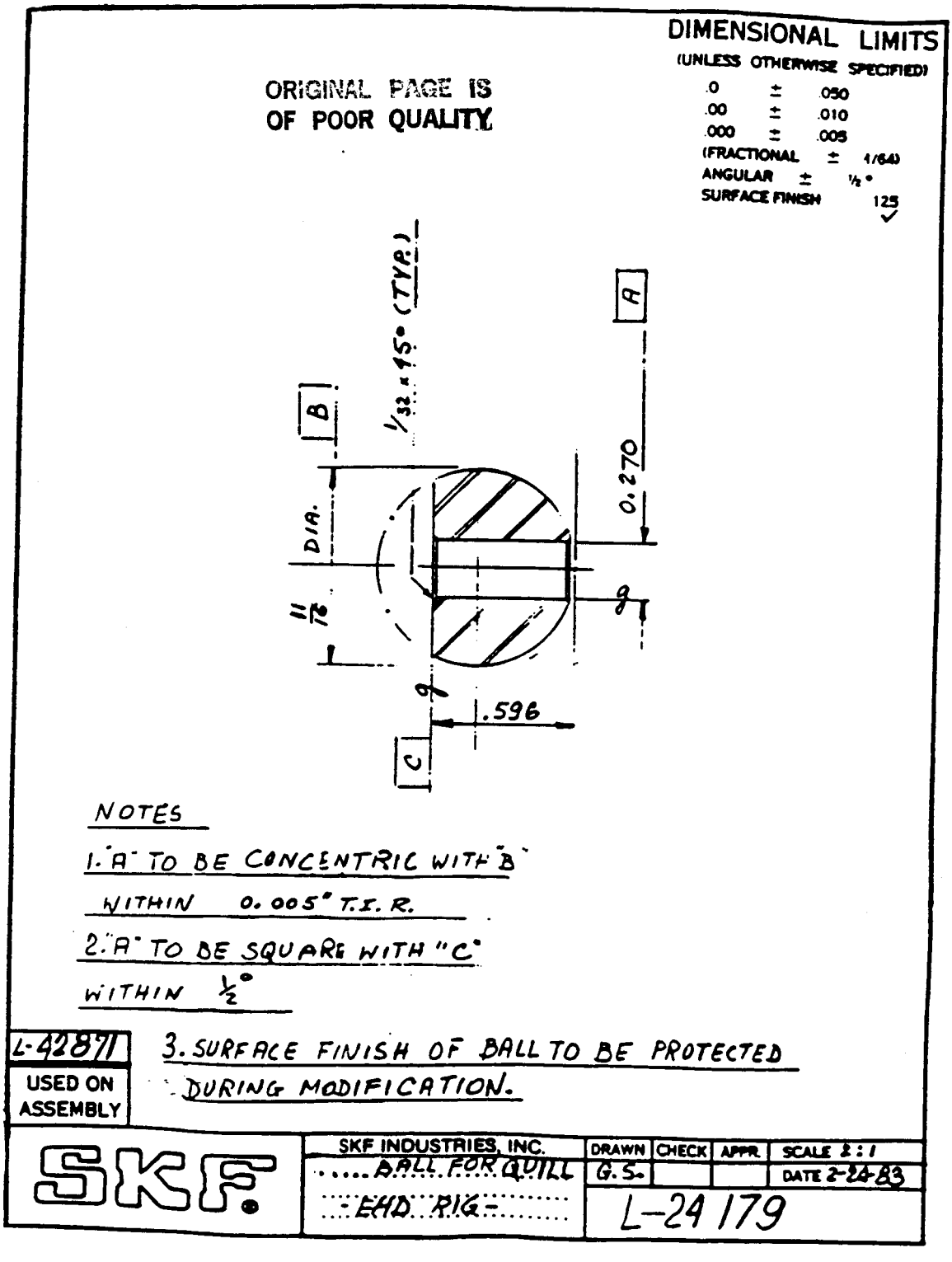

Figure 3.9 Drawing of Ball Specimen

3.3.3 Lubricant Specimens

Only the three graphite based lubricants tested in Phase I were used in the Phase II testing. They are

- P03Ag
- P2003
- P3310

They are all manufactured by Pure Carbon Company. Some of the typical properties are listed in Table 3.1.

The Hughes lubricant compact, although providing the best wear protection in the room temperature tests of Phase I, does not possess the high temperature capability required for the Phase II testing. The polyimide resin used in the weave is temperature limited to about 315°C (600°F) and for that reason was excluded from the Phase II lubricants.

Grade P03 carbons were developed for high speed face seals and have a high thermal conductivity, strength, abrasion resistance and oxidation resistance. P03Ag is base P03 grade carbon impregnated with silver metal to promote thermal conductivity. Grade P2003 is a base P03 type material impregnated with relatively insoluable glass-like phosphates to improve its strength and permeability. In addition, the glass-like phosphates melt at high temperature and

Table 3.1 Average Physical Properties of Graphite Lubricants

PROPERTY	LUBRICANT		
	P03Ag	P2003	P3310
APPARENT DENSITY (gm/cc)	2.40	2.	2.05
COMPRESSIVE STRENGTH (ksi)	29	33	30
TRANSVERSE STRENGTH (ksi)	11	12	11
TENSILE STRENGTH (ksi)	8.5	8.5	8.5
MODULUS OF ELASTICITY (psi x 10^6)	2.4	2.2	2.6
TEMPERATURE LIMIT IN AIR (°F)	950	1250	1000
COEFFICIENT OF THERMAL EXPANSION (μin/in/°F)	2.5	2.7	2.3
THERMAL CONDUCTIVITY (btu/hr/ft^2/°F/ft)	50	45	45

oxidize in preference to the graphite. The melt also helps to retain the graphite in the contact. The P2003 grade graphite tend to absorb moisture. The adsorbed moisture softens the additive and converts it into a gel which upon heating may extrude and harden into a surface glaze. P3310 contains a zinc orthophosphate additive which is water insoluable. it has a higher melting point then the phosphate glass in P2003 but is not as good an oxidation inhibitor. The compositions of these graphite compounds is proprietary information.

3.4 Test Procedure

The Phase II testing procedure benefited from the experience gained during the development of the Phase I testing procedure. Testing consisted of the generation of traction curves, for the conditions desired, using a burnishing method of lubrication. The tests were followed by some cursory tribological evaluations for an assessment of the wear protection provided by the lubricant/material combinations. The test procedure was as follows:

1. Install new ball and locate a new contact position on the disk.
2. Clean specimens with Triclor ether and acetone.
3. Heat specimens to test temperature in the high temperature enclosure while disk and ball surfaces are rotating but

unloaded. Allow specimens to soak at test temperature for one hour.

4. Adjust mounting of test specimen to correct for differential thermal expansion.

5. Burnish lubricant on the ball and disk surfaces for one hour using a burnishing load of 53N for the ball and 62N for the disk.

6. Load disk onto ball specimen at desired test load and with surface speeds set for pure rolling. Continue burnishing the disk specimen. (The ball surface was not lubricated during the test.)

7. Generate a traction curve in the positive and negative directions of slip. (Test duration was generally less than one minute.)

8. Turn off heat and spindle drives. Open enclosure door, loosen specimens and allow to cool.

3.5 Test Matrix

The contact loads, rolling speeds, and temperatures selected for the graphite lubricant testing and the development of traction models is shown in Table 3.2. These tests were for Si_3N_4 balls

Table 3.2 High Temperature Graphite Lubrication Test Matrix

LUBRICANT	AVERAGE SURFACE SPEEDS (IPS)	TEMPERATURE 700°F MAXIMUM HERTZ CONTACT STRESS (KSI)			TEMPERATURE 1000°F MAXIMUM HERTZ CONTACT STRESS (KSI)		
		200	250	300	200	250	300
P03Ag	150	D2	D6	D3	D1	D5	D4
	250	D13	D15	D17	D14	D16	D18
P2003	150	D7	D9	D11	D8	D10	D12
	250	D19	D21	D23	D20	D22	D24
P3310	150	D25	D27	D29	D26	D28	D30
	250	D31	D33	D35	D32	D34	D36

All tests Si_3N_4 ball on Si_3N_4 disk

against Si_3N_4 disks only. The test matrix was selected to cover the range of operating conditions anticipated for rolling and sliding contacts in advanced LHR diesel engines.

In addition to the test matrix for the silicon nitride/graphite combinations of Table 3.2, there were a series of tests run using the same lubricants on an Armoloy coated M50 steel disk. This test matrix appears in Table 3.3.

Several very cursory tests were run on the TiN coated M50 steel disk with no lubricant and M50 steel balls. These tests did not follow any prescribed matrix.

Table 3.3 Armoloy Coated M50 Steel Disk Test Matrix

LUBRICANT	AVERAGE SURFACE SPEEDS (IPS)	TEMPERATURE					
		400 °F MAXIMUM HERTZ CONTACT STRESS (KSI)			600 °F MAXIMUM HERTZ CONTACT STRESS (KSI)		
		200	250	300	200	250	300
NONE	250	-	D38	D43	-	D48	D53
P3310	250	-	D39	D44	-	D49	D54
P03Ag	250	-	D41	D46	-	D51	D56
P2003	250	-	D40	D45	-	D50	D55

All tests Si_3N_4 ball on Armoloy/M50 disk

4.0 SOLID LUBRICANT TRACTION TESTS

4.1 Initial Testing

A series of test rig check-out tests as well as test procedure development tests were run initially. Early high temperature tests were run at 204°C (400°F) using P2003 and P03Ag graphite lubricants. This initial testing showed that the graphite lubricants were not effective at 204°C (400°F). It is a well established that the presence of gases or liquids such as absorbed water imparts good lubricating qualities in graphite. It is felt that at this 204°C (400°F) temperature region, the graphite loses moisture and that the temperature is not high enough for the additives to come into play. Consequently, the graphite acts as an abrasive instead of a lubricant. Based on these initial results testing at 204°C (400°F) was dropped in connection with the silicon nitride ball and disk materials. The high temperature tests conducted were at 370°C (700°F) and 540°C (1000°F). The testing performed at these 2 high temperatures utilized both silicon nitride disks and balls.

4.2 Graphite Lubricants at High Temperature

The three (3) graphite lubricants, described in Section 3.3.3, were tested for effectiveness as solid lubricants at high temperature. The final test matrix for the graphite lubricants at high temperatures is shown in Table 4.1. Traction force vs.

Table 4.1 High Temperature Graphite Lubrication Test Matrix

LUBRICANT	AVERAGE SURFACE SPEEDS (IPS)	TEMPERATURE 700°F MAXIMUM HERTZ CONTACT STRESS (KSI)			TEMPERATURE 1000°F MAXIMUM HERTZ CONTACT STRESS (KSI)		
		200	250	300	200	250	300
P03Ag	150	D2	D6	D3	D1	D5	D4
	250	D13	D15	D17	D14	D16	D18
P2003	150	D7	D9	D11	D8	D10	D12
	250	D19	D21	D23	D20	D22	D24
P3310	150	D25	D27	D29	D26	D28	D30
	250	D31	D33	D35	D32	D34	D36

All tests Si_3N_4 ball on Si_3N_4 disk

slide/roll ratio curves were generated for all 36 tests. A typical traction curve is shown in Figure 4.1. The solid lubricant used in this test was P3310 under test conditions of 370°C (700°F) chamber temperature, 1034 MPa maximum Hertzian pressure (200 ksi) and 6.35 m/s (250 in/sec) rolling speed. The traction curve was generated by initial operation at pure rolling (giving zero net traction in the rolling direction) followed by a gradual increase in rolling speed of one specimen until a maximum traction force is reached. The rolling speed is then adjusted back to pure rolling. The negative portion of the traction curve was obtained by repeating the procedure but lowering the speed below that which represents pure rolling.

The traction curves are characterized by a slope (measured near the pure rolling point) and a maximum traction force. See the curve of Figure 4.1. Typically, both slope and maximum traction force for solid lubricants are several times greater than oil lubricated contacts. The maximum traction coefficient of the test shown in Figure 4.1 is 0.31. The results from the 36 high temperature graphite tests have been tabularized and are presented in Table 4.2. Included in the table are each curve's maximum traction force, as well as, the computed maximum traction coefficient.

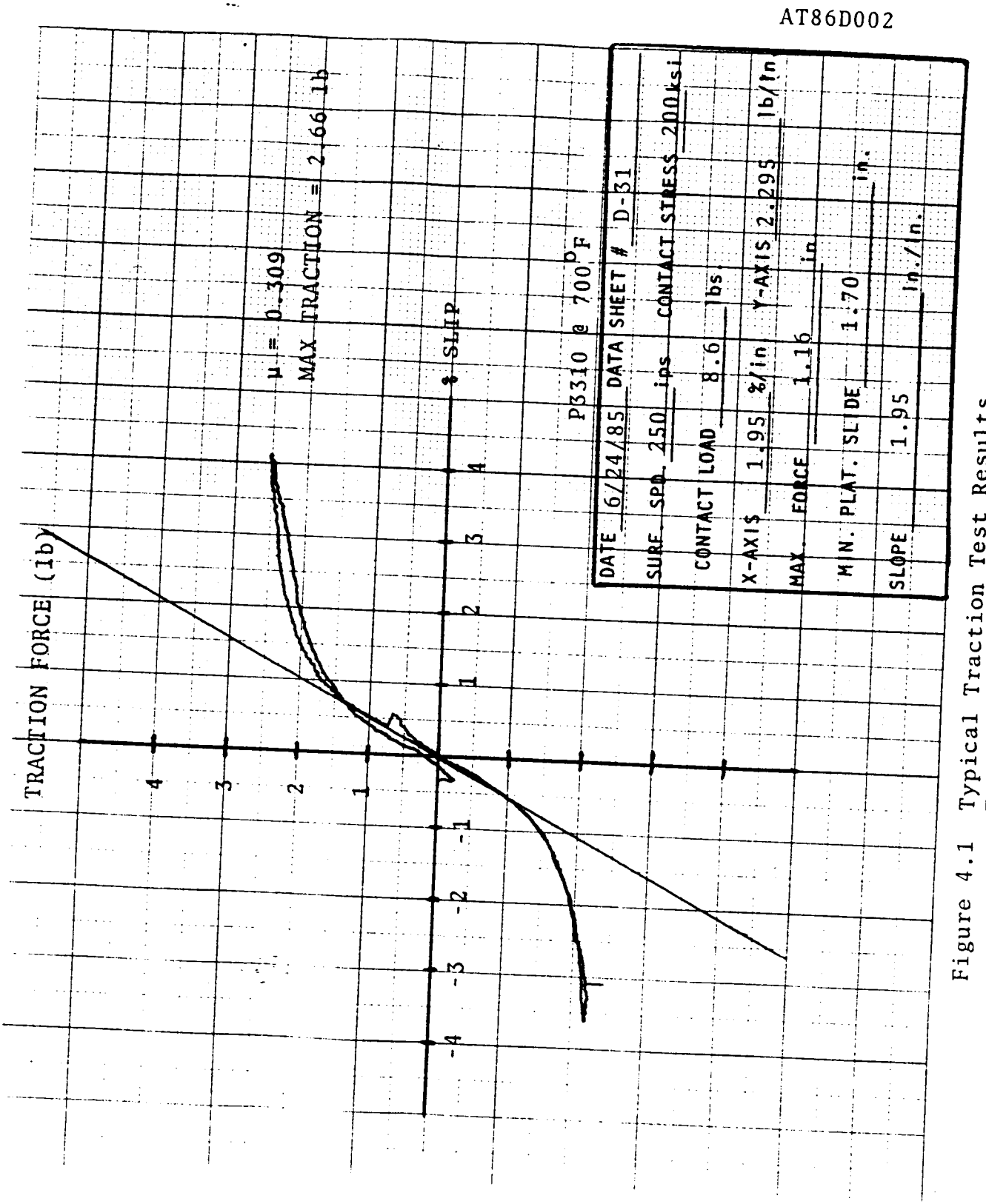

Figure 4.1 Typical Traction Test Results
Traction Force vs. Slip Curve

Table 4.2 Measured Test Results for High Temperature Graphite Lubricants

Test Number	Ball Material	Disc Material	Lubricant	Temperature	Stress	Speed	Max Traction	Max Coefficient
1	SILICON NITRIDE	SILICON NITRIDE	P03AG	1000	200	150	1.6	0.19
2	SILICON NITRIDE	SILICON NITRIDE	P03AG	700	200	150	3.7	0.43
3	SILICON NITRIDE	SILICON NITRIDE	P03AG	700	300	150	12.8	0.44
4	SILICON NITRIDE	SILICON NITRIDE	P03AG	1000	300	150	4.8	0.16
5	SILICON NITRIDE	SILICON NITRIDE	P03AG	1000	250	150	1.2	0.07
6	SILICON NITRIDE	SILICON NITRIDE	P03AG	700	250	150	7.2	0.43
7	SILICON NITRIDE	SILICON NITRIDE	P2003	700	200	150	5.2	0.60
8	SILICON NITRIDE	SILICON NITRIDE	P2003	1000	200	150	3.6	0.42
9	SILICON NITRIDE	SILICON NITRIDE	P2003	700	250	150	8.9	0.53
10	SILICON NITRIDE	SILICON NITRIDE	P2003	1000	250	150	11.8	0.70
11	SILICON NITRIDE	SILICON NITRIDE	P2003	700	300	150	10.0	0.34
12	SILICON NITRIDE	SILICON NITRIDE	P2003	1000	300	150	4.7	0.16
13	SILICON NITRIDE	SILICON NITRIDE	P03AG	700	200	250	5.7	0.66
14	SILICON NITRIDE	SILICON NITRIDE	P03AG	1000	200	250	1.2	0.14
15	SILICON NITRIDE	SILICON NITRIDE	P03AG	700	250	250	5.8	0.34
16	SILICON NITRIDE	SILICON NITRIDE	P03AG	1000	250	250	2.6	0.15
17	SILICON NITRIDE	SILICON NITRIDE	P03AG	700	300	250	7.6	0.26
18	SILICON NITRIDE	SILICON NITRIDE	P03AG	1000	300	250	2.9	0.10
19	SILICON NITRIDE	SILICON NITRIDE	P2003	700	200	250	3.1	0.36
20	SILICON NITRIDE	SILICON NITRIDE	P2003	1000	200	250	4.7	0.55
21	SILICON NITRIDE	SILICON NITRIDE	P2003	700	250	250	9.1	0.54
22	SILICON NITRIDE	SILICON NITRIDE	P2003	1000	250	250	7.2	0.43
23	SILICON NITRIDE	SILICON NITRIDE	P2003	700	300	250	15.0	0.52
24	SILICON NITRIDE	SILICON NITRIDE	P2003	1000	300	250	11.4	0.39
25	SILICON NITRIDE	SILICON NITRIDE	P3310	700	200	150	2.0	0.23
26	SILICON NITRIDE	SILICON NITRIDE	P3310	1000	200	150	2.3	0.27
27	SILICON NITRIDE	SILICON NITRIDE	P3310	700	250	150	4.9	0.29
28	SILICON NITRIDE	SILICON NITRIDE	P3310	1000	250	150	3.8	0.23
29	SILICON NITRIDE	SILICON NITRIDE	P3310	700	300	150	10.3	0.36
30	SILICON NITRIDE	SILICON NITRIDE	P3310	1000	300	150	6.2	0.21
31	SILICON NITRIDE	SILICON NITRIDE	P3310	700	200	250	2.7	0.31
32	SILICON NITRIDE	SILICON NITRIDE	P3310	1000	200	250	2.6	0.30
33	SILICON NITRIDE	SILICON NITRIDE	P3310	700	250	250	4.8	0.29
34	SILICON NITRIDE	SILICON NITRIDE	P3310	1000	250	250	4.4	0.26
35	SILICON NITRIDE	SILICON NITRIDE	P3310	700	300	250	6.7	0.40
36	SILICON NITRIDE	SILICON NITRIDE	P3310	1000	300	250	6.1	0.21

Temperature in ^{o}F
Stress in ksi
Speed in in/s
Traction in lb

4.2.1 P3310

The test that produced the traction curve of Figure 4.1 was test number D31[1]. Scanning electron microscope (SEM) micrographs of the test ball are shown in Figure 4.2. A low power (25X) magnification of the contact track is shown in Figure 4.2a. The actual wear track (Hertzian contact zone) is the sharp white band in the center of the wide light area. The remainder of the wide light area is excess solid lubricant transferred to the ball from burnishing and/or solid lubricant which has been squeezed or forced out of the contact zone.

The orientation of the SEM photomicrographs with respect to the ball and the test arrangement is shown in Figure 4.3. Note the location of left and right edges on Figure 4.3 and then on the photo of Figure 4.2a. This orientation will be used consistently throughout the remainder of this report. Figures 4.2c and 4.2d are higher magnification (250X) photomicrographs of the edges, respectively, of test ball #31. Figure 4.2b shows the center of the contact zone under 1000X magnification. For comparison purposes, Figure 4.4 presents two 1000X photomicrographs of unrun, as-finished ball surface. This is the same magnification as the photo of Figure 4.2b. Notice the characteristic porous appearance to the ball surface. To the naked eye this surface appears smooth and lusterous, and stylus traces verify the surface finish to meet the

[1]All the test number designations were preceeded by the letter D. For the purpose of this report the tests will be referred to by number only. The D will appear only in the SEM photos.

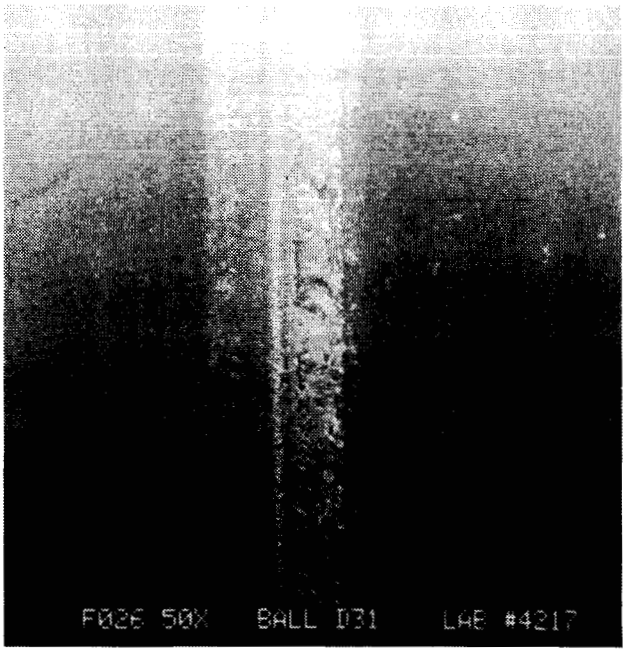

(a) Contact Track

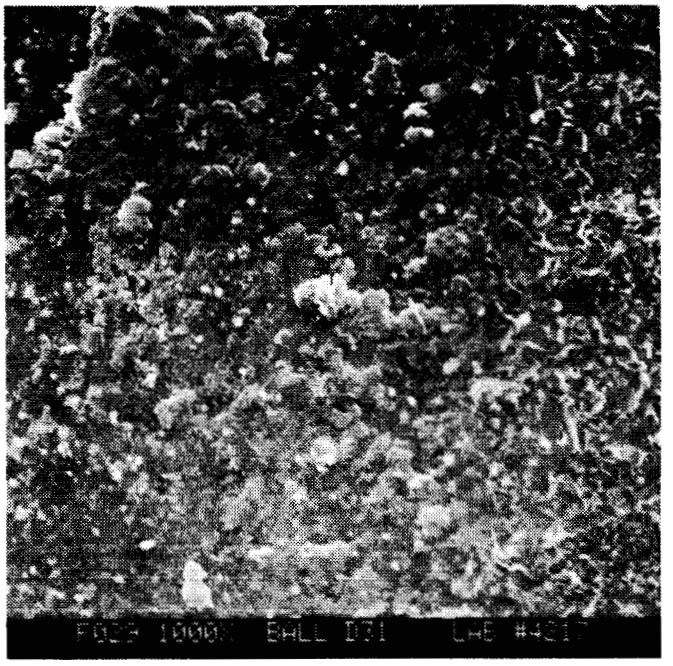

(b) Center of Contact

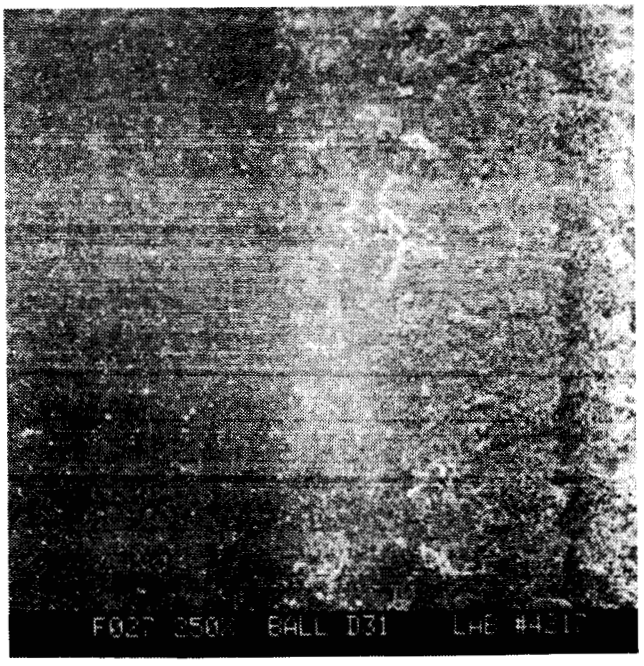

(c) Left Edge of Contact

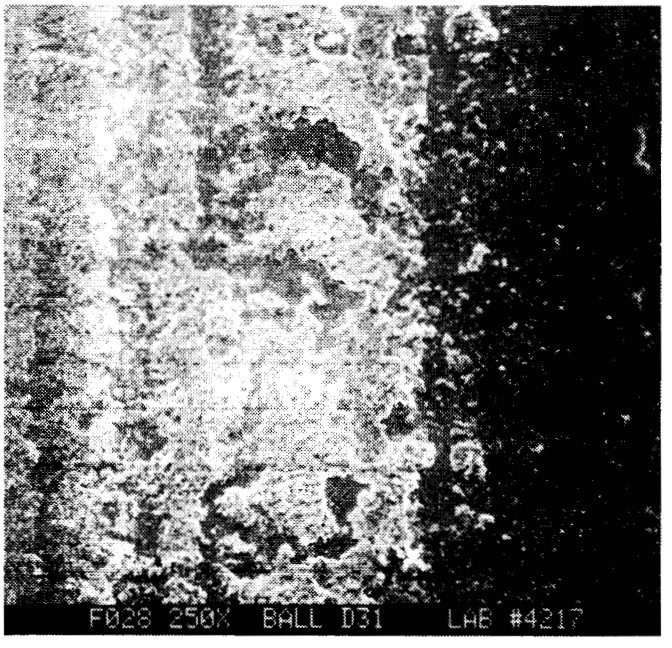

(d) Right Edge of Contact

Figure 4.2 Silicon Nitride Test Ball
P3310, T = 370°C
Contact Stress = 1378 MPa
Rolling Speed = 6.35 m/s

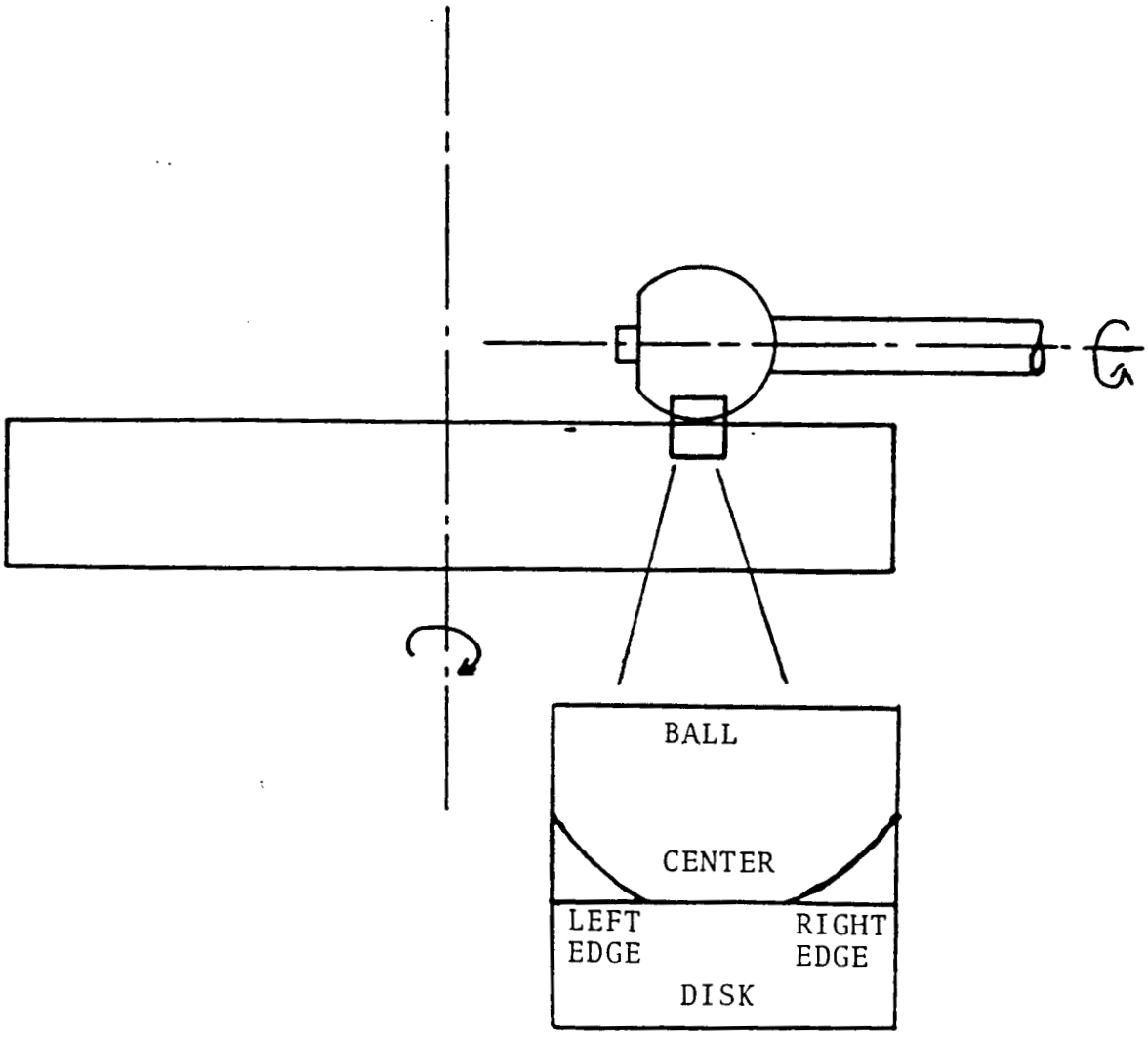

Figure 4.3 Location of Edges and Center of Wear Track in SEM Photomicrographs

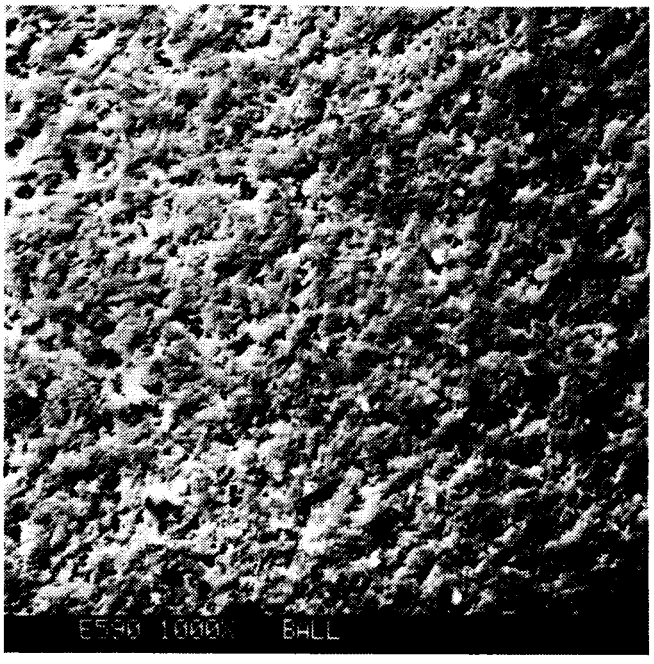

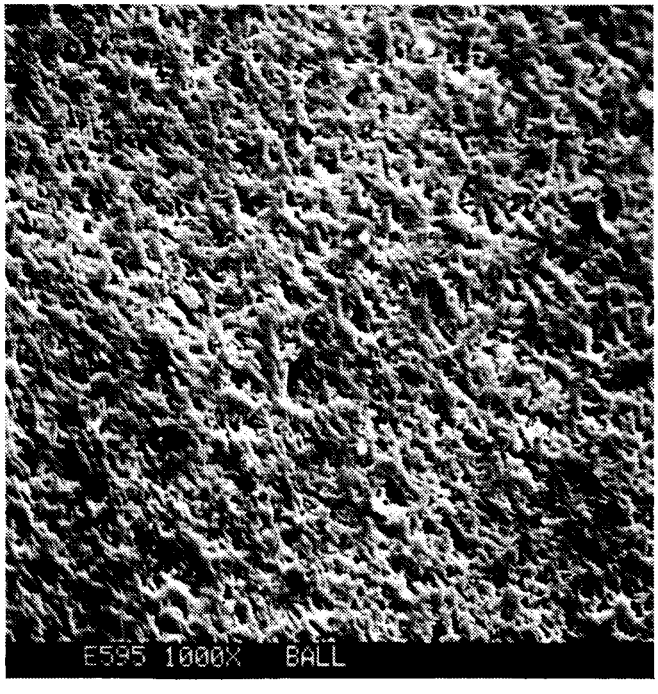

Figure 4.4 Unrun Silicon Nitride Ball Surface

specifications of an AFBMA (Anti-Friction Bearing Manufacturers Association) Grade 10 quality ball.

Returning to the results shown in the photos of Figure 4.2, the contact zone shows what appears to be patches of worked lubricant and a well protected ball surface. The thin surface layer of lubricant has undergone some plastic deformation.

Some test runs with the P3310 lubricant showed little or no apparent wear damage of the ball surface. This is shown in Figure 4.5 for test #29 which was also at 370°C (700°F) but with higher contact stress, 2068 MPa (300 ksi) and lower rolling speeds, 3.8 m/s (150 in/s). The format of Figure 4.5 is the same as Figure 4.2. In this test there is very little excess material along the sides of the contact zone. The track center, Figure 4.5b appears to be very smooth and somewhat glossy. The measured traction coefficient for this test was 0.36. The P3310 results, from a surface appearance viewpoint, at 370°C (700°F) and 540°C (1000°F) were consistent as evidenced by Figures 4.6, 4.7 and 4.8.

Figure 4.9 presents the SEM micrographs of test ball #28. Here we see a departure from the typical P3310 results of the previous photos. The test conditions were a temperature of 540°C (1000°F), contact stress of 3.8 m/s (150 in/s). The measured traction coefficient was only 0.28, however, the SEM micrographs show a thick,

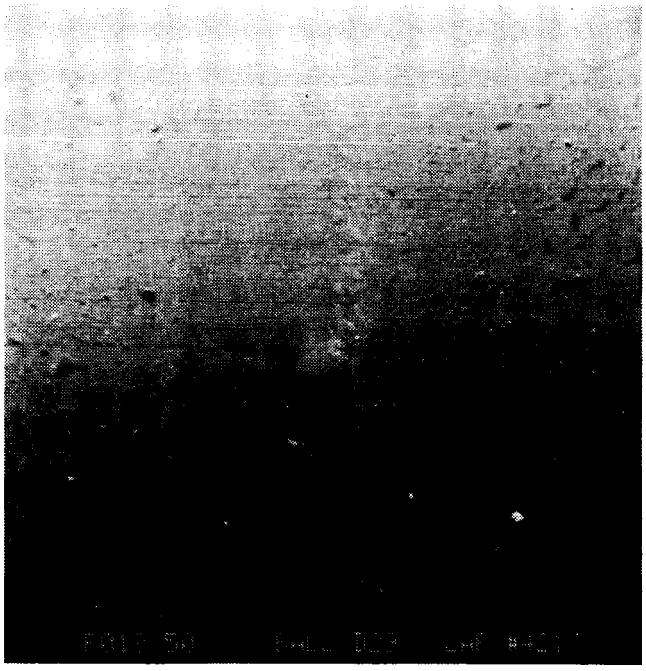

(a) Contact Track

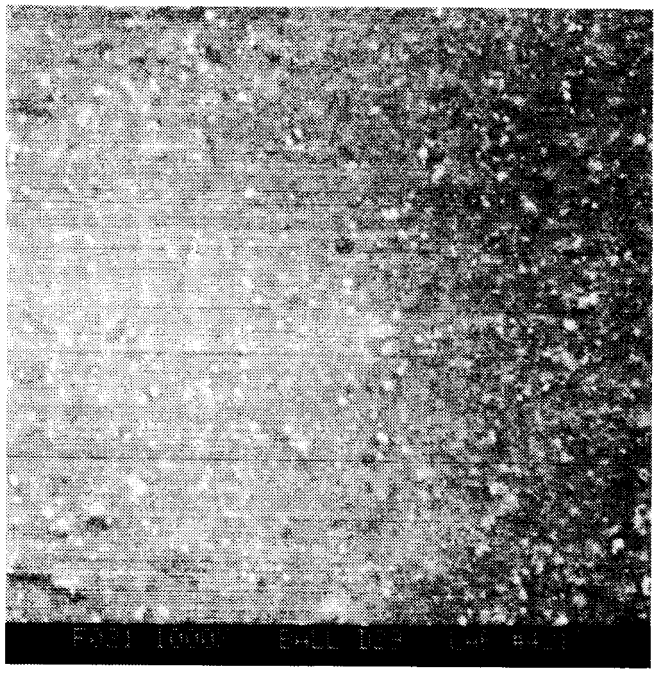

(b) Center of Contact

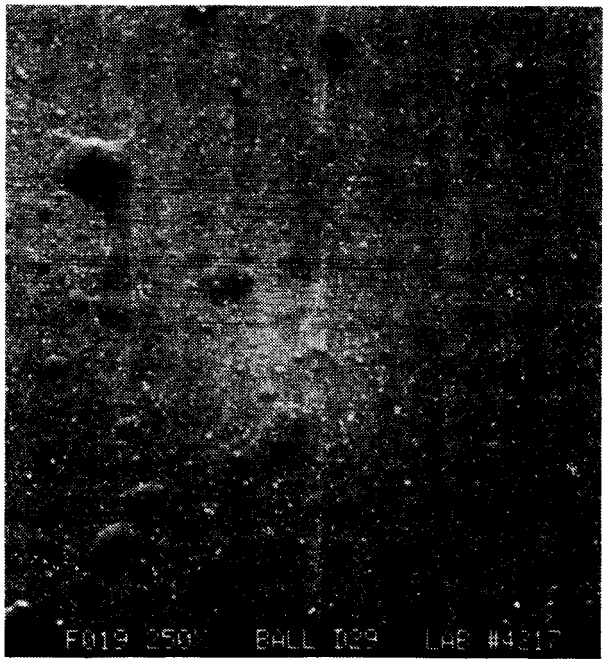

(c) Left Edge of Contact

(d) Right Edge of Contact

Figure 4.5 Silicon Nitride Test Ball
P3310, T = 370°C
Contact Stress = 2068 MPa
Rolling Speed = 3.8 m/s

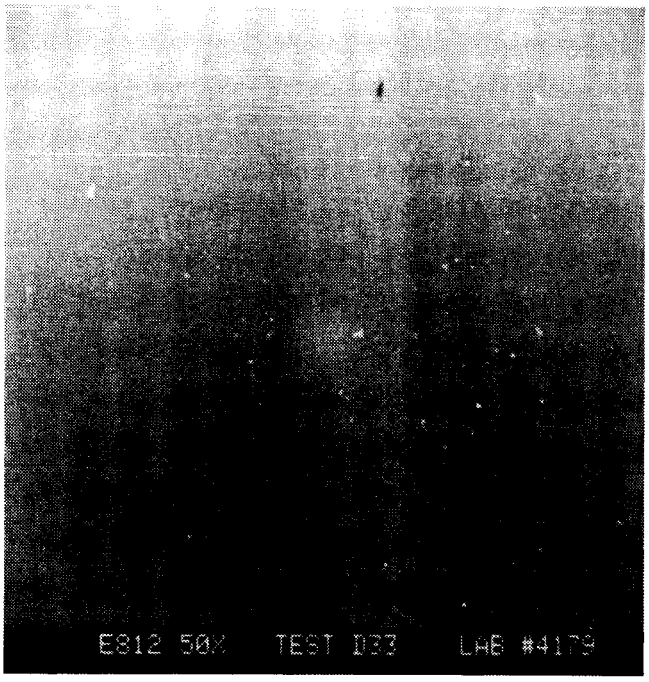

(a) Contact Track

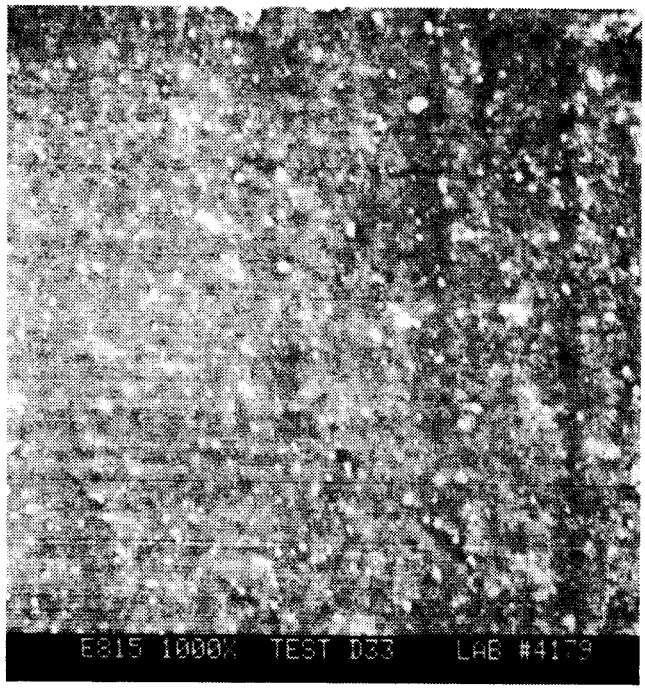

(b) Center of Contact

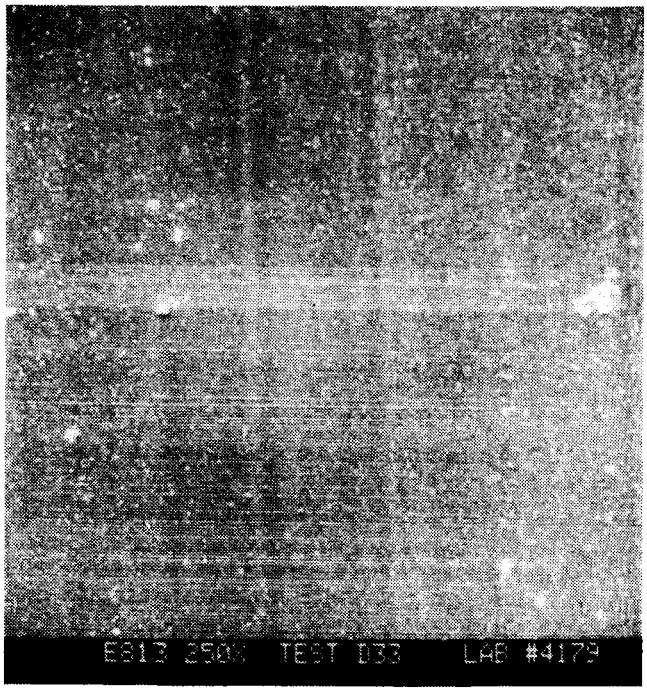

(c) Left Edge of Contact

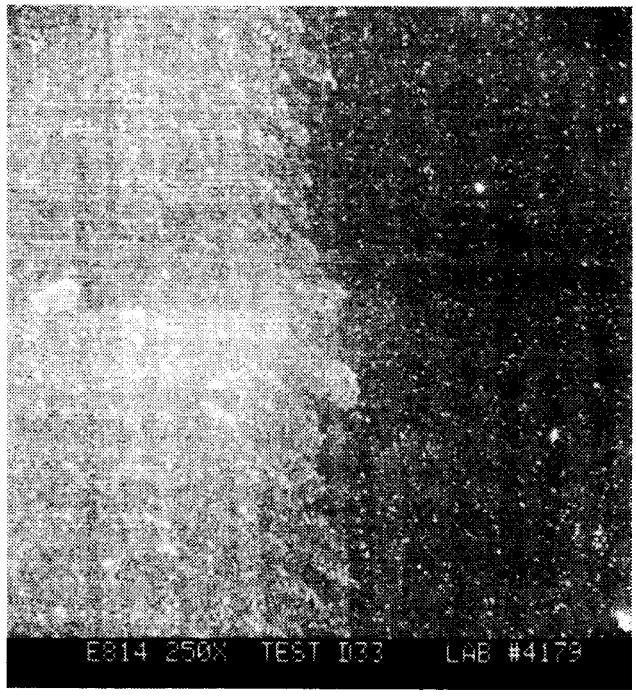

(d) Right Edge of Contact

Figure 4.6 Silicon Nitride Test Ball
P3310, T = 370°C
Contact Stress = 1723 MPa
Rolling Speed = 6.35 m/s

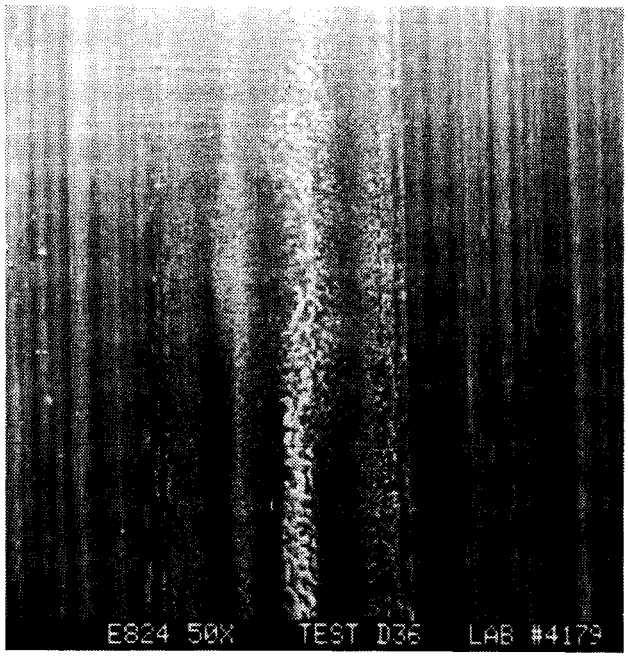

(a) Contact Track

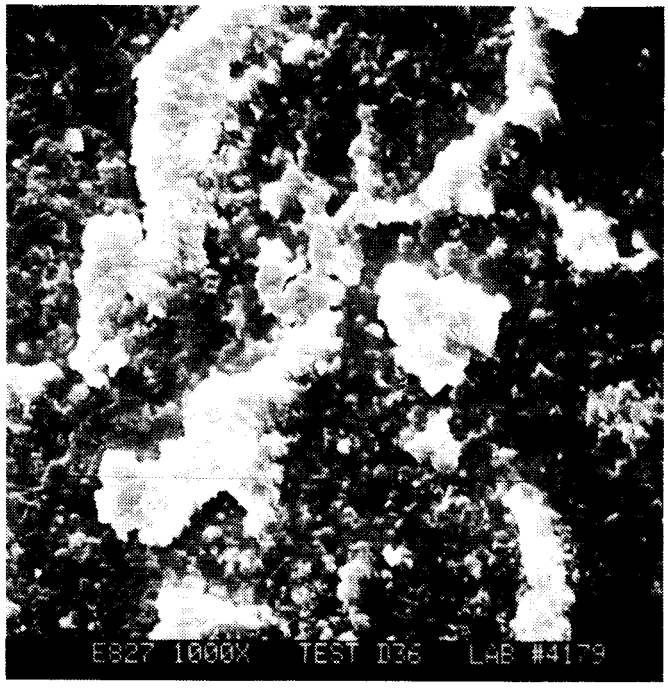

(b) Center of Contact

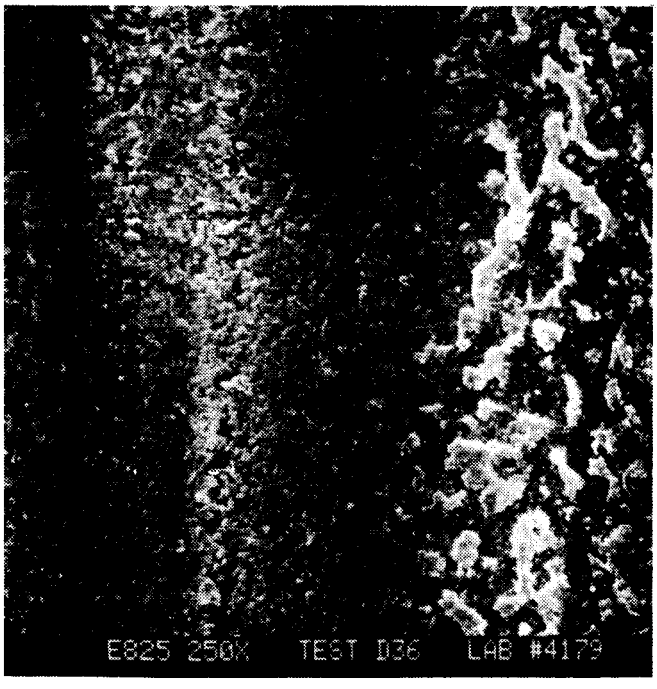

(d) Left Edge of Contact

(d) Right Edge of Contact

Figure 4.7 Silicon Nitride Test Ball
P3310, T = 540°C
Contact Stress = 2068 MPa
Rolling Speed = 6.35 m/s

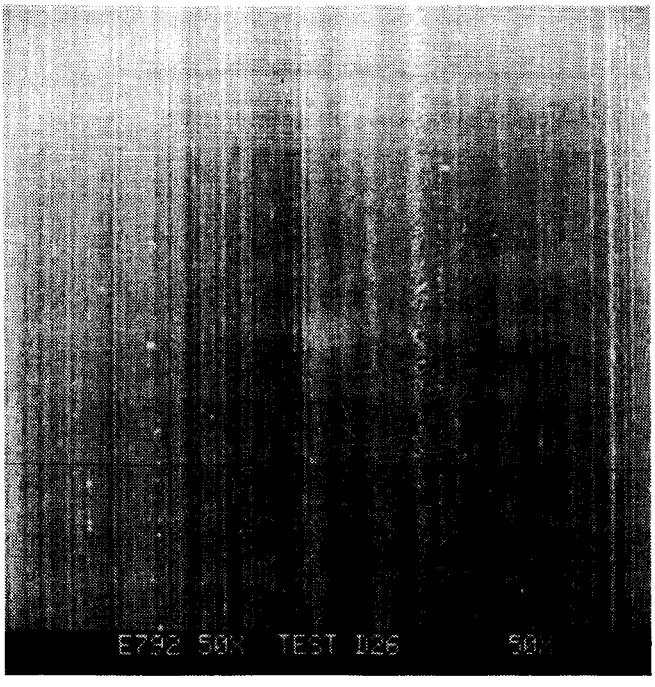

(a) Contact Track

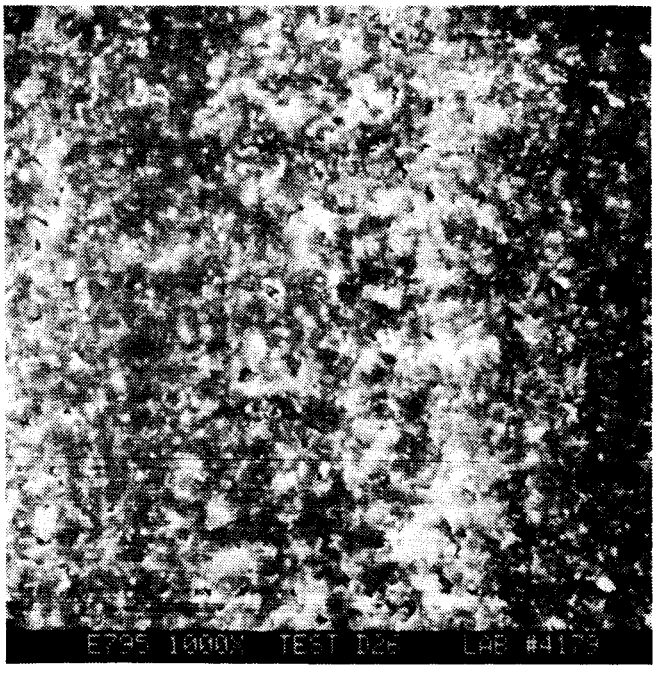

(b) Center of Contact

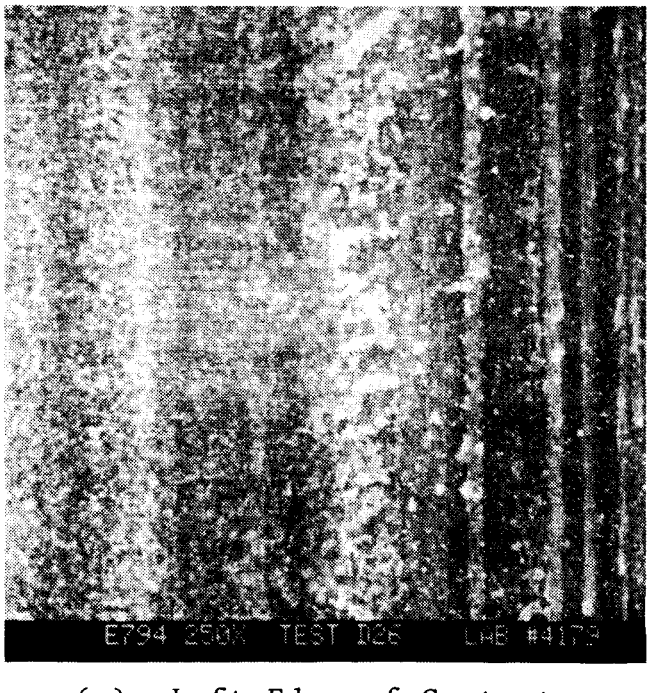

(c) Left Edge of Contact

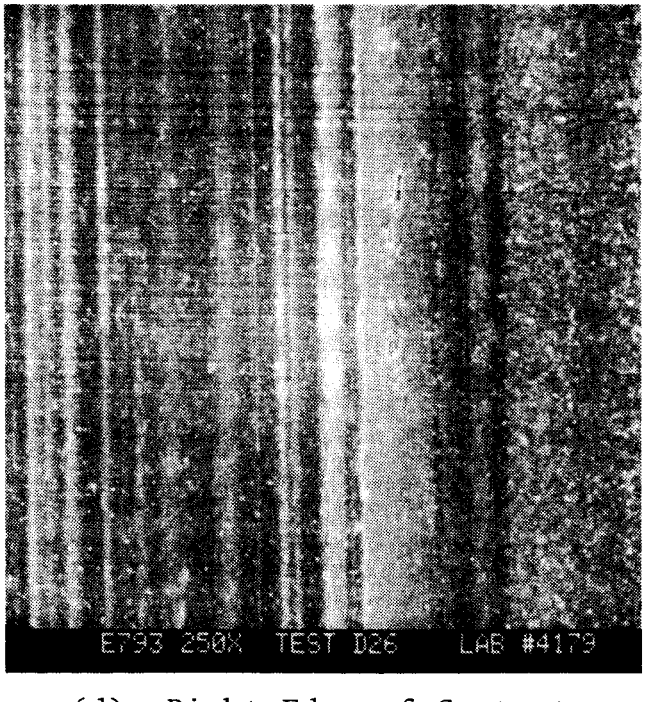

(d) Right Edge of Contact

Figure 4.8 Silicon Nitride Test Ball
P3310, T = 540°C
Contact Stress = 1378 MPa
Rolling Speed = 3.8 m/s

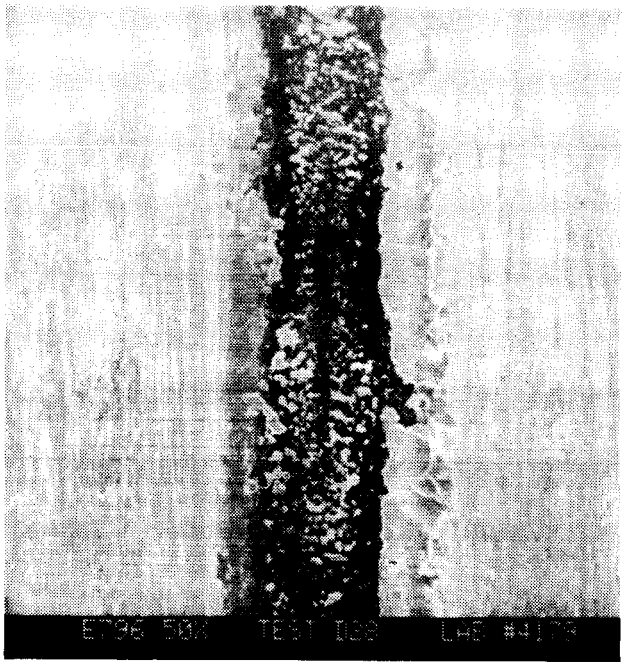

(a) Contact Track

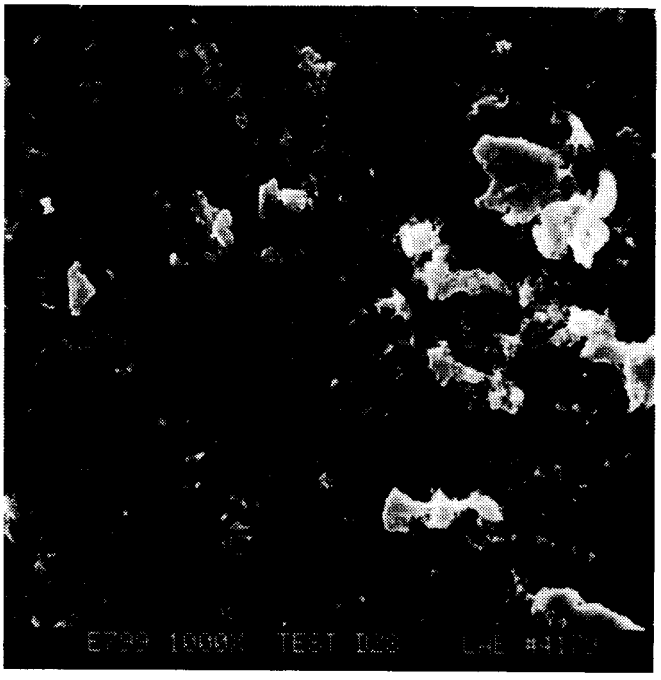

(b) Center of Contact

(c) Left Edge of Contact

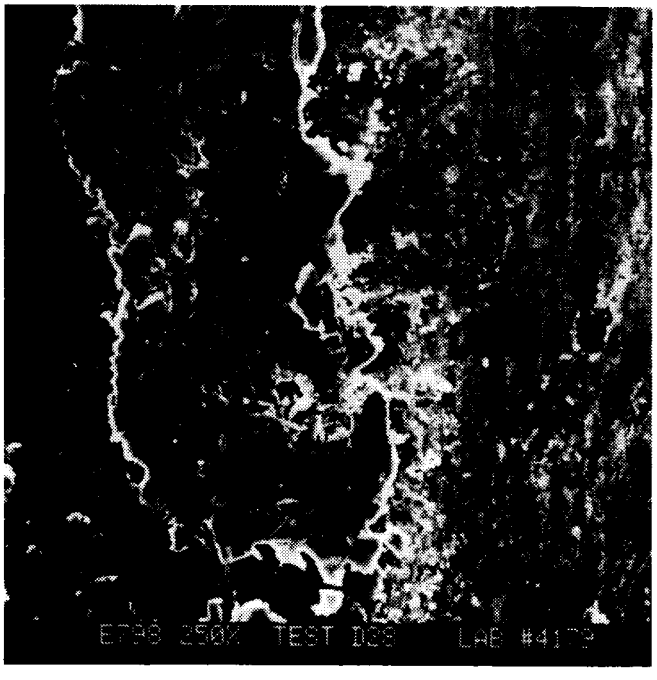

(d) Right Edge of Contact

Figure 4.9 Silicon Nitride Test Ball
P3310, T = 540°C
Contact Stress = 1723 MPa
Rolling Speed = 3.8 m/s

brittle looking coating of lubricant. The lubricant which has been pushed out of the contact zone is brittle and cracked. There is also very little lubricant left in the center of the contact zone. Figure 4.9b shows the center region at high magnification (1000X) and oxidation of the silicon nitride surface is evident. The documented oxidation of silicon nitride [4] states that it oxidizes by forming silica (SiO_2) which appears very glassy and fills in the original surface pores. This has been verified for NC132 silicon nitride in tests at SKF [5].

4.2.2 PO3Ag

The tests conducted with PO3Ag were much more inconsistent then the P3310 results but, frequently yielded lower traction levels, particularly at 540°C (1000°F). Measured traction values for the PO3Ag lubricant ranged from as low as 0.07 to as high as 0.66.

There appears to be some correlation between the high traction values and the appearance of the PO3Ag lubricant on and around the contact zone as evidenced by the photomicrographs of Figure 4.10 and 4.11.

Figure 4.10 demonstrates this for test #2 which had a test temperature of 370°C (700°F), contact stress of 1279 MPa (200

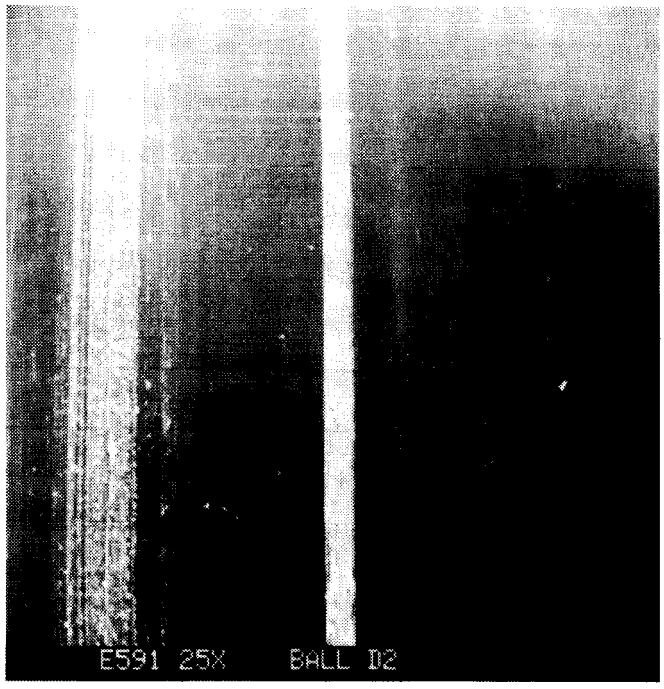

(a) Contact Track

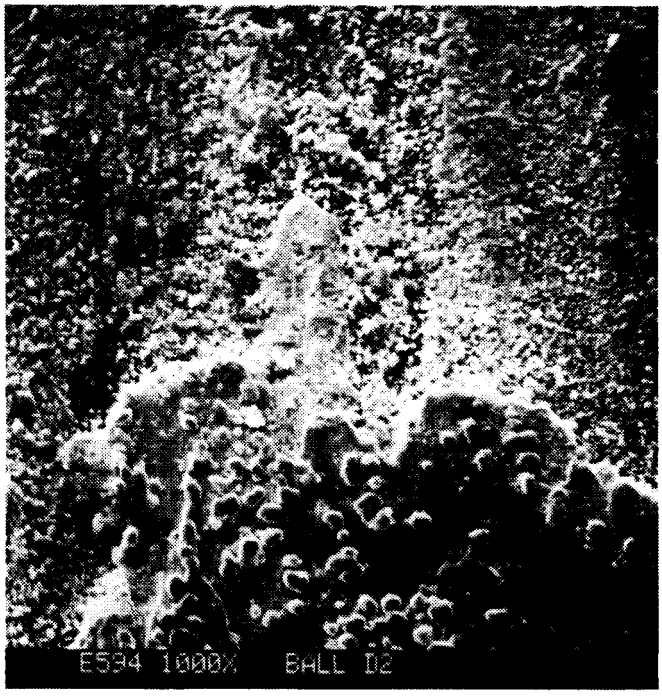

(b) Center of Contact

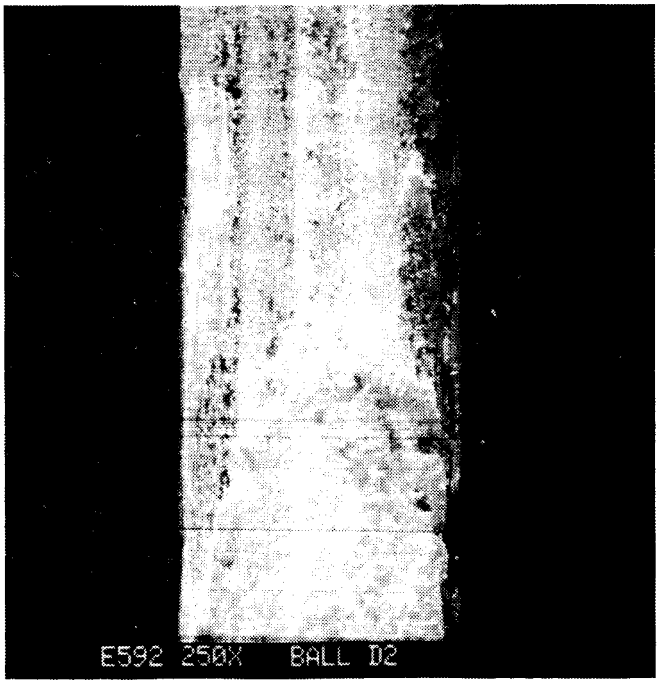

(c) Contact Track

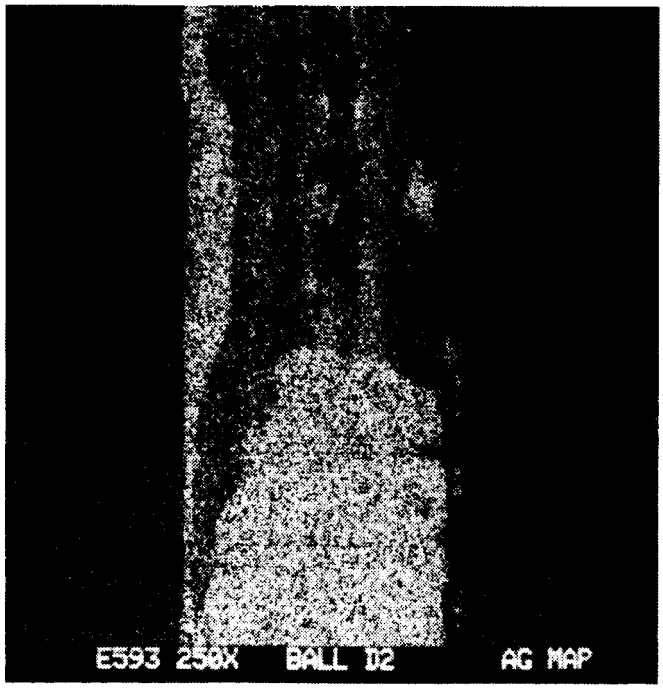

(d) Silver (Ag) Map of Track

Figure 4.10 Silicon Nitride Test Ball
P03Ag, T = 370°C
Contact Stress = 1378 MPa
Rolling Speed = 3.8 m/s

(a) Contact Track

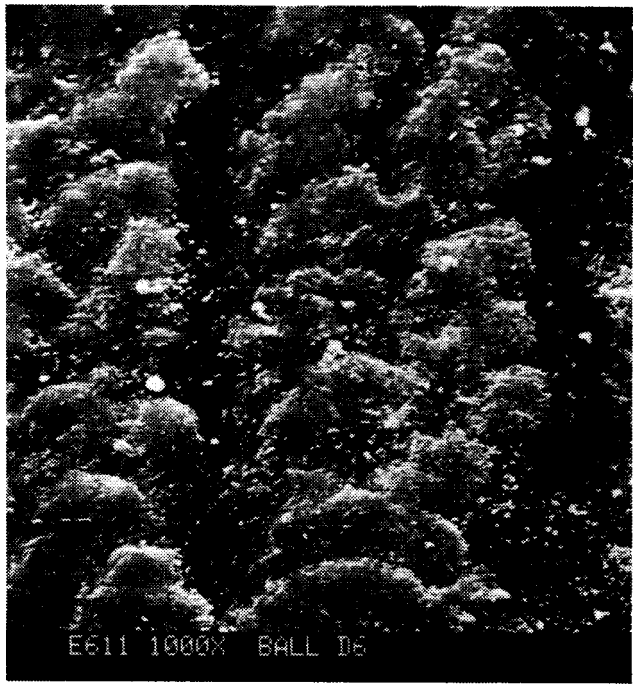

(b) Center of Contact

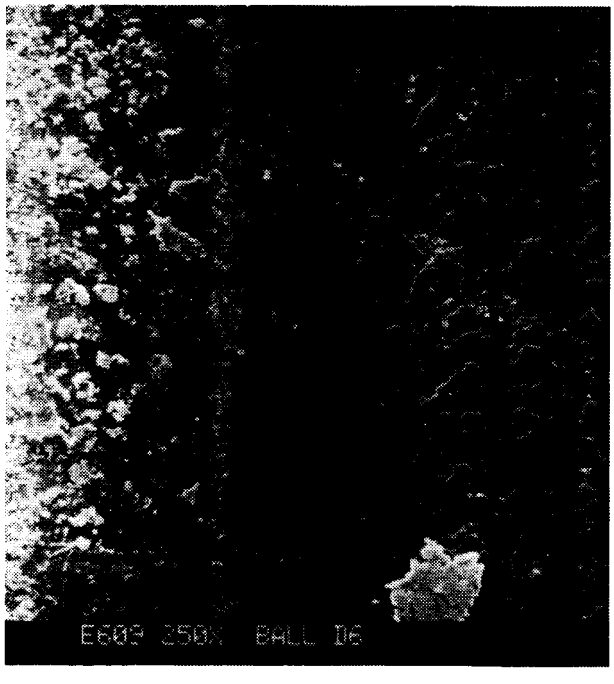

(c) Left Edge of Contact

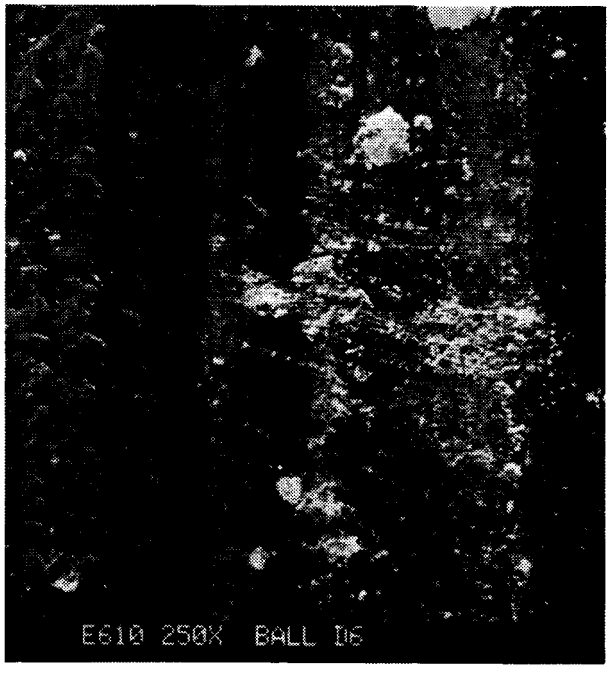

(d) Right Edge of Contact

Figure 4.11 Silicon Nitride Test Ball
P03Ag, T = 370°C
Contact Stress = 1723 MPa
Rolling Speed = 3.8 m/s

ksi), and a rolling speed of 3.8 m/s (150 in/s). The low magnification (25X) micrograph, Figure 4.10, shows the contact zone as a well defined white streak on the left most side of what appears to be a well polished surface. The polished appearance is the result of the graphite/silver filling the pores and pits of the original ball surface and being smoothed over by continued burnishing. Figure 4.10c is a medium magnification (250X) micrograph of the heavier white streak to the right of the contact region. Here we clearly see a heavy deposit of lubricant which is verified by the silver (Ag) map of Figure 4.10d. The measured traction coefficient of 0.43 could be a reflection of this type of deposit behavior.

Test #6 which was run with the same temperature and speed but at a contact stress of 1723 MPa (250 ksi) had the same measured traction coefficient (0.43) but very different in appearance, as shown in Figure 4.11. At low magnification (Figure 4.11a) we see that the surface areas alongside of the contact zone do not have the same polished appearance as did the test ball of Figure 4.10. There are still zones of heavy lubricant deposit, however, high magnification examination (Figures 4.11c and d) shows a lack of lubricant deposits and a bumpy and rutted surface.

The inconsistent nature of the results can be seen in the results and photomicrographs of test #17. Here the temperature

was the same 370°C (700°F) but the contact stress and rolling speed were higher, 2068 MPa (300 ksi) and 6.35 m/s (250 in/s), respectively. The measured traction coefficient was 0.26. Despite the low measured traction level the photomicrographs (Figure 4.12) show a discontinuous lubricant film and evidence of wear damage in the contact zone. The high magnification picture (1000X) indicates a high degree of plastic deformation in the center of the contact zone.

The PO3Ag tests conducted at 540°C (1000°F) consistently provided low traction values, 0.07 to 0.19. This may be attributed to high temperature behavior of the lubricant during burnishing. The PO3Ag burnished by leaving heavy streaked deposits of lubricant that were high in silver content. Figures 4.13 to 4.15 illustrate this as well as the general behavior of the PO3Ag at 540°C (1000°F). Figure 4.13 shows the ball specimen of test #16 after a traction test at 540°C (1000°F), 1723 MPa (250 ksi) and 6.35 m/s (250 in/s). Low magnification (25X), Figure 4.13a shows a significant amount of lubricant burnished on the ball. A thin glossy layer appears to form in the track (Figure 4.13b) which provide good protection of the ball surface and a low maximum traction coefficient of 0.15.

The photomicrographs of Figures 4.13c and 4.13d show the unrun burnished areas on either side of the contact zone. Here

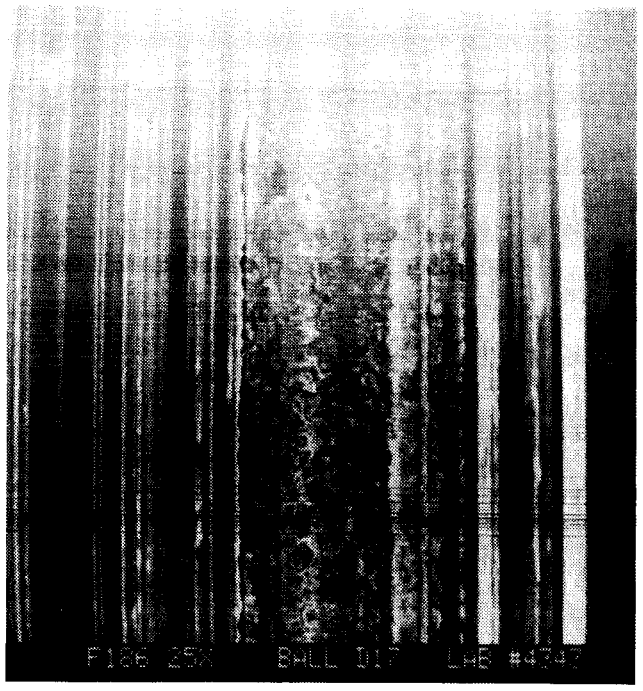

(a) Contact Track

(b) Center of Contact

(c) Left Edge of Contact

(d) Right Edge of Contact

Figure 4.12 Silicon Nitride Test Ball
P03Ag, T = 370°C
Contact Stress = 2068 MPa
Rolling Speed = 6.35 m/s

(a) Contact Track

(b) Center of Contact

(c) Left Edge of Contact

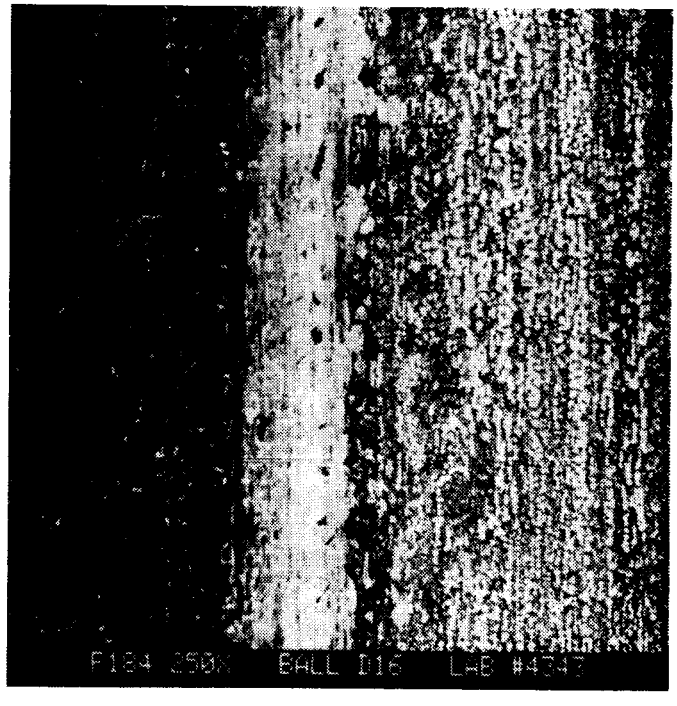

(d) Right Edge of Contact

Figure 4.13 Silicon Nitride Test Ball
P03Ag, T = 540°C
Contact Stress = 1723 MPa
Rolling Speed = 6.35 m/s

we see that the lubricant is deposited in the form of streaks of little nodules or spheres. As you look closer to the edge of the contact zone, it becomes apparent that the lubricant spheres have been plastically deformed and have flowed together giving a flatened and smeared appearance. This is evident in the photos of Figure 4.14 showing test ball #14. Here only the contact stress was changed to a lower, 1379 MPa (200 ksi) value. The same nodular streaks are apparent, however in this instance, the burnishing seems to have given a rutted or grooved appearance to the ball surface.

Some inconsistency did occur in the results of the PO3Ag, as evidenced by Figure 4.15. The figure shows the photomicrographs of test ball specimen #1 after running at 540°C (1000°F), contact stress of 1379 MPa (200 ksi) and a rolling speed of 3.8 m/s (150 in/s). Although providing a low traction value of 0.19, which is consistent with other results, the observed visual behavior is different. Figure 4.15a shows the burnished areas to be smooth and polished looking as opposed to the streaky appearance of the previous figures. Also the track area has a much more smeared and deformed appearance. Higher magnification (250X) of the track area (Figures 4.15c and 4.15d) indicate deformation and damage of the lubricant film and possibly the original ball surface. Figure 4.15b is a higher (1000X) magnification view of the

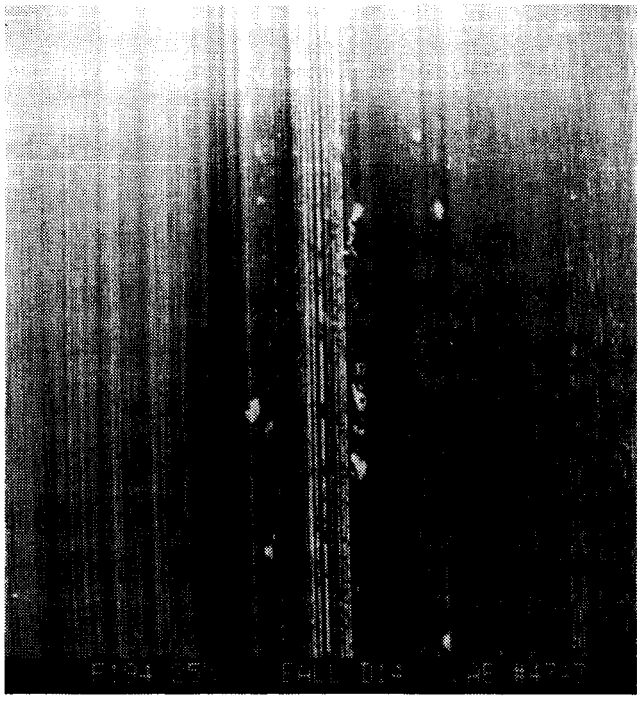

(a) Contact Track

(b) Center of Contact

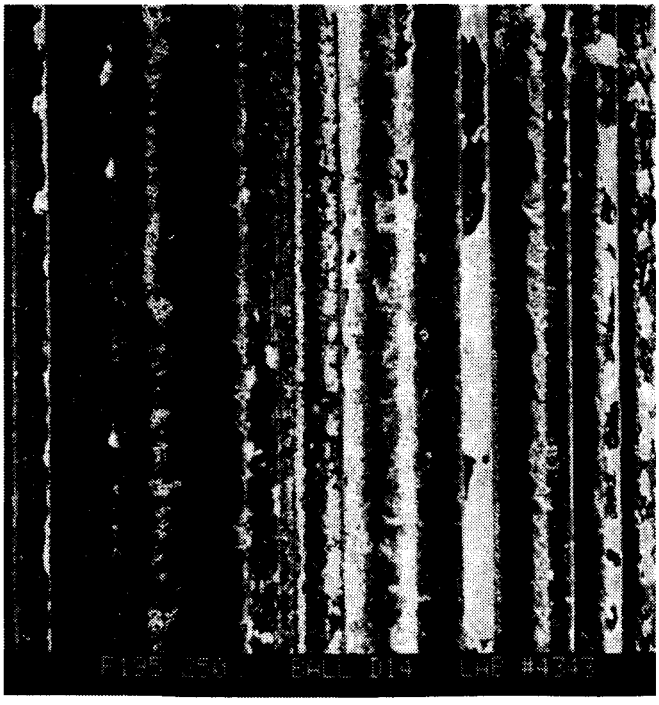

(c) Left Edge of Contact

(d) Right Edge of Contact

Figure 4.14 Silicon Nitride Test Ball
P03Ag, T = 540°C
Contact Stress = 1378 MPa
Rolling Speed = 6.35 m/s

(a) Contact Track

(b) Center of Contact

(c) Left Edge of Contact

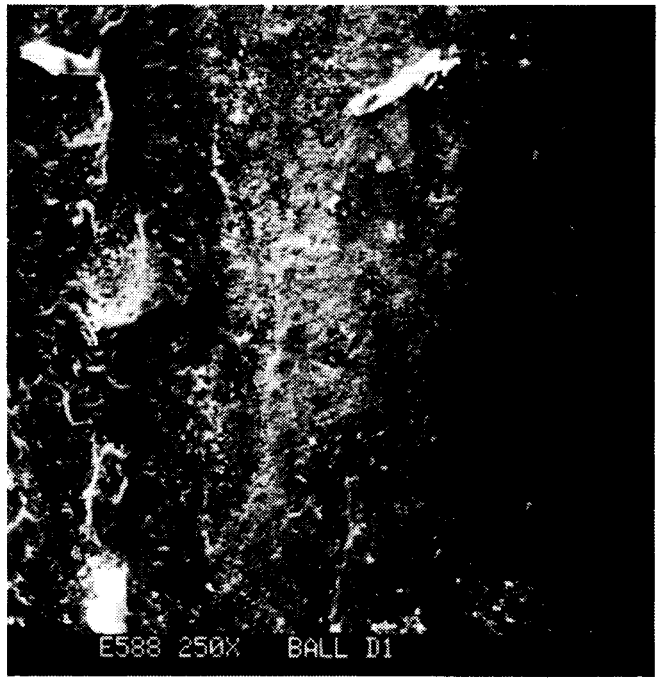

(d) Right Edge of Contact

Figure 4.15 Silicon Nitride Test Ball
P03Ag, T = 540°C
Contact Stress = 1378 MPa
Rolling Speed = 3.8 m/s

center of the track zone indicating a highly plastic behavior of the surface film. This photo suggests that the surface film may be the result of oxidation and partial melting of the lubricant.

4.2.3 P2003

The most inconsistent results were obtained with the P2003 lubricant. The traction coefficients measured ranged widely from a low of 0.16 to a high of 0.6 with the majority of the tests yielding coefficients that were higher than the other two graphite lubricants. The results showed a general trend of material removal and surface damage, especially at the lower, 370°C (700°F), temperature. These results seem contradictory to results reported from tests where P2003 material was used as a "self-lubricating" cage material [5,6].

The results are demonstrated in the photomicrographs of Figures 4.16 to 4.20. Figures 4.16 and 4.17 demonstrate the general appearance of the P2003 test balls. The figures present test balls #9 and #11, respectively. Both tests were run at a temperature of 370°C (700°F) and speed of 3.8 m/s (150 in/s). Test #9 had a contact stress of 1279 MPa (200 ksi) while test #11 had a contact stress of 2068 MPa (300 ksi). Both sets of micrographs depict a ball surface with a very wide wear track and the loss of a significant amount of material during the short

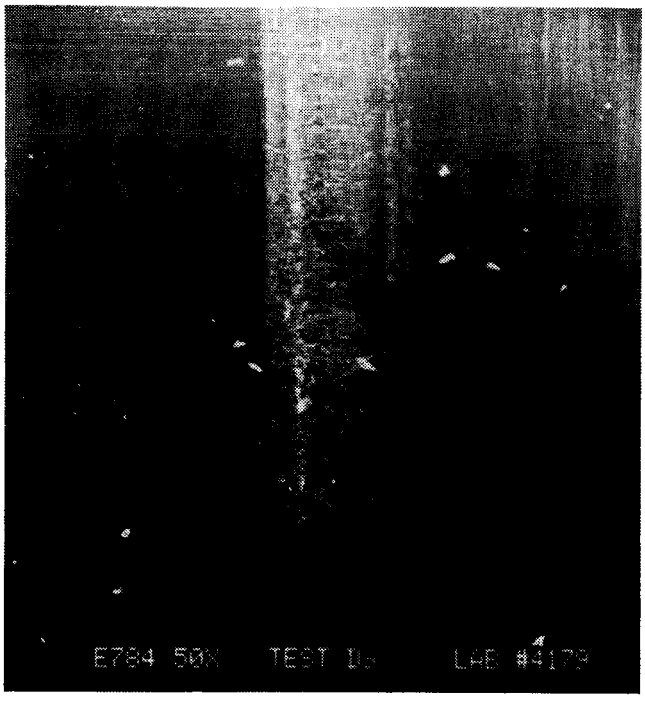

(a) Contact Track

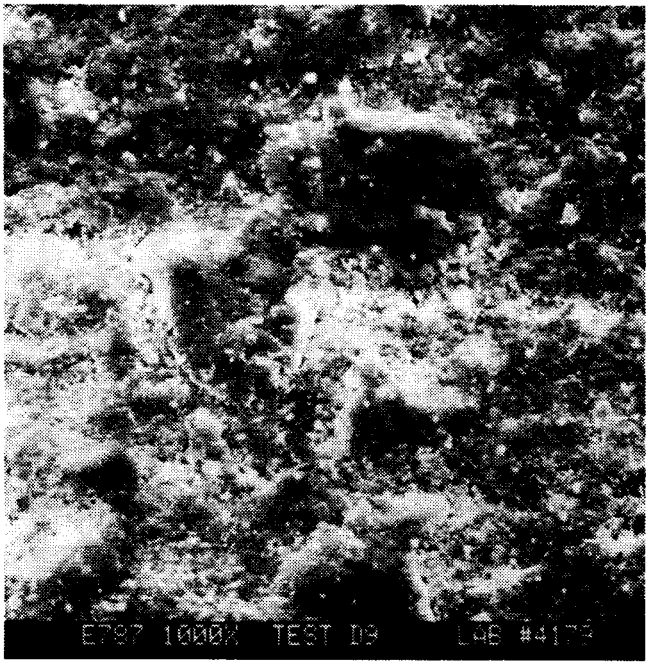

(b) Center of Contact

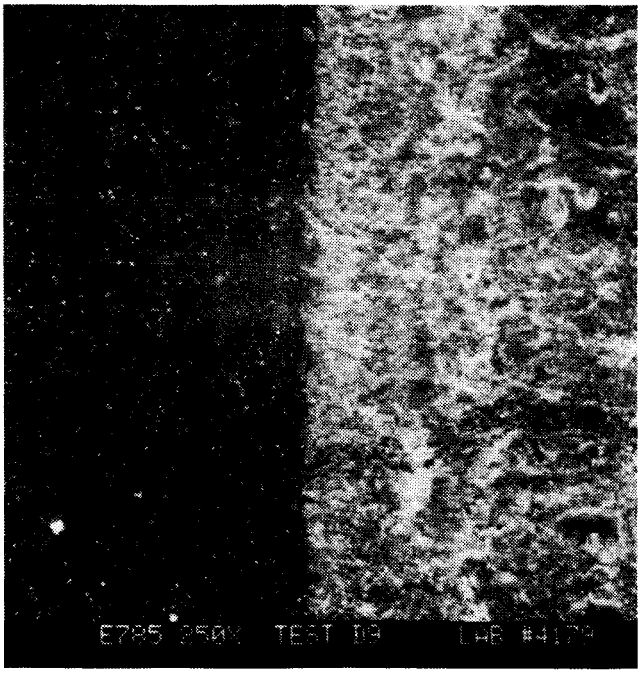

(c) Left Edge of Contact

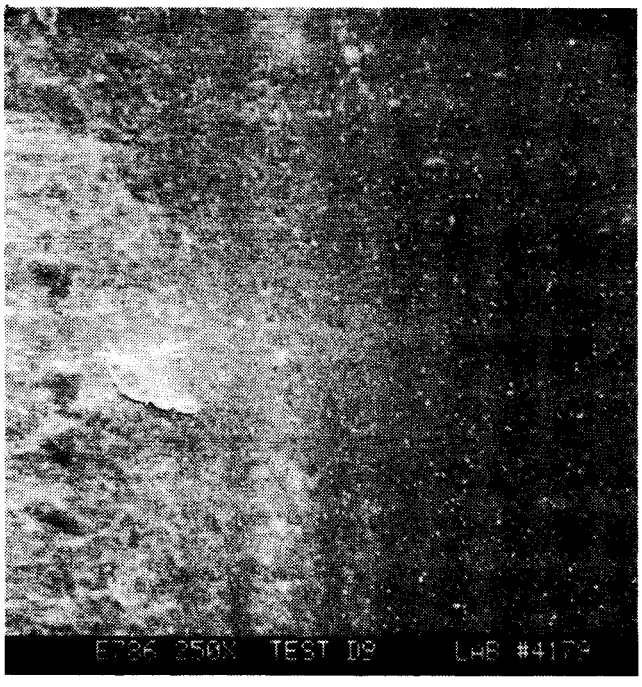

(d) Right Edge of Contact

Figure 4.16 Silicon Nitride Test Ball
P2003, T = 370°C
Contact Stress = 1723 MPa
Rolling Speed = 3.8 m/s

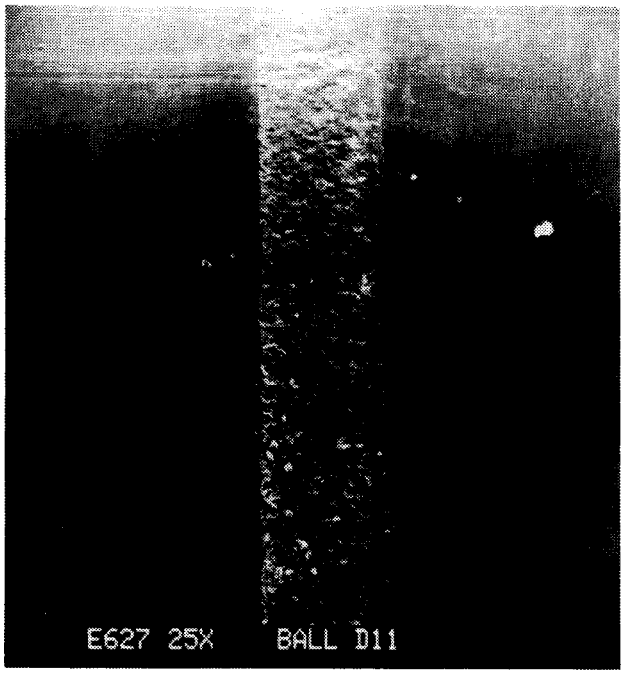

(a) Contact Track

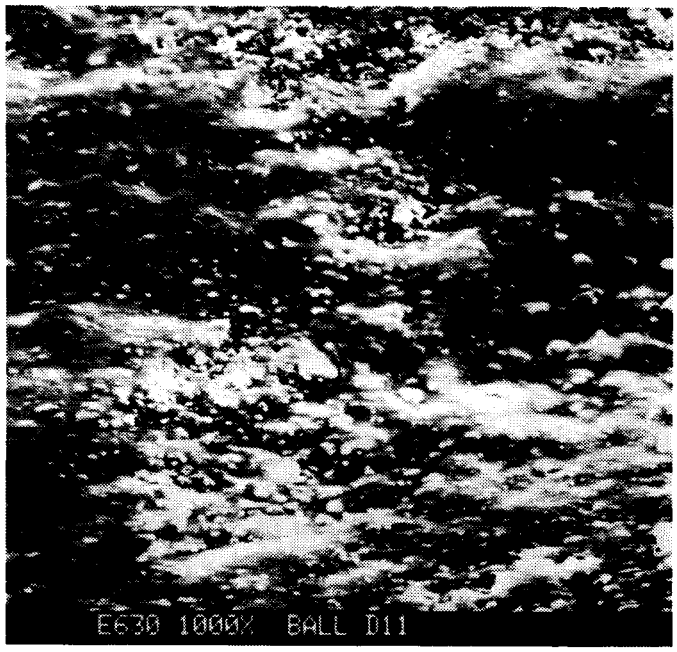

(b) Center of Contact

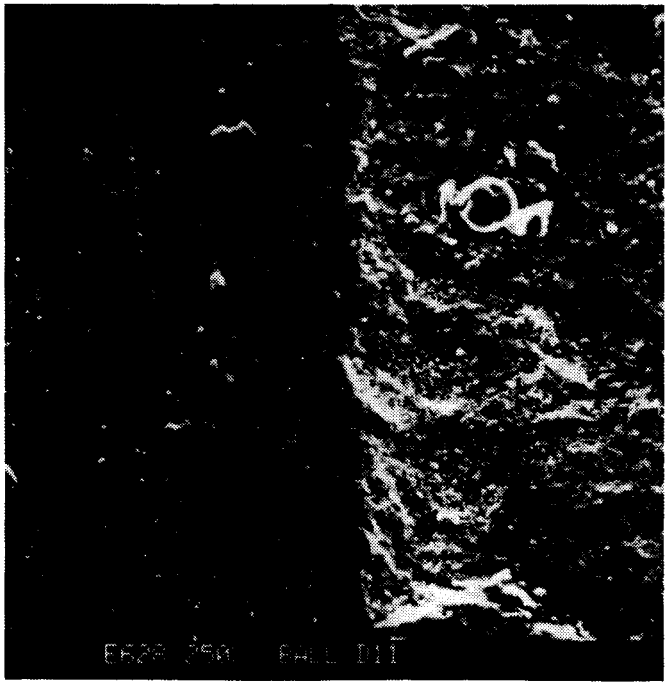

(c) Left Edge of Contact

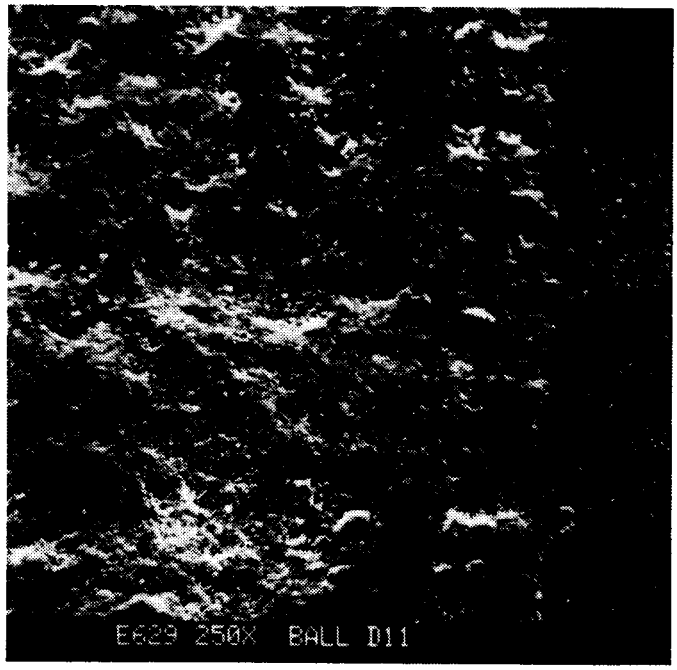

(d) Right Edge of Contact

Figure 4.17 Silicon Nitride Test Ball
P2003, T = 370°C
Contact Stress = 2068 MPa
Rolling Speed = 3.8 m/s

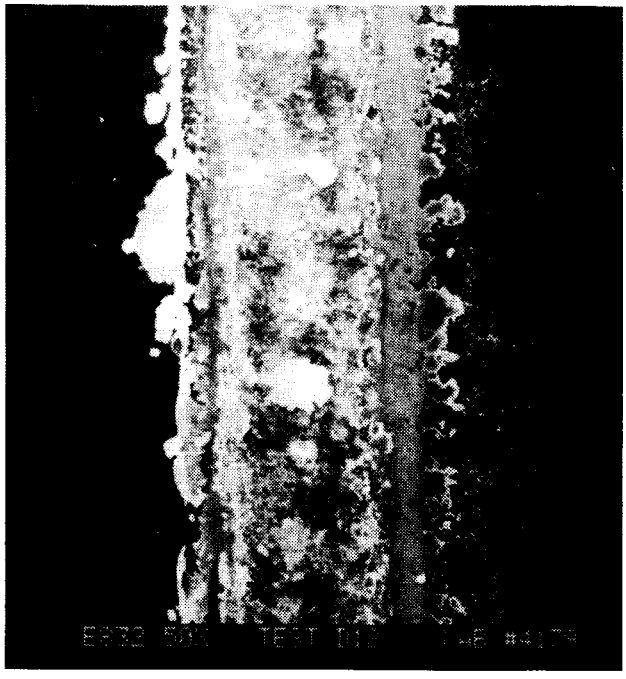

(a) Contact Track

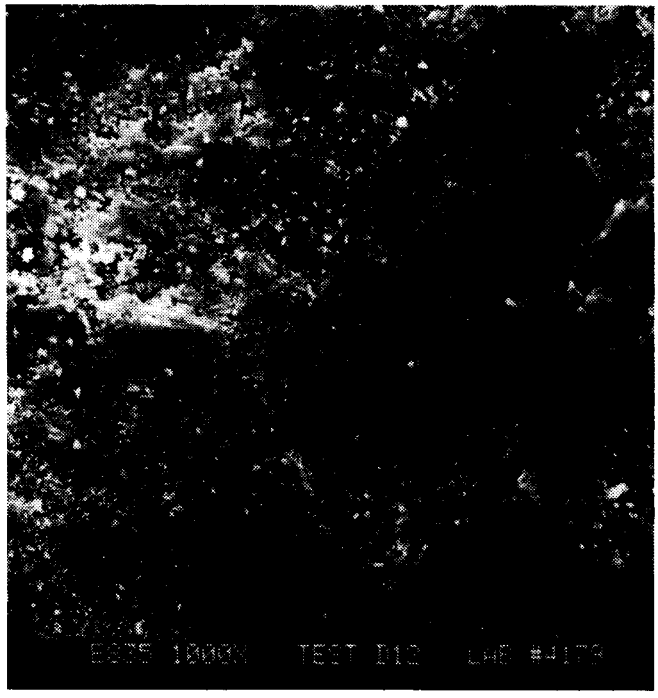

(b) Center of Contact

(c) Left Edge of Contact

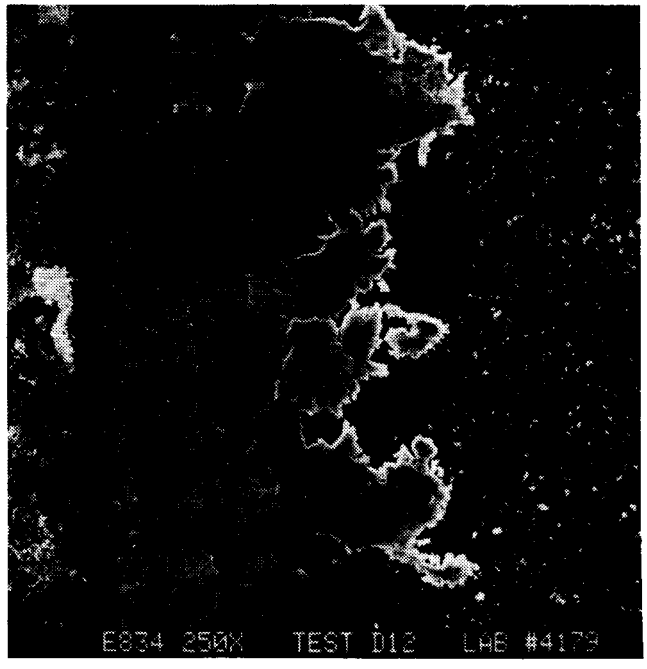

(d) Right Edge of Contact

Figure 4.18 Silicon Nitride Test Ball
P2003, T = 540°C
Contact Stress = 2068 MPa
Rolling Speed = 3.8 m/s

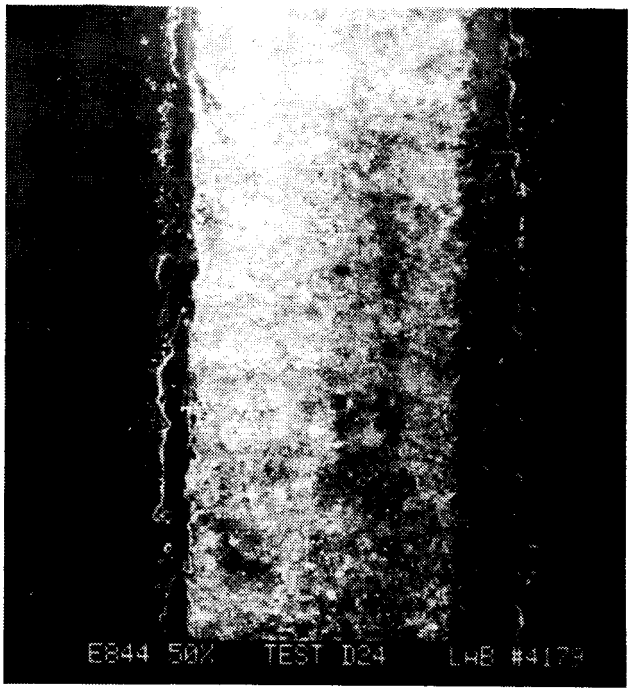

(a) Contact Track

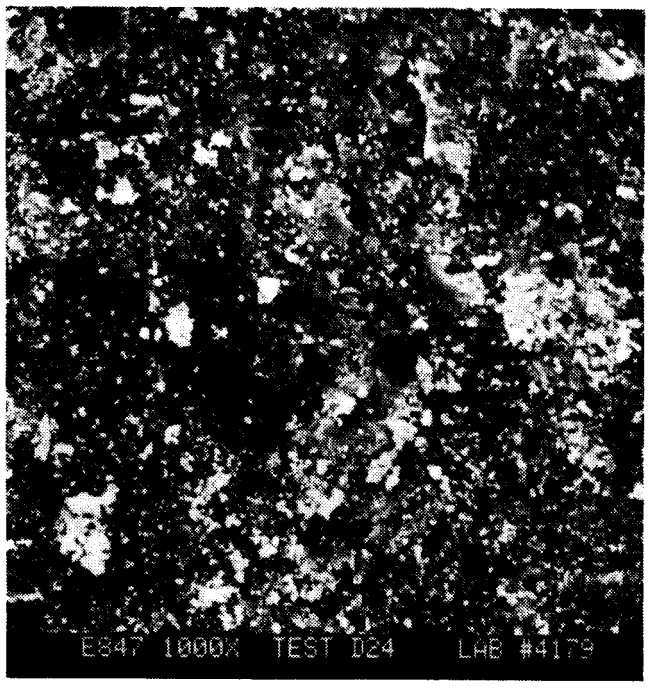

(b) Center of Contact

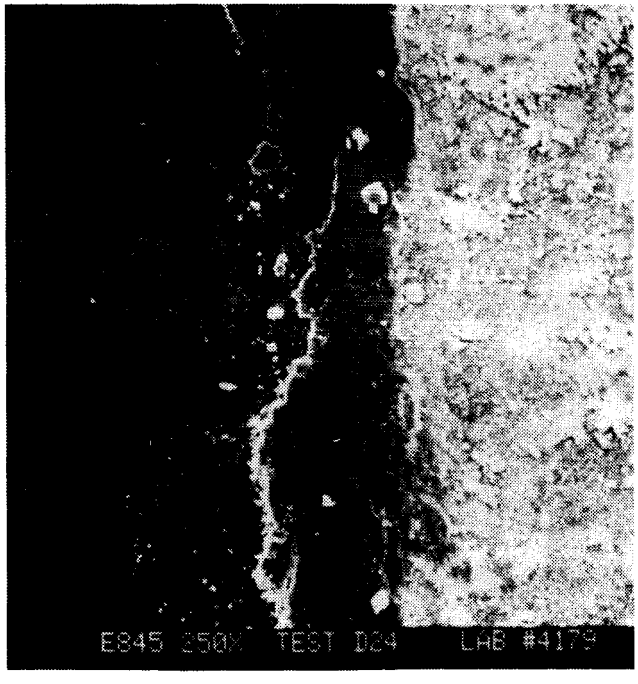

(c) Left Edge of Contact

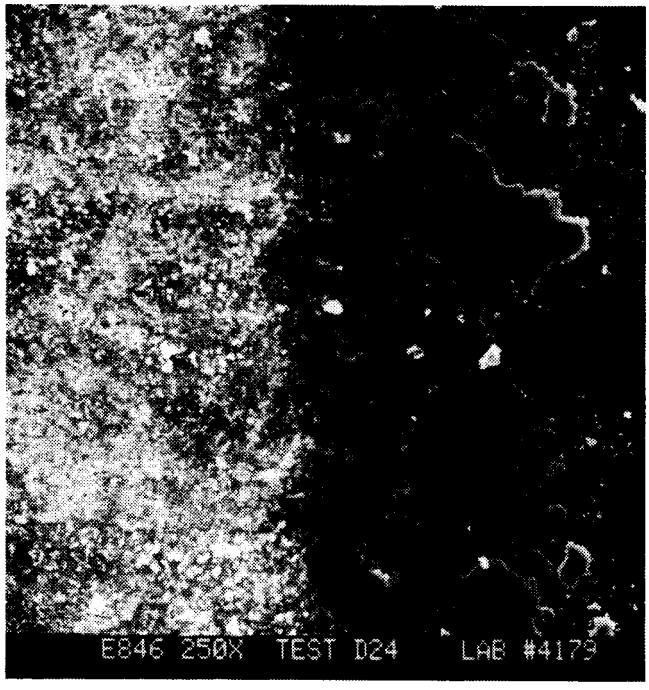

(d) Right Edge of Contact

Figure 4.19 Silicon Nitride Test Ball
P2003, T = 540°C
Contact Stress = 2068 MPa
Rolling Speed = 6.35 m/s

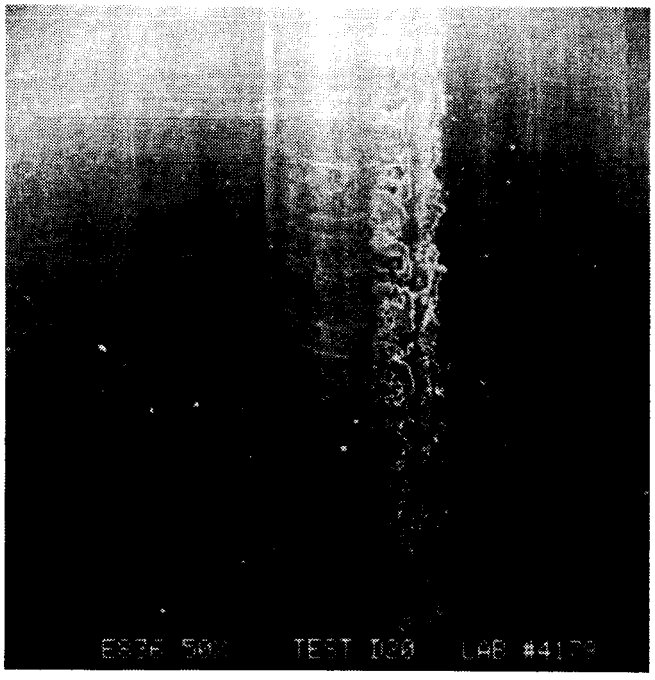

(a) Contact Track

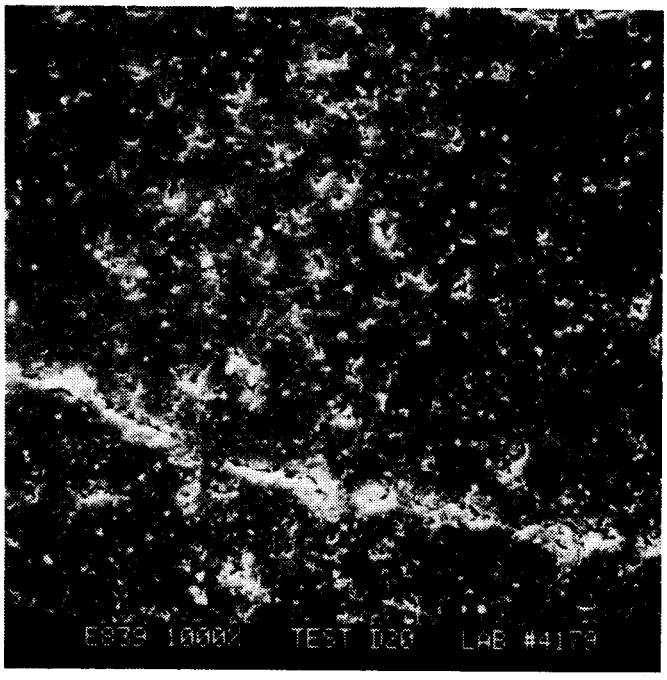

(b) Center of Contact

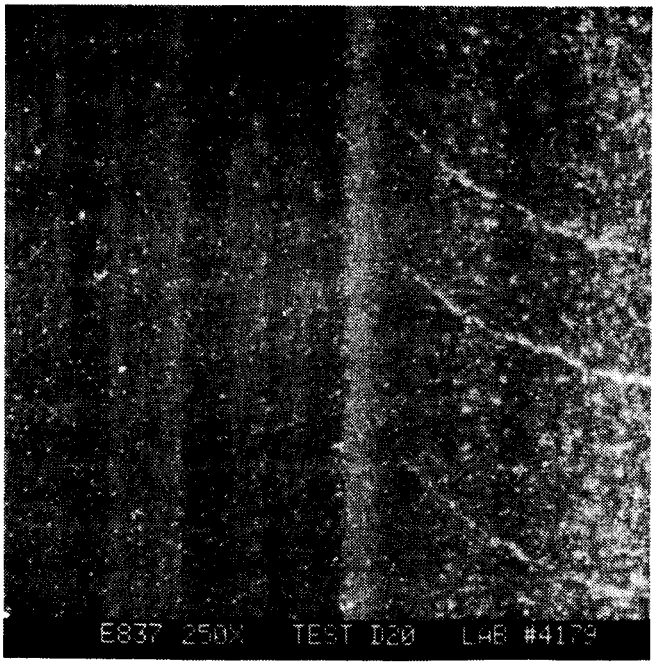

(c) Left Edge of Contact

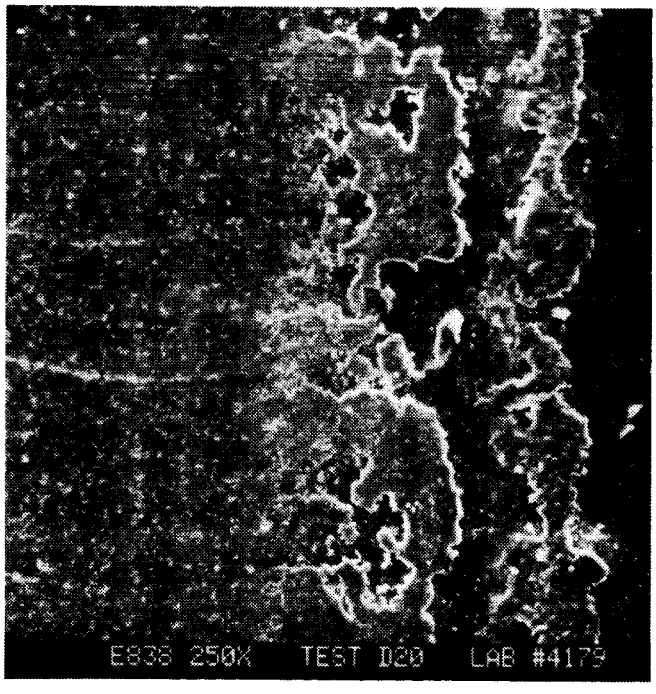

(d) Right Edge of Contact

Figure 4.20 Silicon Nitride Test Ball
P2003, T = 540°C
Contact Stress = 1378 MPa
Rolling Speed = 6.35 m/s

duration of the test. Figure 4.17b (1000X) suggests that some oxidation of the ball surface may have occurred. The measured maximum traction coefficient for these tests were 0.53 and 0.34, respectively.

Figure 4.18 presents the photomicrographs for test ball #12, which provided the lowest recorded traction coefficient for P2003, 0.16. The test conditions were a temperature of 540°C (1000°F), a contact stress of 2068 MPa (300 ksi), and a rolling speed of 3.8 m/s (150 in/s). It is obvious from the photos of Figure 4.18, that the success (low traction) of this particular test resulted from the extensive plastic flow and deformation of the surface film, in the areas along the edges of the contact zone. Figure 4.18c indicates that the P2003, in this test, formed its surface film in a nodular, streaky fashion similar to the more successful PO3Ag tests. However, the high magnification (1000X) view of Figure 4.18b, indicates that in the center of the contact zone wear protection was not at an acceptable level, as evidenced by the loss of material.

The same plastic behavior at the contact zone edges, but poor wear protection in the center of the contact zone is evident in the photomicrographs of test ball #24, Figure 4.19. However, the measured traction coefficient of this test was 0.39. Here the test conditions were identical to that of test #12 with the exception of a higher rolling speed of 6.35 m/s (250 in/s).

Figure 4.20 presents the photomicrographs for test ball #20. Under test conditions of a chamber temperature of 540°C (1000°F), contact stress of 1378 MPa (200 ksi) and a rolling speed of 6.35 m/s (250 in/s), the P2003 provided little or no protection and resulted in an extremely high measured traction coefficient of 0.55. Examination of the photos of Figure 4.20 reveals the presence of transverse cracks at random intervals that run across the contact zone perpendicular to the direction of rolling. Cracks like these can be the result of high surface tensile stresses, which occur in a situation where normal forces in a Hertzian contact zone combine with high traction. Low friction is essential for preserving surface integrity as well as energy conservation.

Macro stresses are really the integration of normal and tangential micro stresses distributed within the contact region. These local stresses may be many times greater than the macro stresses and can arise from local surface depressions or pits (Figure 4.20b) or surface asperities. The high surface tensions around these depressions causes micro cracks which progress from pit to pit giving rise to the macro cracks evident in Figure 4.20a.

4.3 "ARMOLOY" Coated M50 Steel

Armoloy is a special process chromium electrodeposit that has demonstrated significant potential for use in rolling contact bearing applications [7]. This coating is free from the surface cracks that characterize conventional hard chromium electrodeposits, providing for enhanced corrosion resistance. A coefficient of friction value of 0.16 is claimed by the Armoloy Corporation for uncoated steel against coated steel. A maximum coating thickness of 5 μm (200 μinch) is specified by the Armoloy Corporation.

The Armoloy coated M50 disks were tested for its effectiveness as a low friction adjunct to the solid lubricants. The test matrix used for these tests is shown in Table 4.3. Traction force vs. slide/roll ratio curves were generated for all 19 tests. The results of the traction tests are presented in Table 4.4. As can be seen, the traction values measured varied widely from a low of 0.21 to a high of 0.52.

In general the results indicate that the combination of a silicon nitride ball run on an Armoloy surface is not a compatible situation. The presence of lubricant did not seem to improve the situation.

The photomicrographs of Figure 4.21 illustrate the typical behavior. Test ball #43 is shown in this figure. The test con-

Table 4.3 Armoloy Coated M50 Steel Disk Test Matrix

LUBRICANT	AVERAGE SURFACE SPEEDS (IPS)	TEMPERATURE					
		400 °F MAXIMUM HERTZ CONTACT STRESS (KSI)			600 °F MAXIMUM HERTZ CONTACT STRESS (KSI)		
		200	250	300	200	250	300
NONE	250	-	D38	D43	-	D48	D53
P3310	250	-	D39	D44	-	D49	D54
P03Ag	250	-	D41	D46	-	D51	D56
P2003	250	-	D40	D45	-	D50	D55

All tests Si_3N_4 ball on Armoloy/M50 disk

Table 4.4 Measured Test Results for Armoloy Coated M50 Steel

Test Number	Ball Material	Disc Material	Lubricant	Temperature	Stress	Speed	Max Traction	Max Coefficient
37	M50	M50 ARMOLOY	NONE	400		250	7.2	0.43
38	SILICON NITRIDE	M50 ARMOLOY	NONE	400	250	250	7.7	0.30
39	SILICON NITRIDE	M50 ARMOLOY	P3310	400	250	250	10.1	0.39
40	SILICON NITRIDE	M50 ARMOLOY	P2003	400	250	250	10.0	0.39
41	SILICON NITRIDE	M50 ARMOLOY	P03AG	400	250	250	11.1	0.44
42	M50	M50 ARMOLOY	NONE	400	300	250	33.8	0.52
43	SILICON NITRIDE	M50 ARMOLOY	NONE	400	300	250	26.3	0.42
44	SILICON NITRIDE	M50 ARMOLOY	P3310	400	300	250	19.6	0.31
45	SILICON NITRIDE	M50 ARMOLOY	P2003	400	300	250	19.5	0.31
46	SILICON NITRIDE	M50 ARMOLOY	P03AG	400	300	250	25.0	0.39
47	M50	M50 ARMOLOY	NONE	600	250	250	7.8	0.21
48	SILICON NITRIDE	M50 ARMOLOY	NONE	600	250	250	13.1	0.51
49	SILICON NITRIDE	M50 ARMOLOY	P3310	600	250	250	11.6	0.45
51	SILICON NITRIDE	M50 ARMOLOY	P03AG	600	250	250	5.5	0.22
52	M50	M50 ARMOLOY	NONE	600	300	250	21.6	0.33
53	SILICON NITRIDE	M50 ARMOLOY	NONE	600	300	250	24.8	0.39
54	SILICON NITRIDE	M50 ARMOLOY	P3310	600	300	250	13.3	0.52
55	SILICON NITRIDE	M50 ARMOLOY	P2003	600	300	250	15.1	0.24
56	SILICON NITRIDE	M50 ARMOLOY	P03AG	600	300	250	17.9	0.28

Temperature in ^{o}F
Stress in ksi
Speed in in/s
Traction in lb.

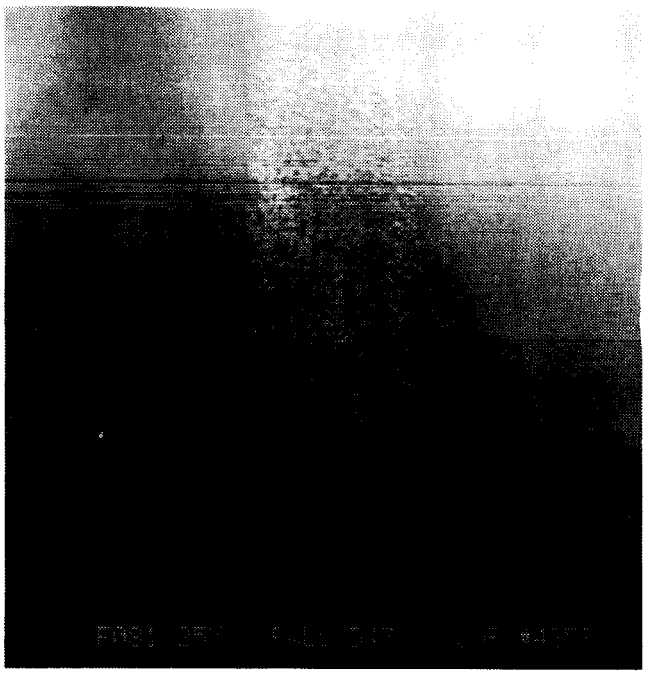

(a) Contact Track

(b) Center of Contact

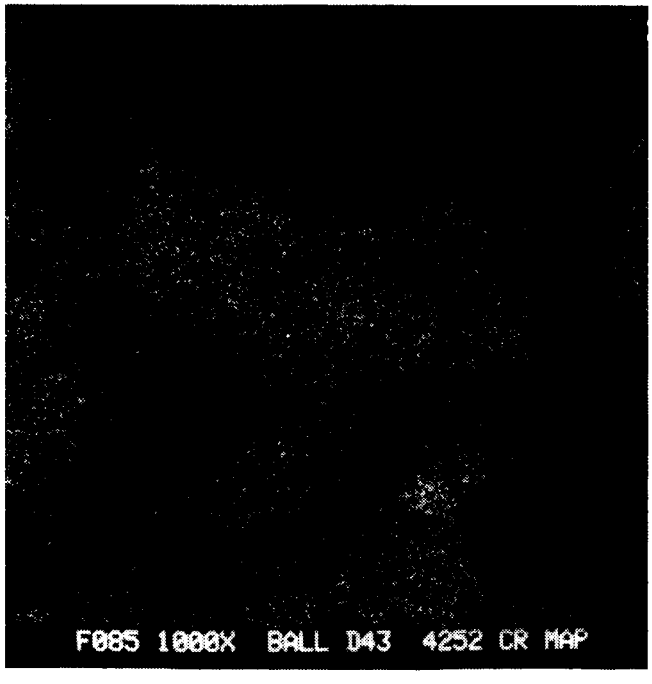

(c) Chrome Map of Center

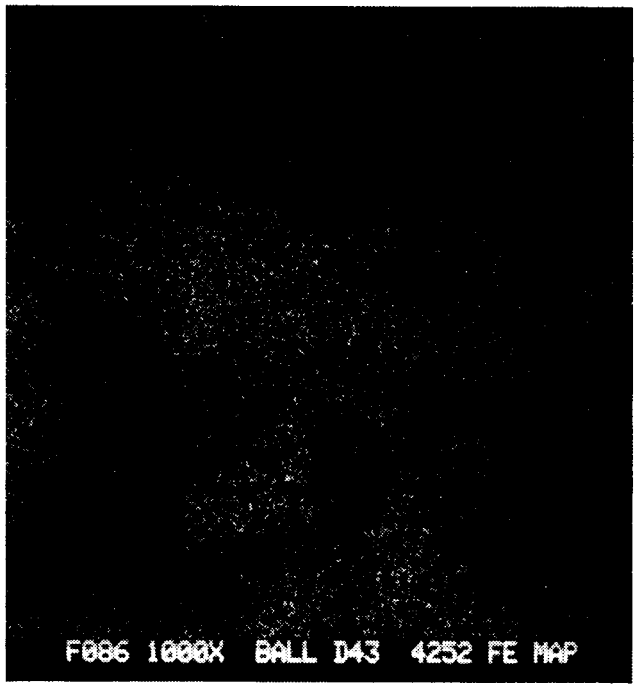

(d) Iron Map of Center

Figure 4.21 Silicon Nitride Test Ball
Armoloy, T = 200°C
Contact Stress = 2068 MPa
Rolling Speed = 6.35 m/s

ditions were a temperature of 200°C (400°F), a contact stress of 2068 MPa (300 ksi) and a rolling speed of 6.35 m/s (250 in/s). No lubricant was used in this test. The measured maximum traction coefficient was 0.42. Even in the short amount of time of the test (~2 minutes) there appears to be evidence of ball surface damage (Figure 4.21a). At higher magnification (1000X) there also appears to be material deposited in the contact zone (Figure 4.21b). Subsequent X-ray dispersion examination (EDAX) revealed the deposits to be iron (Fe) and chrome (Cr), the two major constituents of the Armoloy coating and the disk. This would indicate that in a short time the integrity of the coating was destroyed.

Test #49 (Figure 4.22) run at 315°C (600°F) and with the aid of P3310 lubricant (the best performing graphite) provided no better results. The measured traction coefficient was 0.45 and there was also considerable chrome and iron pick up on the ball (Figures 4.22a to 4.22d).

The disk surface appeared typically as illustrated by Figures 4.23a to 4.23d. These are progressively higher magnification of the contact zone on the disk of test #46, as well as low magnification of the test ball. The ball (Figure 4.23d) shows itself to be very similar in appearance to the ball of Figure 4.22a. That is the appearance of streaks of deposited material across the

(a) Contact Track

(b) Center of Contact

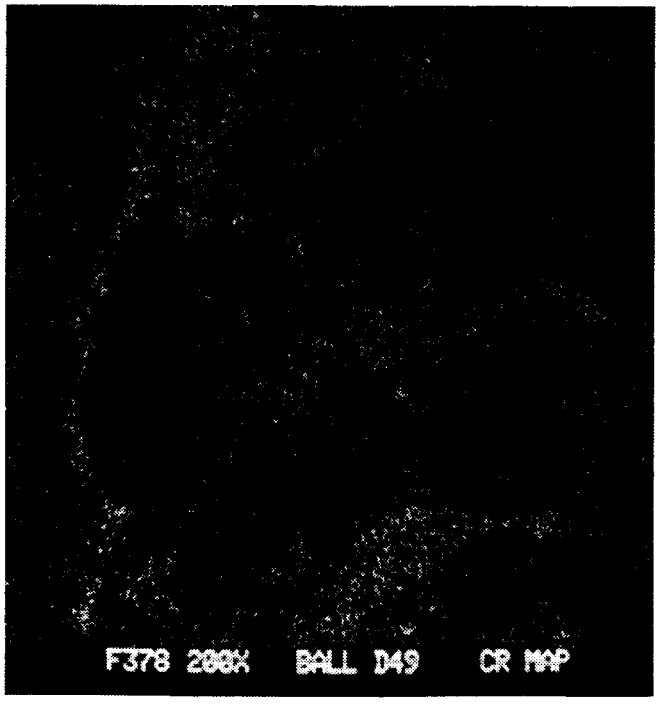

(c) Chrome Map of Center

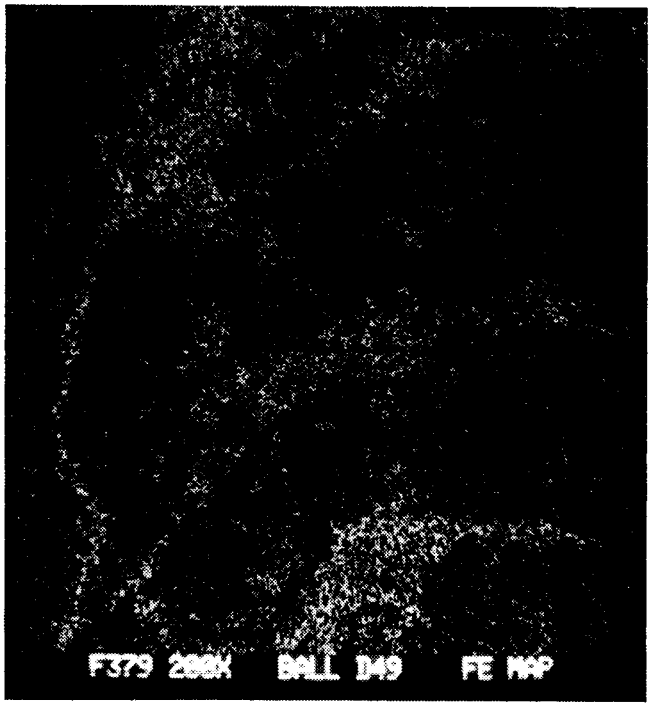

(d) Iron Map of Center

Figure 4.22 Silicon Nitride Test Ball
Armoloy - P3310, T = 315°C
Contact Stress = 1723 MPa
Rolling Speed = 6.35 m/s

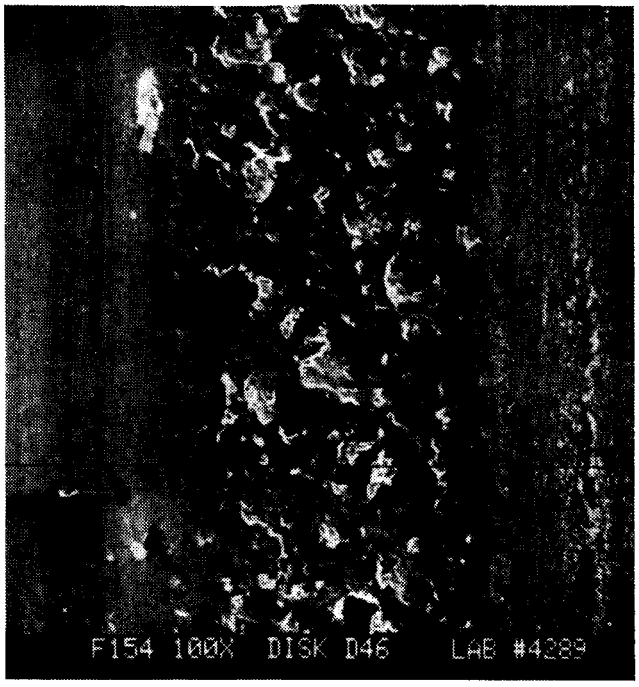

(a) Disk Contact Track

(b) Center of Contact

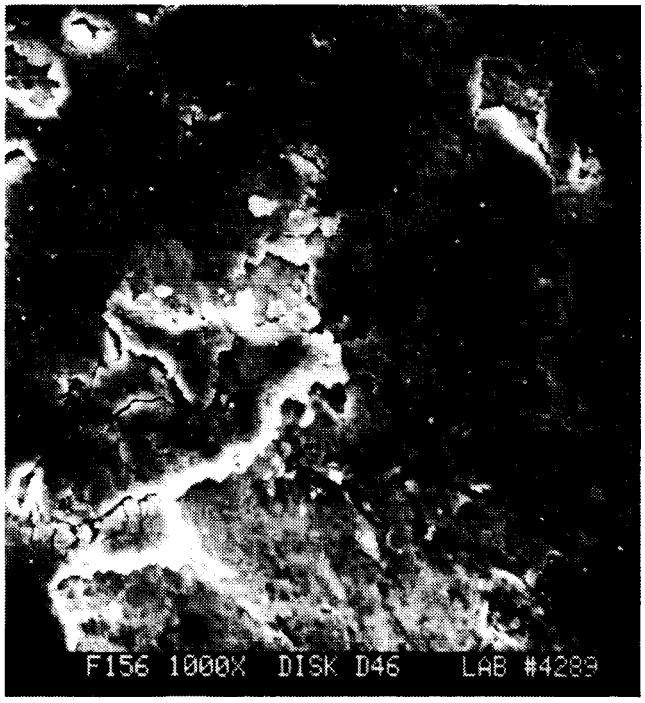

(c) Center of Contact

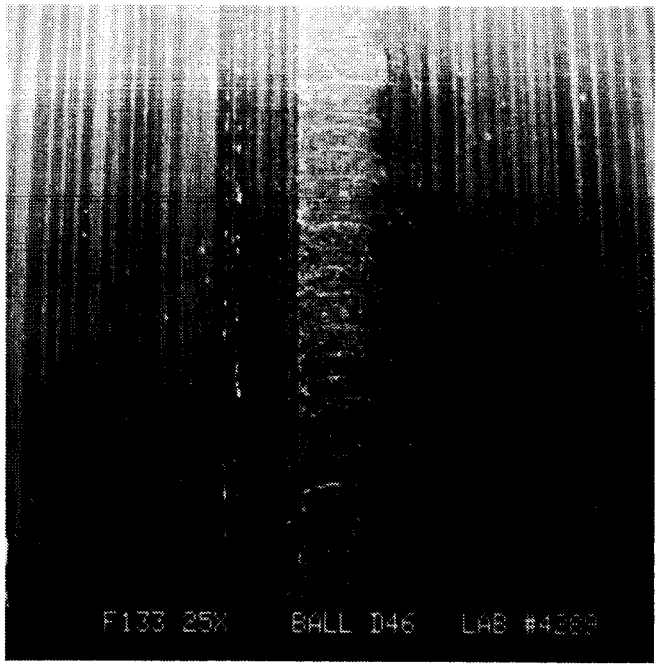

(d) Ball Contact Track

Figure 4.23 Test Specimens Si_3N_4/Armoloy/P03Ag
T = 200°C
Contact Stress = 2068 MPa
Rolling Speed = 6.35 m/s

contact zone. Figures 4.23a to 4.23c show the damaged disk surface. The contact zone is characterized by material removed resulting pits or craters which in turn have had their edges smeared over by the motion of the ball.

Figure 4.24 presents the photomicrographs of test #51 which was the only test with both a reasonable traction level and some wear protection. The lubricant was silver filled graphite (PO3Ag). The temperature was 315°C (600°F) and may have been high enough for the PO3Ag to behave as demonstrated previously. The measured traction coefficient was 0.22 and examination of the photos reveals some wear protection of the disk surface.

4.4 Titanium Nitride Coated M50 Steel

A series of five (5) tests were run to investigate the performance of a titanium nitride (TiN) coated M50 disk. Thin coatings of TiN (3 to 5 μm) deposited by a physical vapor deposition (PVD) technique have been reported to increase the life of cutting tools as much as 20 times [8]. PVD TiN coatings offer tremendous potential for friction, wear and corrosion control in rolling bearings. Applicability to bearing materials such as AISI M50 steel without inducing metallurgical damage makes it a prime candidate for evaluation in friction and wear programs.

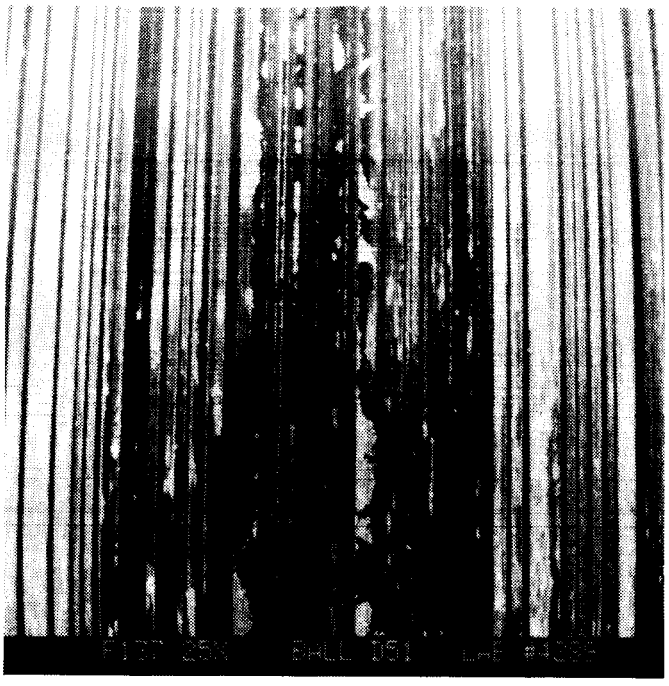

(a) Ball Contact Track

(b) Center of Ball Contact

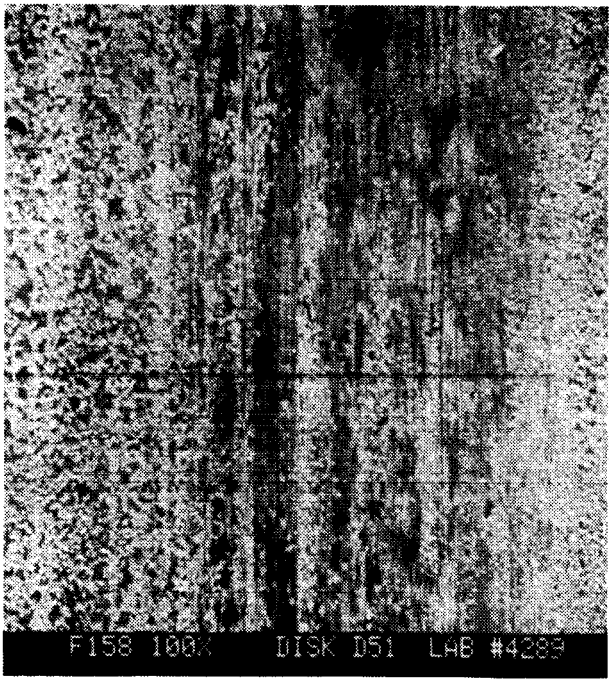

(c) Disk Contact Track

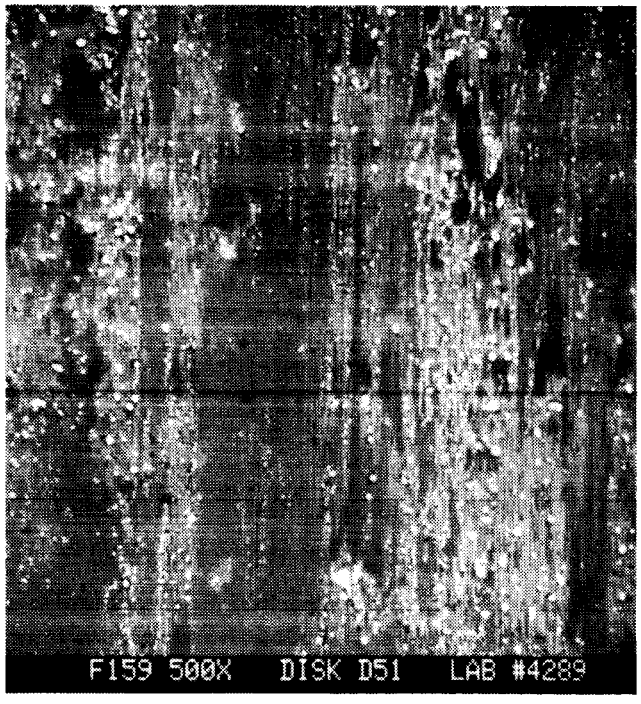

(d) Center of Disk Contact

Figure 4.24 Test Specimens Si_3N_4/Armoloy/P03Ag
T = 315°C
Contact Stress = 1723 MPa
Rolling Speed = 6.35 m/s

All the tests involving the TiN coated disk were run at room temperature and with M50 steel ball specimens. The rolling speed was the same for all five tests at 3.8 m/s (150 in/s). There were, however, 3 tests run dry or without the presence of any lubricant and 2 tests with oil lubrication. A table showing the five tests and their running conditions is included as Table 4.5.

The three unlubricated tests provided similar results but surprisingly high traction, 0.42 to 0.56. However, these very cursory tests do not provide enough data to issue any factual judgement on the frictional characteristics of the coated disk.

Figure 4.25 illustrates the typical appearance of the test ball specimens after the traction test. Figure 4.25 is for test #57 which was run at a contact stress of 1379 MPa (200 ksi). Ball wear was negligible as can be seen in Figure 4.25a, however, there is evidence of material transfer to the ball. Upon further examination and EDAX evaluation (Figures 4.25c and 4.25d) it was determined that the material is largely titanium (Ti) which would indicate removal of coating material from the disk. Figure 4.25b is a 1000X magnification micrograph of the unrun ball surface.

Even at the higher contact stress of 1723 MPa (250 ksi) the results appear the same (Figure 4.26). Perhaps the most interesting result about these tests revolves around the disk.

Table 4.5 Test Results for TiN Coated M50 Steel Disk

TEST NO.	BALL MATERIAL	DISK MATERIAL	STRESS	SPEED	MAX TRACTION	COEFFICIENT	LUBRICANT
D57	M50	TiN/M50	200	150			NONE
D58	M50	TiN/M50	300	150	35.6	0.51	NONE
D59	M50	TiN/M50	250	150	16.9	0.42	NONE
D60	M50	TiN/M50	250	150	-	-	OIL
D61	M50	TiN/M50	250	150	-	-	OIL

All Tests at Room Temperature
Stress in ksi
Speed in in/s
Traction in lb.

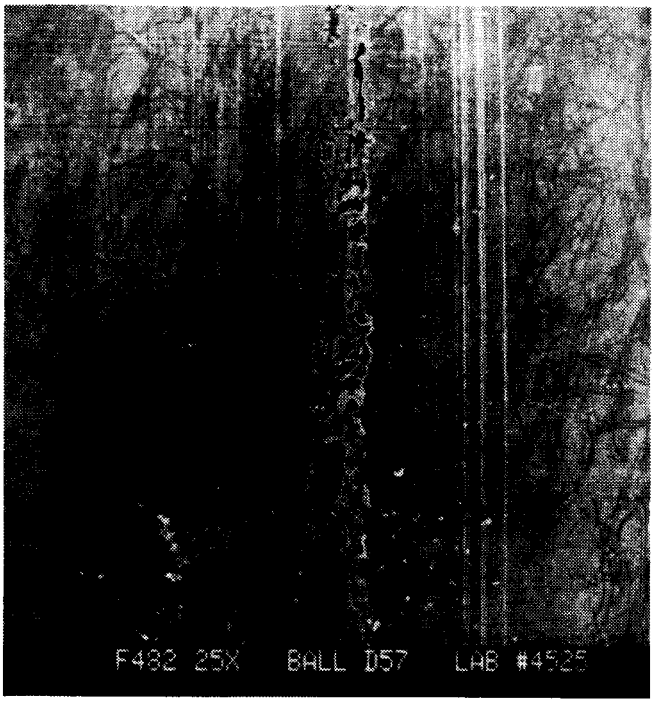

(a) Contact Track

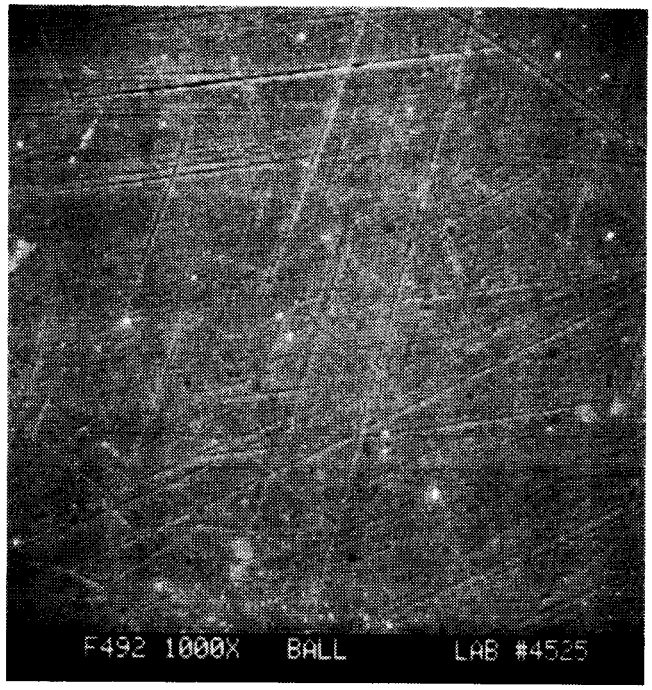

(b) Unrun M50 Ball Surface

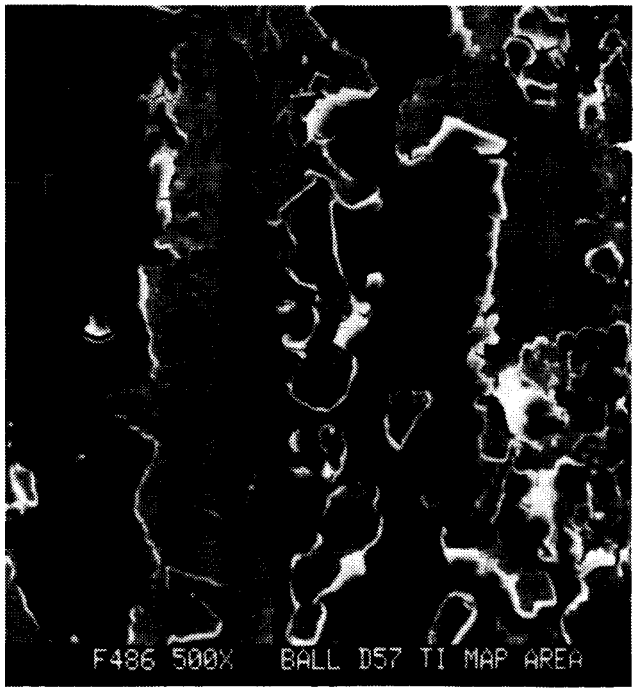

(c) Center of Contact

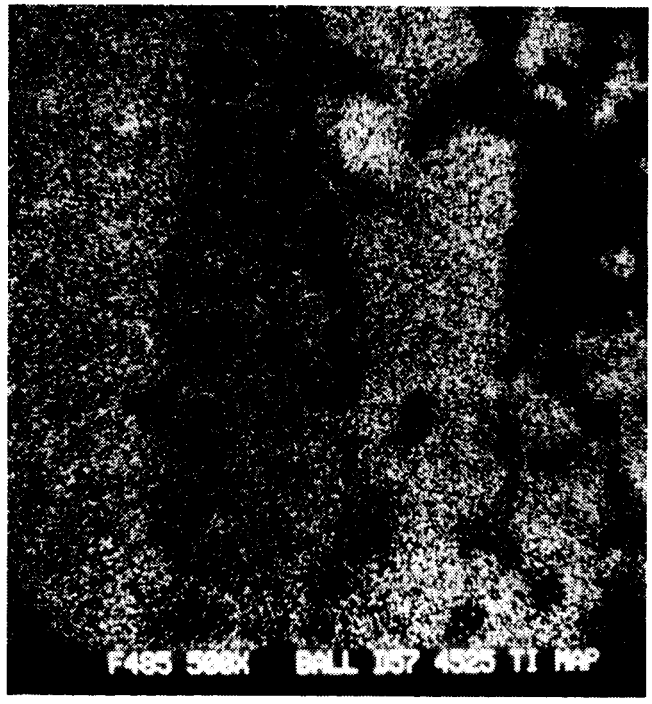

(d) Titanium Map of Center

Figure 4.25 M50 Test Ball
TiN Coated Disk
Room Temperature
Contact Stress = 1378 MPa

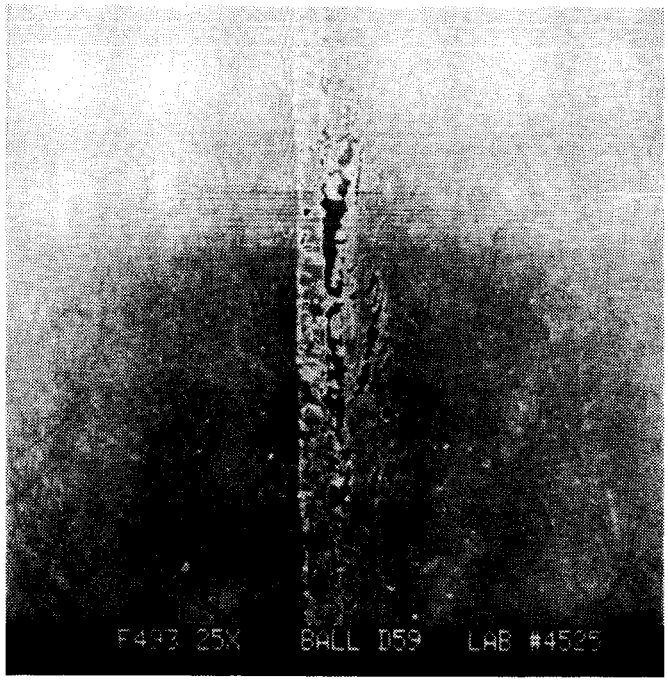

(a) Contact Track

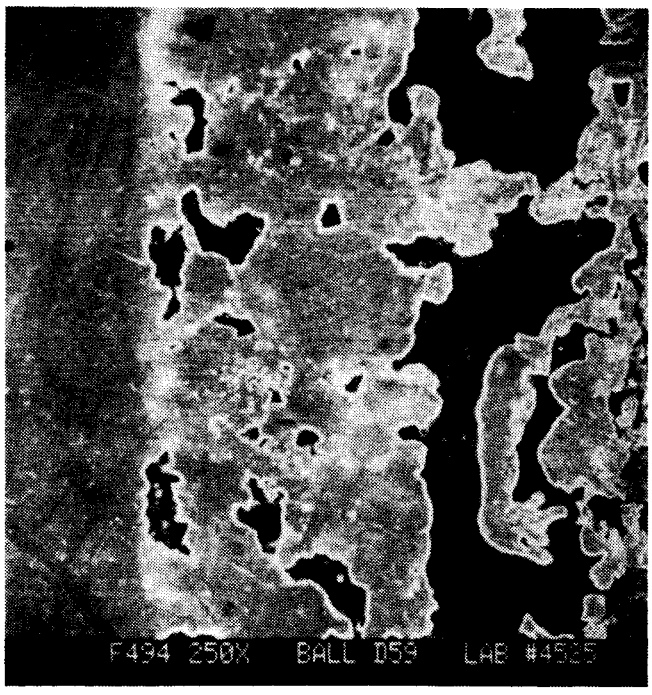

(b) Left Edge of Contact

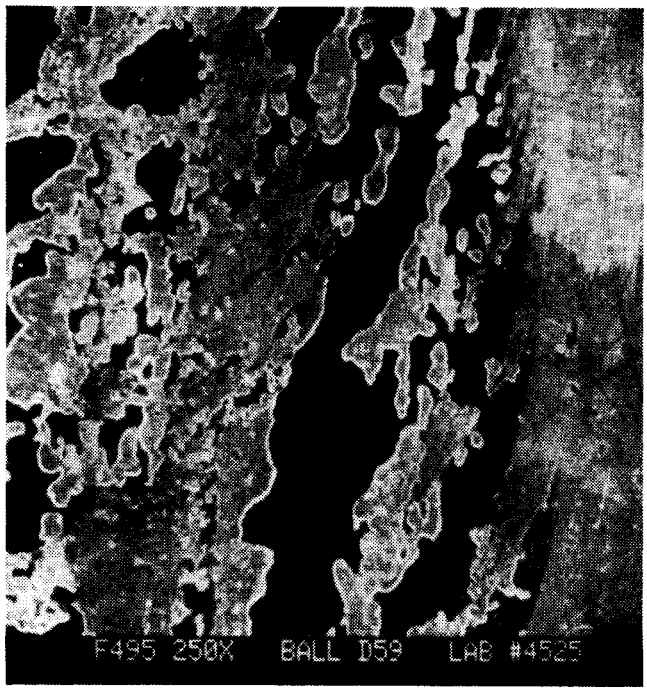

(c) Right Edge of Contact

Figure 4.26 M50 Test Ball
TiN Coated Disk
Room Temperature
Contact Stress = 1723 MPa

Figure 4.27 presents photomicrographs of the disk surface. Figure 4.27a is a 250X magnification view of the unrun, coated surface. Notice the appearance of grinding lines or scratches, owing to the thin nature of the TiN coating. There also appears to be a substantial amount of surface pits or voids in the surface coating.

Figures 4.27b and 4.27c show the track (contact zone) areas on the disk surface where the traction tests were run. The black marks or stains are ink spots made to mark the location. Note that the only evidence of contact is a slight discoloration band. There is nothing on the surface that would correlate with the material pick up on the balls. Thus, one possible scenario concerning the deposits on the test balls is that it is an oxide of titanium, formed by the heat and tribo-conditions of the contact.

Upon further examination, track #3, which is the track that corresponds to test #58 (2068 MPa (300 ksi)), reveals the early stages of disk surface damage. Figure 4.28 presents the micrographs of this area on the disk. The photos indicate that the surface coating is beginning to break down along the edges of what appears to be a prominent grinding mark or scratch. This would lead one to believe that the coatings and their success are very dependent upon the substrate preparation and surface integrity.

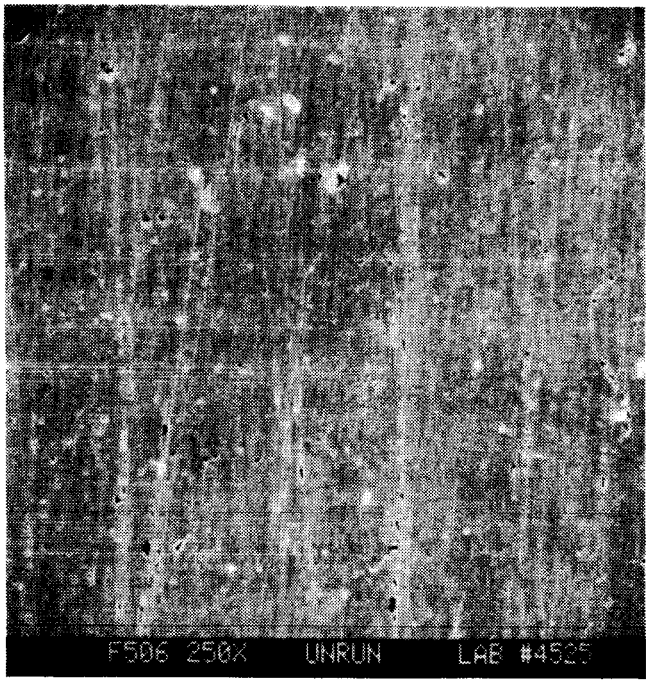

(a) Unrun Disk Surface

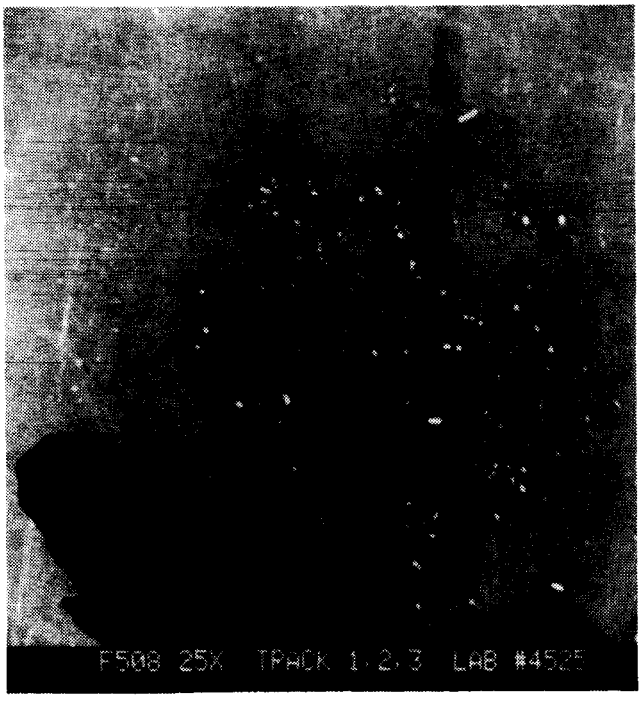

(b) Disk Tracks

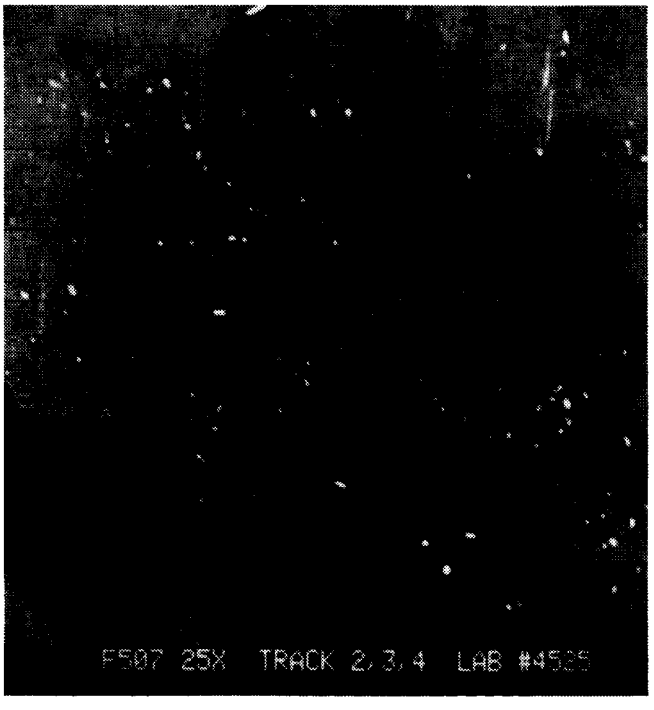

(c) Disk Tracks

Figure 4.27 TiN Coated Disk
Traction Test Contact Paths

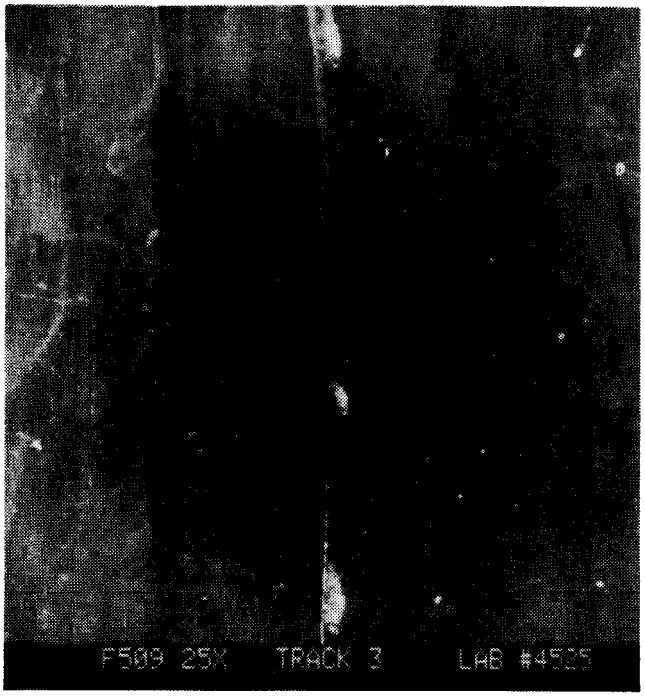

(a) Disk Track #3

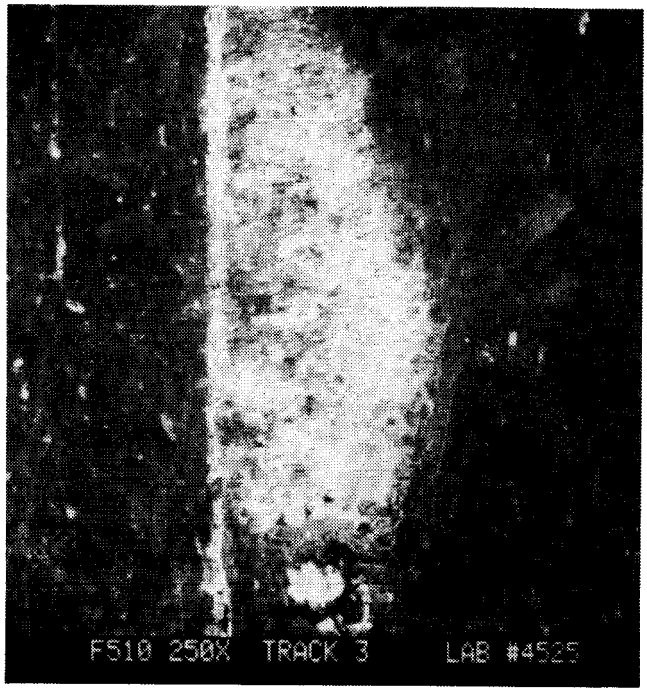

(b) Track #3 Damage Area

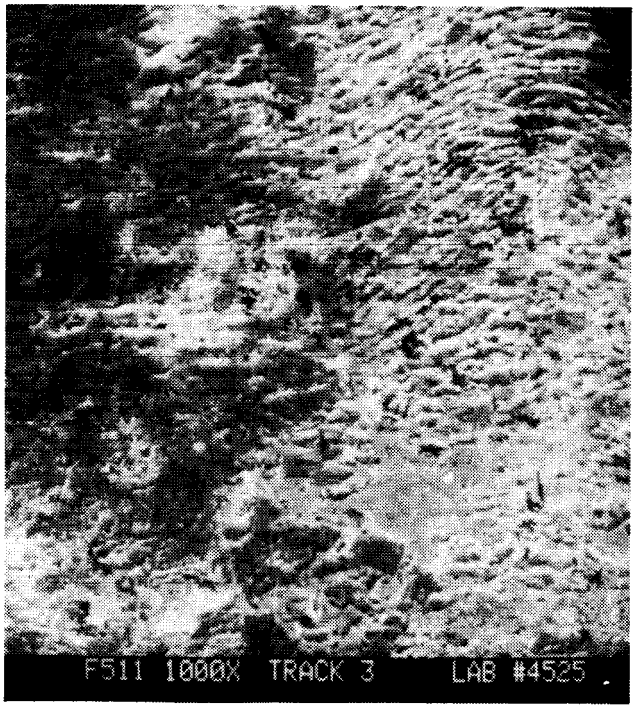

(c) Track #3 Damage Area

Figure 4.28 TiN Coated Disk
Contact Path for 2068 MPa Test

4.5 Discussion of Traction Results

The rolling element-lubricant combinations tested using the test matrix of Table 4.1 were listed in Table 4.2 with the measured (recorded) results. The table lists as one of the key results the limiting traction force. This is the actual traction force acting on the ball measured at the point where the traction vs. slide/roll curve levels to a maximum. Working with this value (as opposed to coefficient) allows better direct comparison of the trends in the results and lends itself better to the process of judging lubricant effectiveness.

Values of limiting traction force for the high temperature graphite tests are plotted in Figures 4.29, 4.30 and 4.31 for P3310, P03Ag and P2003, respectively. The results show that the limiting traction force was a function of the contact stress and rolling speed, much like was found in Phase I [3]. The effect of contact stress was greater then the effect of rolling speed with the latter showing its greatest effect at high contact stress levels. For any given lubricant there is a noticeable decline in the traction levels as temperature was increased from 370°C (700°F) to 540°C (1000°F). This is indicative of the fact that these lubricants are designed for use at high temperatures.

The best performing lubricant from an overall traction level standpoint was the P3310. This correlates well with the SEM exa-

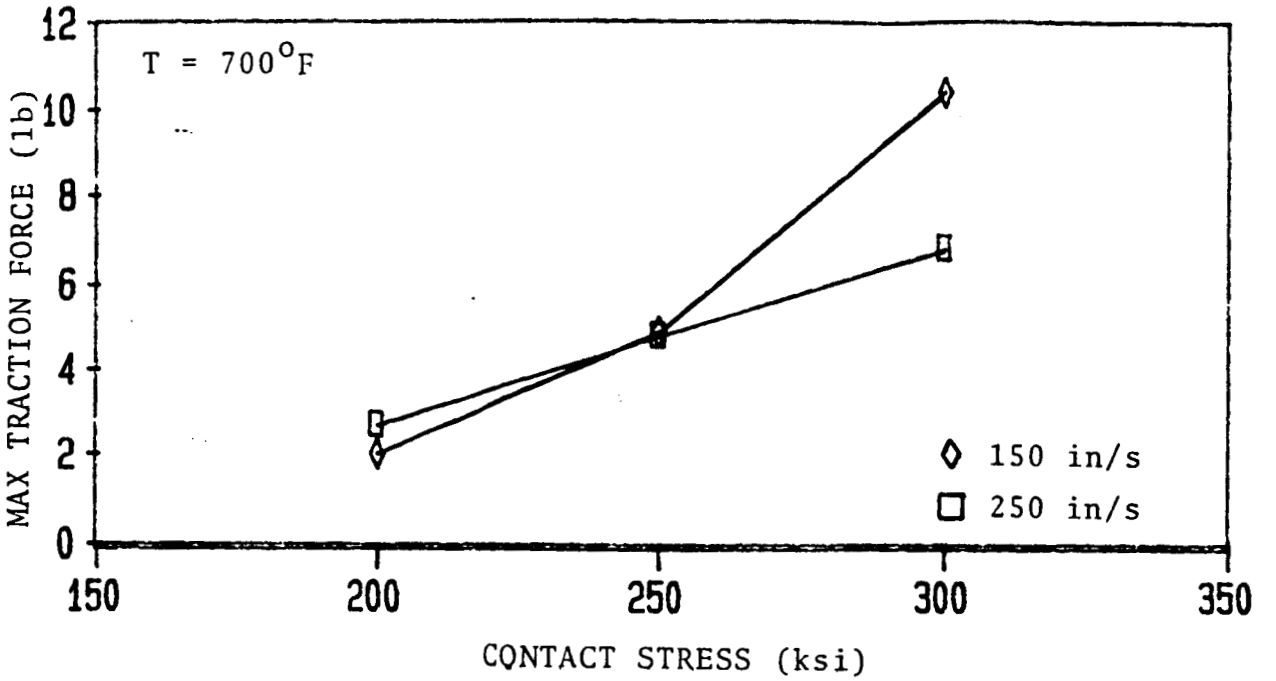

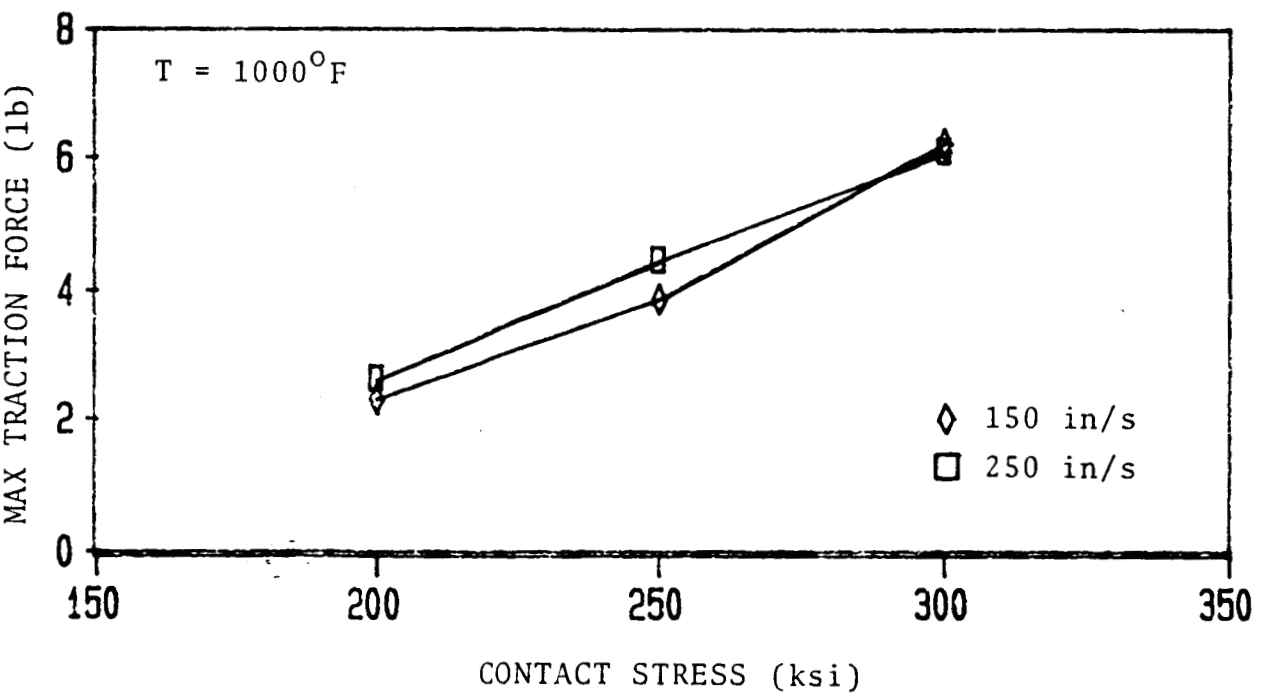

Figure 4.29 Traction Tests Results
P3310 Lubricant

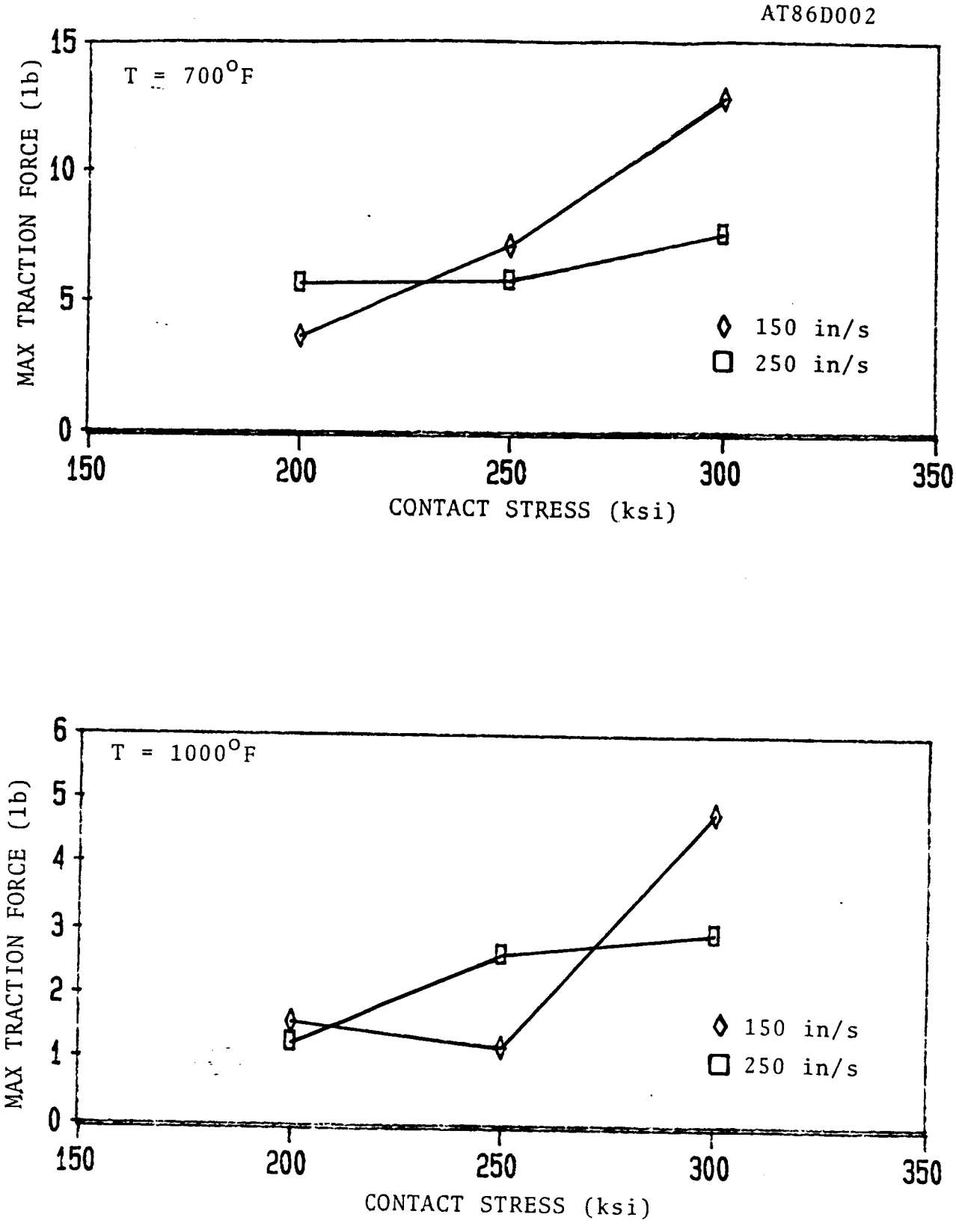

Figure 4.30 Traction Test Results
P03Ag Lubricant

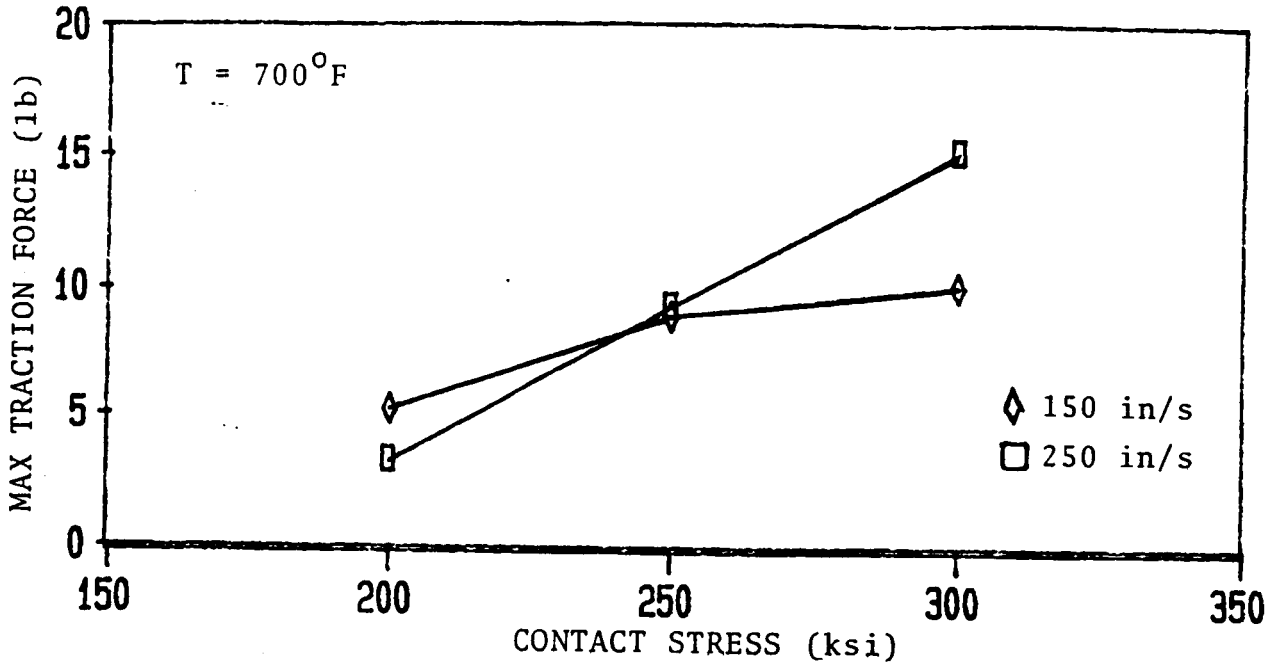

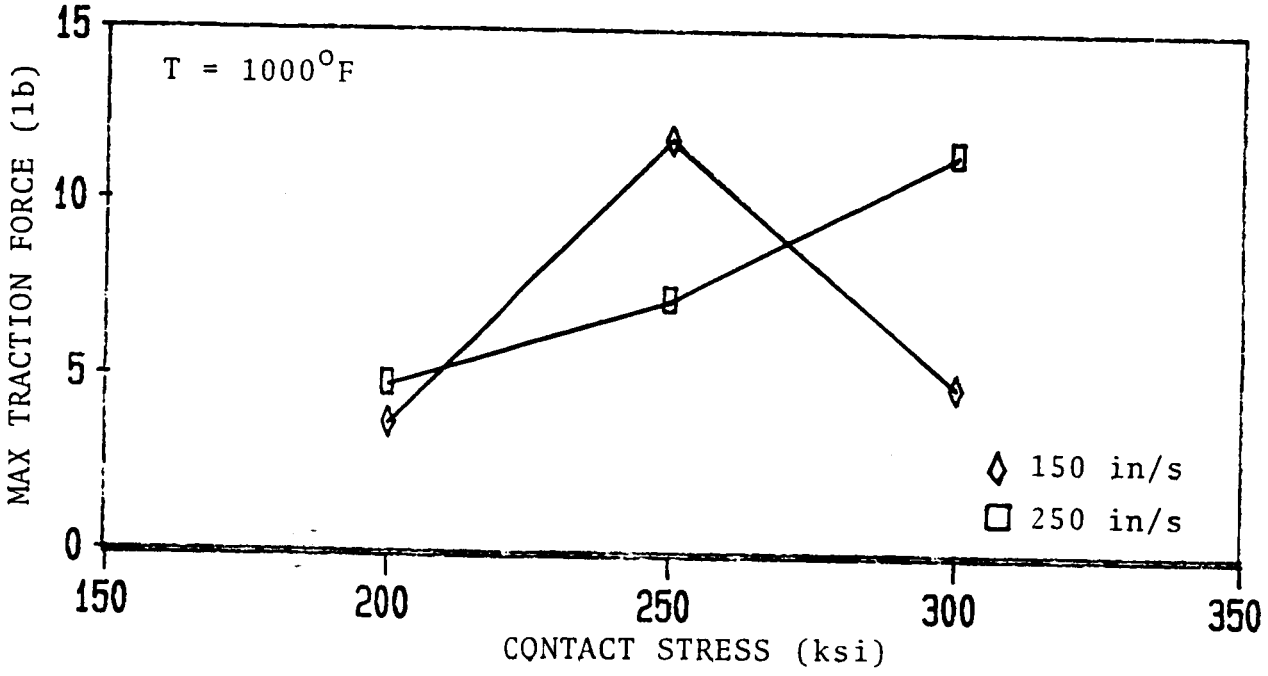

Figure 4.31 Traction Test Results
P2003 Lubricant

minations which revealed the P3310 better than the other two graphites with regard to wear protection. Given the fact that the span in measured traction force was not of large magnitude (at a given temperature) wear protection is a weighty factor in lubricant selection. On this basis P3310 would appear to be the graphite of choice at high temperatures.

Values of limiting traction force for tests using silicon nitride balls on the Armoloy coated M50 disk are plotted in Figure 4.32. Similar trends are noted in the data with regard to contact stress effects. However, the traction levels are substantially higher. This latter fact correlates well with the observed lack of wear protection noted in the SEM examination of these test pairs. One interesting trend is the lack of any sizeable difference in the traction levels at the two different temperature levels. All three lubricants yielded very similar traction levels and neither of them provided any substantial improvement over no lubricant.

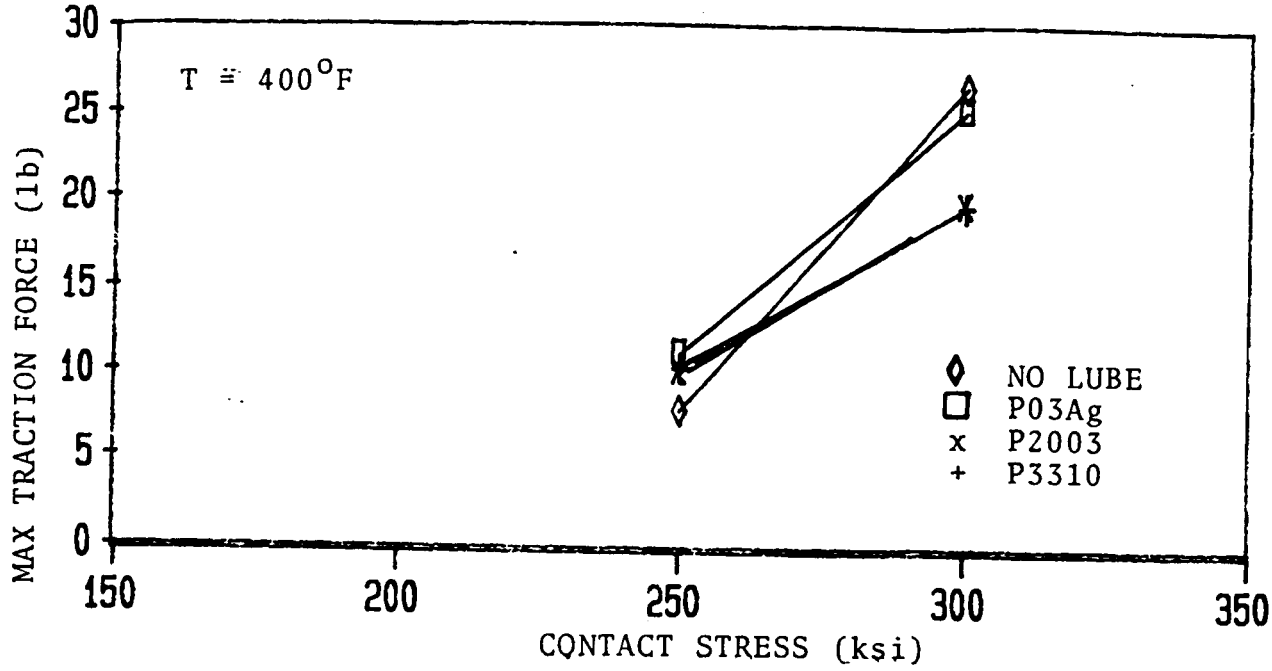

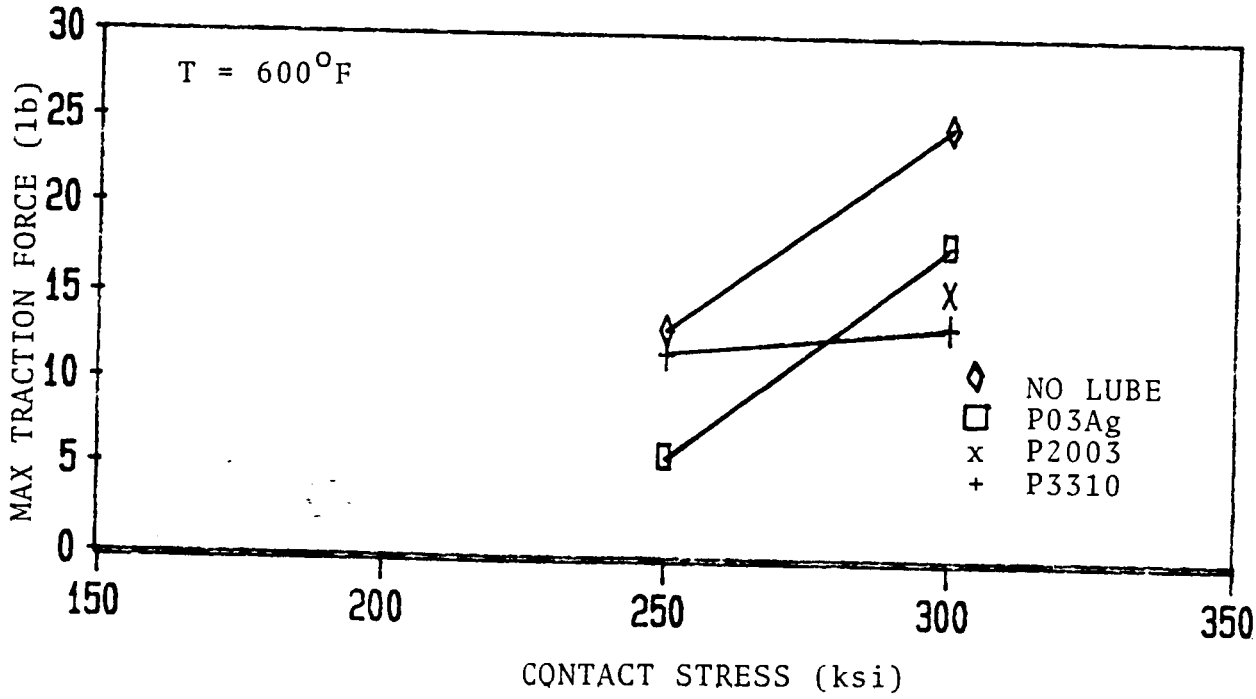

Figure 4.32 Traction Test Results
Si_3N_4 Ball on Armoloy/M50 Disk

4.6 Surface Analysis of Test Specimens

Post test examination of the surface of several ball specimens was conducted using Infrared (IR) Emission Spectroscopy. The detection of thin films, such as solid lubricant films, or oxides can be obtained by careful study of detailed IR-emission spectra. Work ongoing at Rensselaer Polytechnic Institute (RPI) under the leadership of Dr. James Lauer is advancing the state-of-the-art of this process. In an effort to understand the surface films on the silicon nitride test balls and to assess the merits of the IR-emission process, several test specimens were examined at RPI. In the case of films on metal substrates the process revolves about the fact that metal is an infrared reflector and has a low emittance over a given spectral range. The spectrum of a film on a metal substrate is obtained by subtracting the spectrum of a bare substrate from the total spectrum. It became quite clear that the analysis would be much more complex for the silicon nitride substrate material. Silicon nitride exhibits large gradients of the optical constants in the spectral region of interest. They interferred with those of the films that were to be analyzed. Also the gold-palladium coating which was put on the balls to enhance the SEM analysis interferred as well. Nevertheless, some IR results were obtained which demonstrate the merits of the process and point the way for further and future work.

As an example, we will discuss here the results for the analysis of several of the silicon nitride test balls that were run with the P03Ag graphite lubricant.

Balls #3 and #6: P03Ag - T = 370°C

Two balls were tested with the lubricant P03Ag at 370°C. The maximum traction coefficient was almost the same for both balls: .44 for #3 and .43 for #6.

The IR-emittance spectra are shown in Figures 4.33 and 4.34. The spectra of the silicon nitride surface are almost identical for both balls except for a slightly higher emittance for ball #6 between 930 and 1070 cm^{-1}. The spectra of contact track and burnished area are quite different for these balls, although they were tested under very similar conditions. There is no indication of any silver from the lubricant in the spectra of ball #3. The contact track of ball #6 contains silver as indicated by its flat spectrum. The ratioed spectra (Figure 4.35 and 4.36) indicate a band around 850 cm^{-1} for the burnished area of ball #3 as well as for the contact track of ball #6.

Balls #4, 14 and #16: P03Ag - T = 540°C

Three balls were tested with the lubricant P03Ag at 540°C. Again the maximum traction coefficient was almost identical with

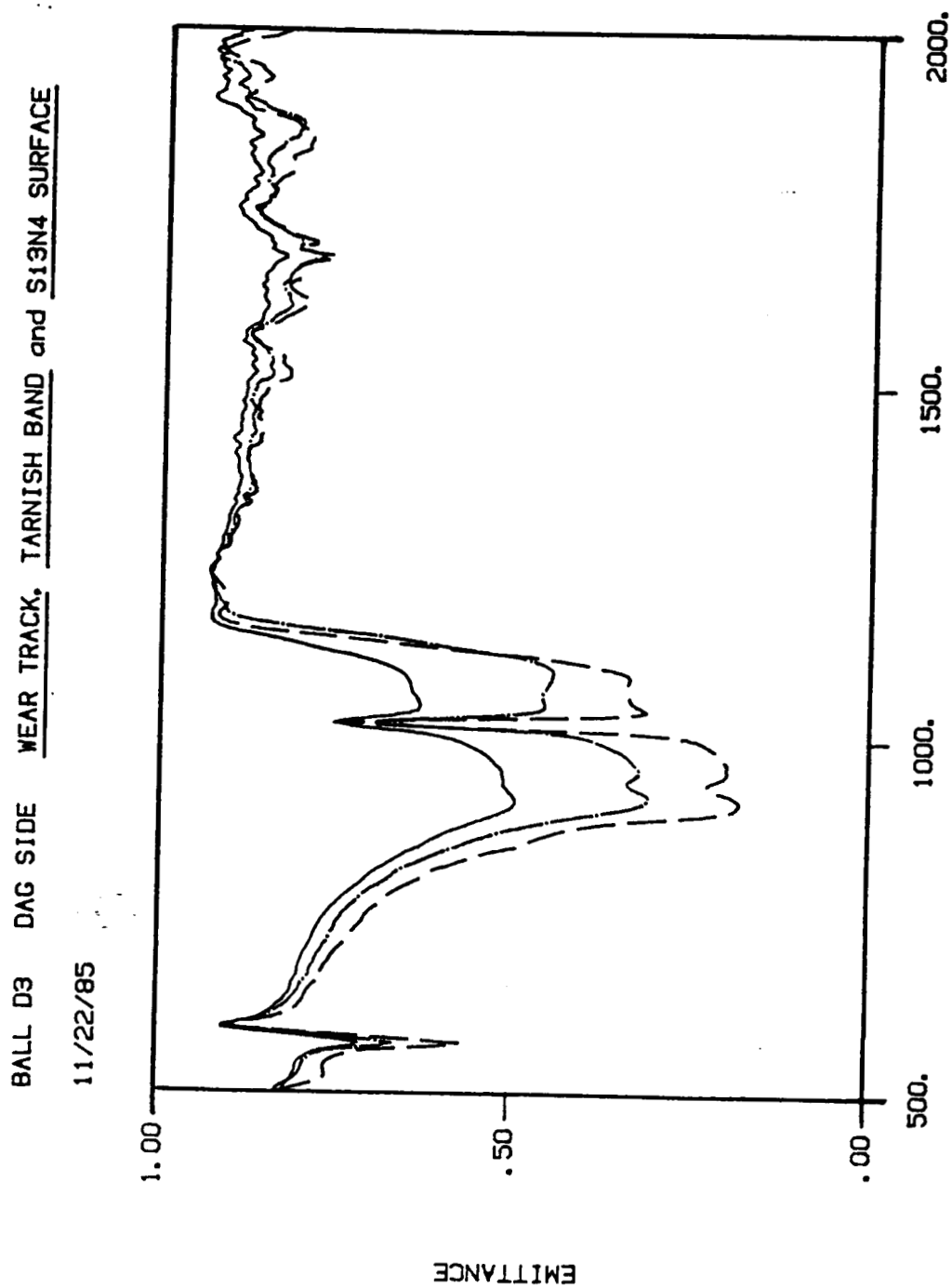

Figure 4.33 IR Spectrum Ball #3

Figure 4.34 IR Spectrum Ball #6

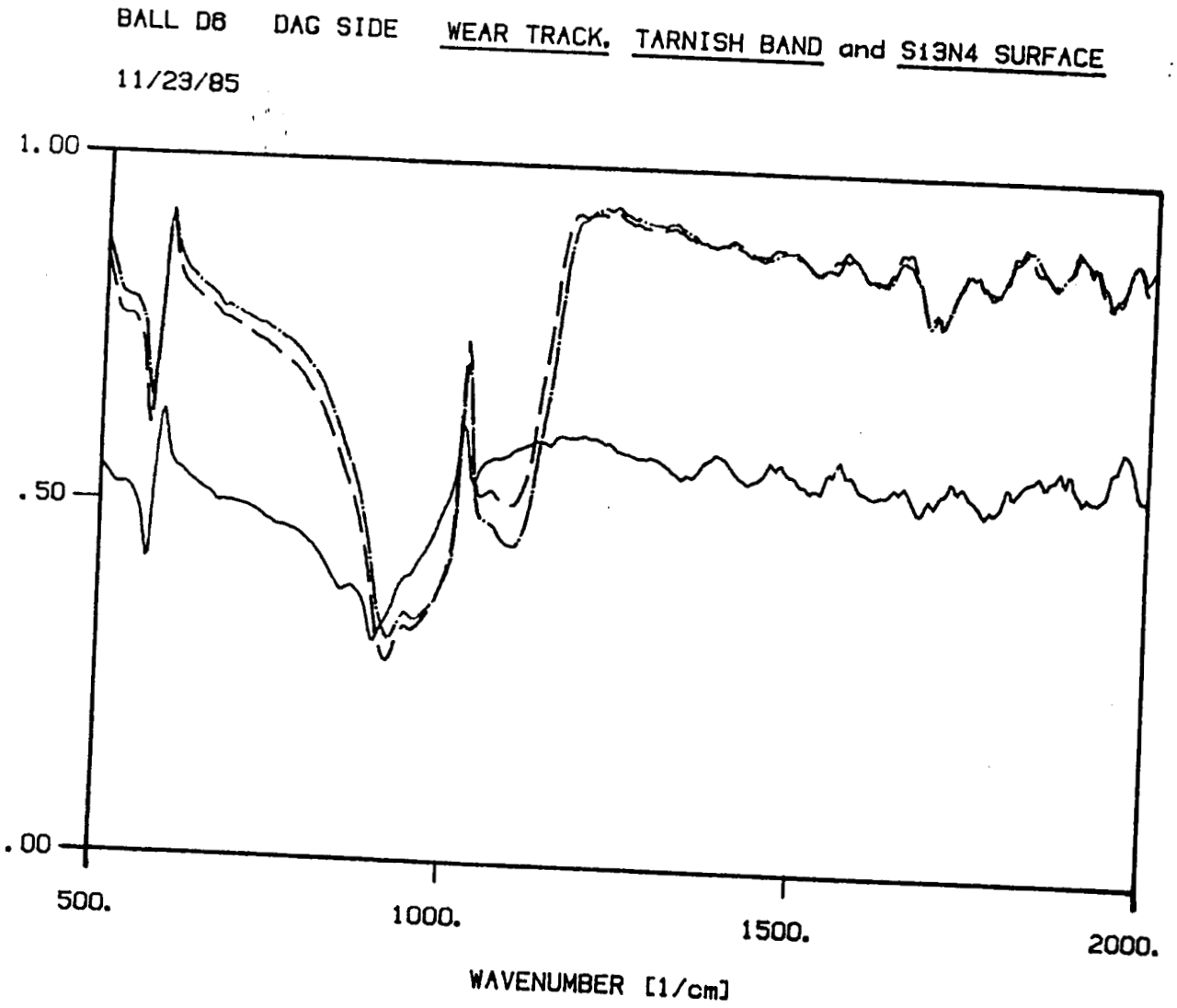

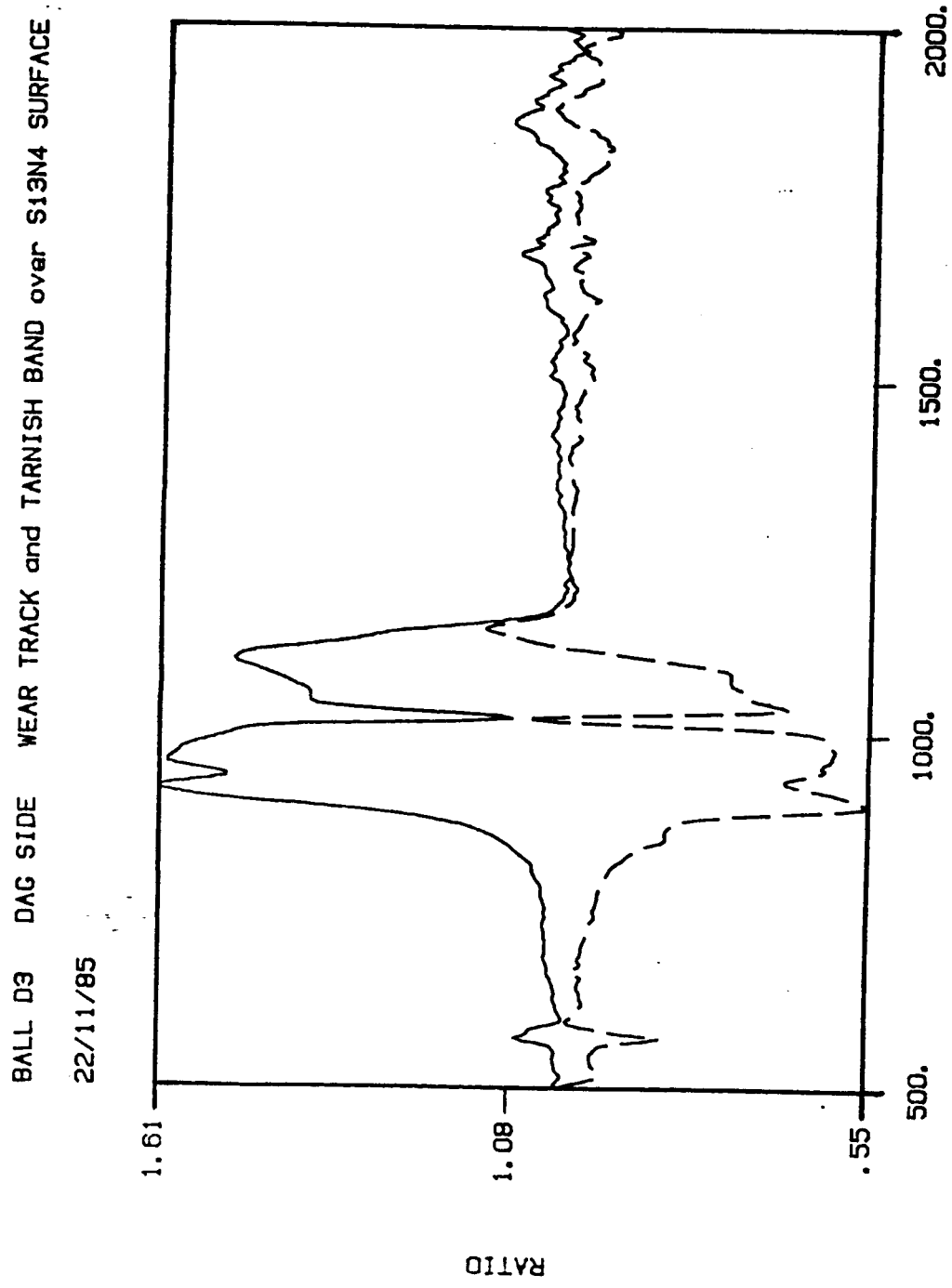

Figure 4.35 Ratioed Spectrum Ball #3

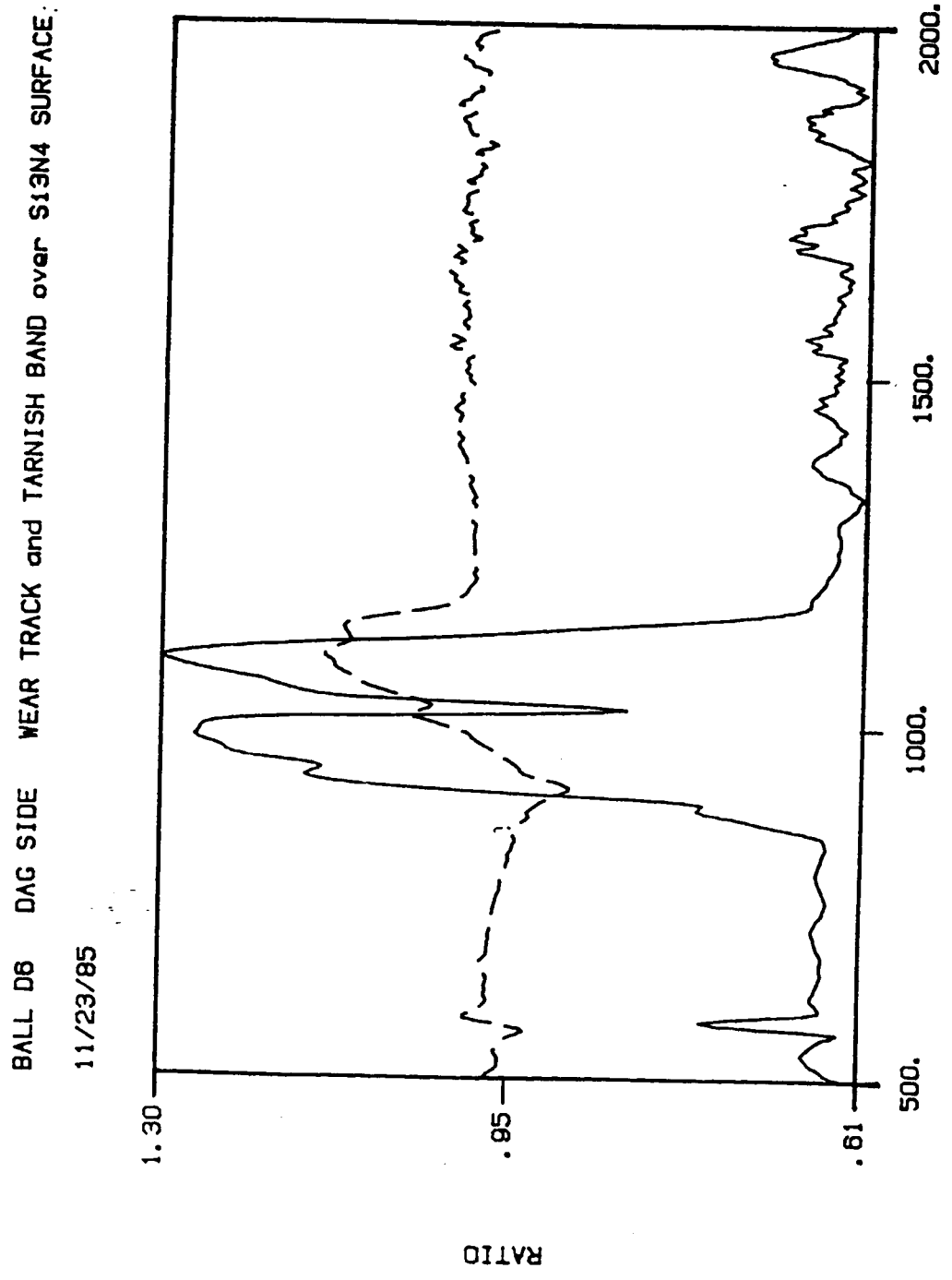

Figure 4.36 Ratioed Spectrum Ball #6

the low values of .16, .14 and .15 for balls #4, 14 and #16 respectively.

The IR-emittance spectra are shown in (Figures 4.37, 4.38 and 4.39). The spectrum of the surface of ball #4 is almost identical to that of ball #3 except for a slightly lower emittance between 1060 and 1110 cm^{-1}. The surfaces of the balls #14 and #16 seem to be oxidized SiO or SiOH as their spectra are of similar shape as those of the theoretical broad band oscillator on top of the silicon nitride substrate (Figure 4.40). Note that the emittance towards the low and high frequency end of the spectrum is about the same as for the unrun ball, whereas with a metal overcoat it is generally lower. All the contact tracks seem to contain silver with the highest content for ball #4 with an almost flat spectrum and an approximately identical lower content for balls #14 and #16. In all the contact tracks as well as in the burnished areas there is the 850 cm^{-1} band present. The burnished area of ball #4 is almost identical to that of ball #3. There seems to be some silver in the burnished area of ball #14 and #16 with the higher content for #16. The ratioed spectrum ball #4 (Figure 4.41) is again similar to that of ball #3.

This work seems to suggest that the presence of surface oxides (SiO and SiOH) may be a large contributor to the success of the lubricant at high temperature. Further work is needed in these areas.

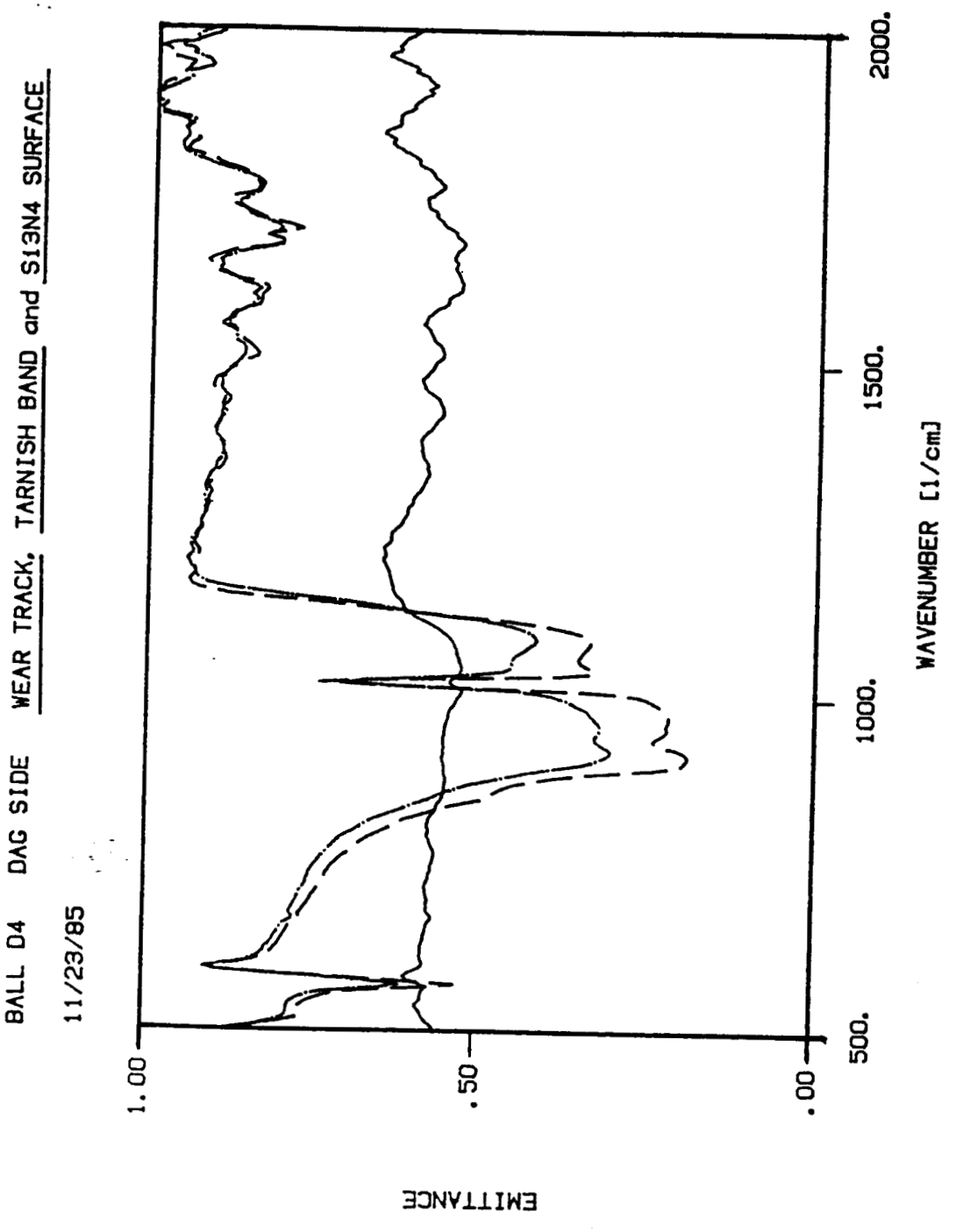

Figure 4.37 IR Spectrum Ball #4

Figure 4.38 IR Spectrum Ball #14

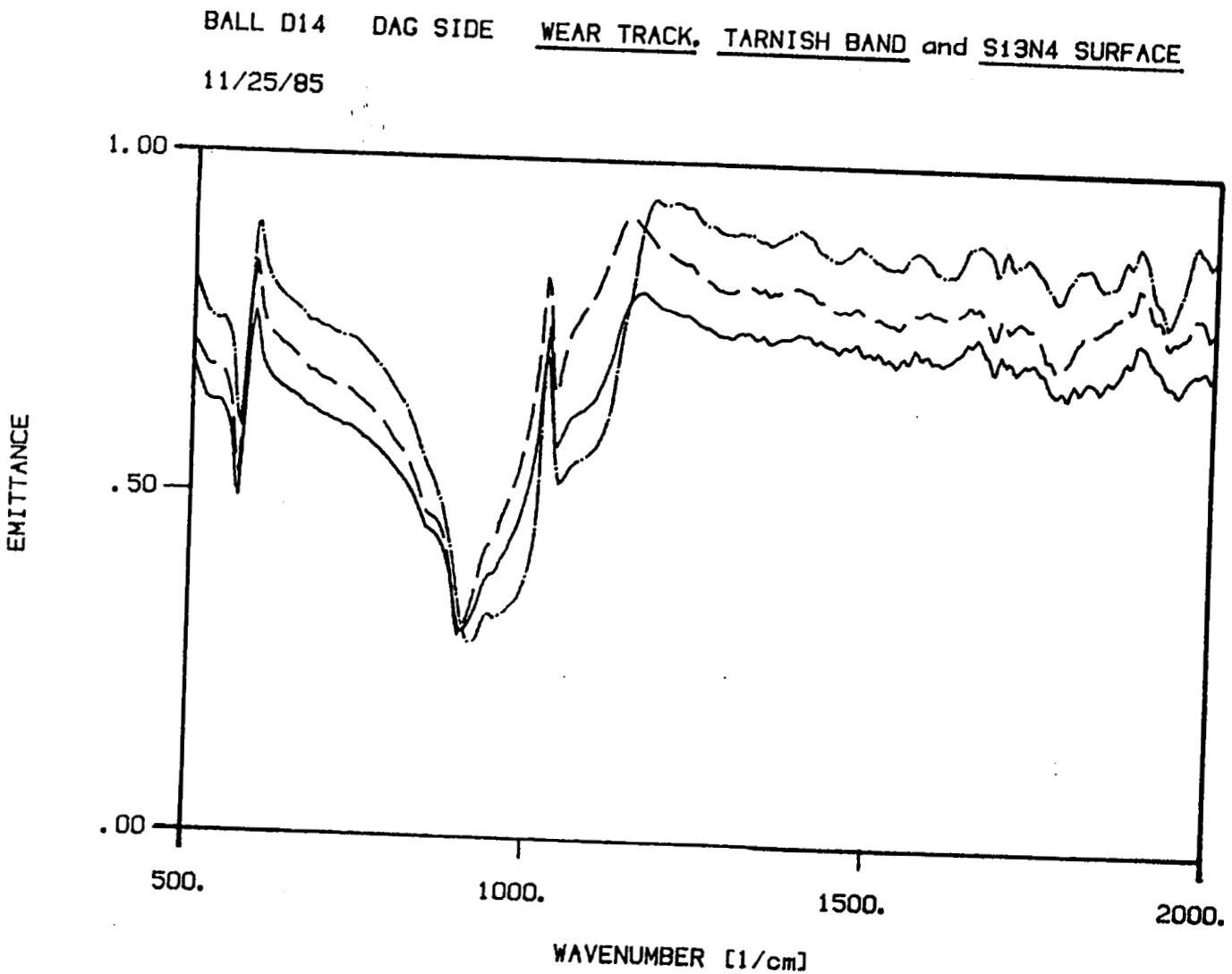

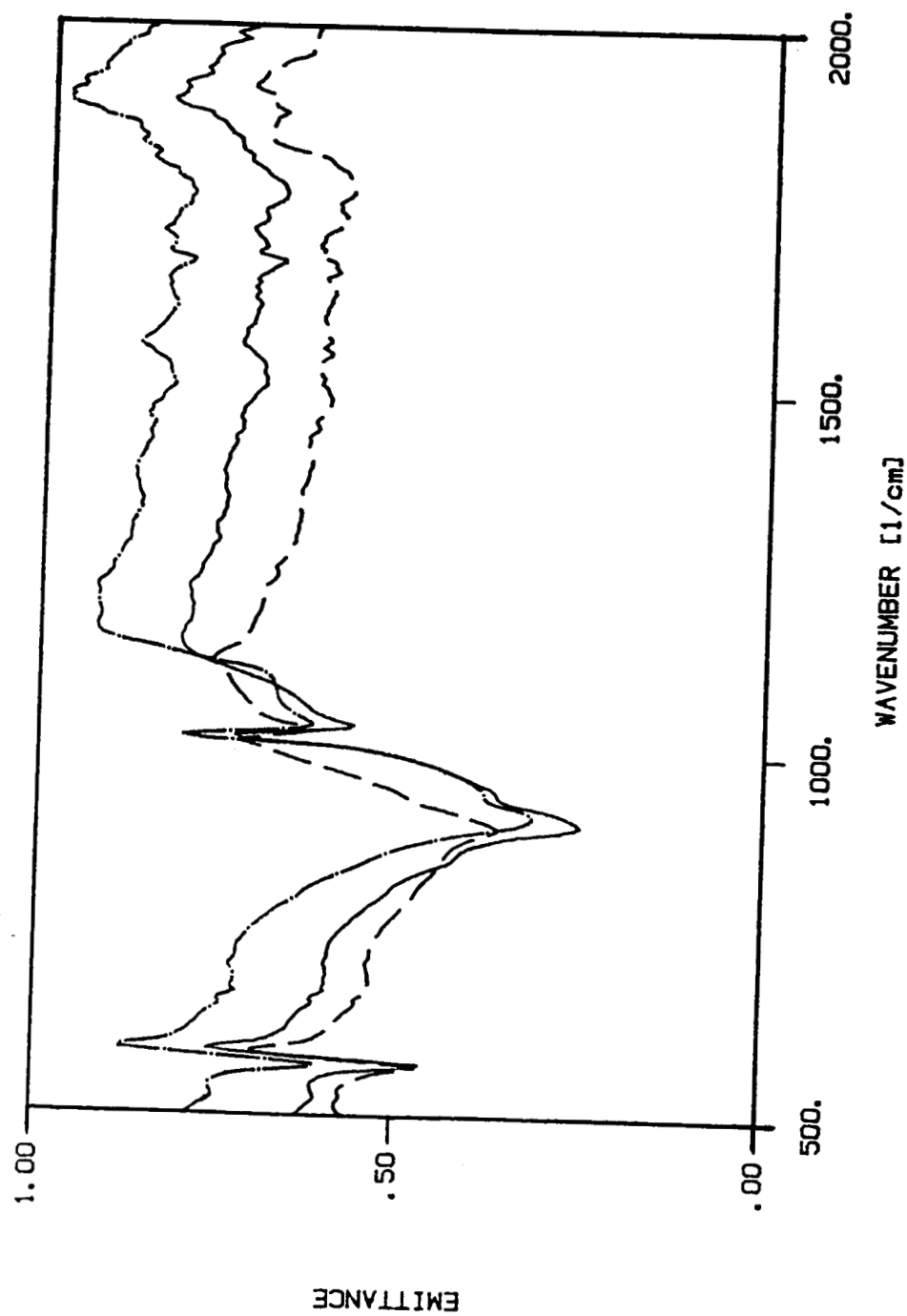

Figure 4.39 IR Spectrum Ball #16

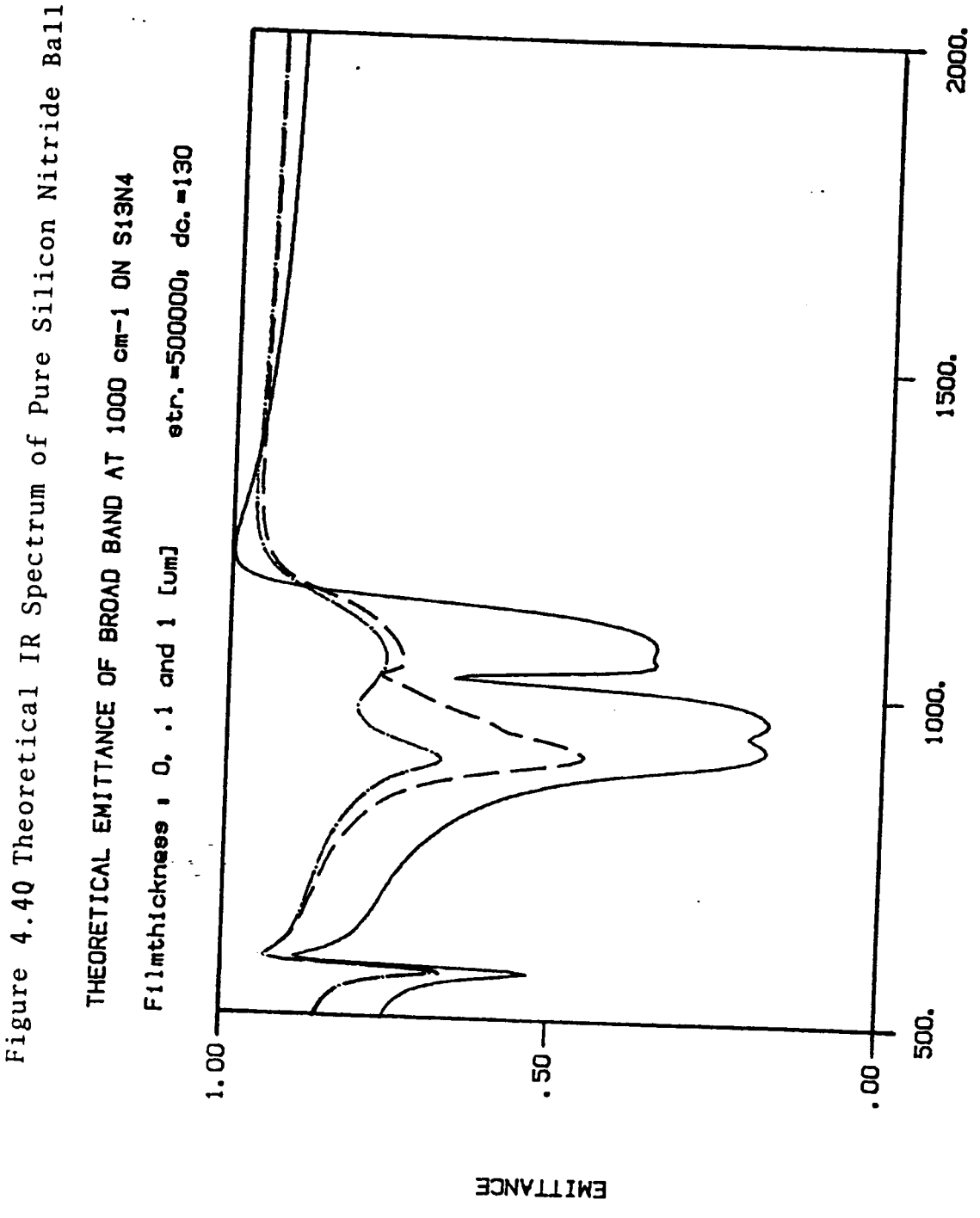

Figure 4.40 Theoretical IR Spectrum of Pure Silicon Nitride Ball

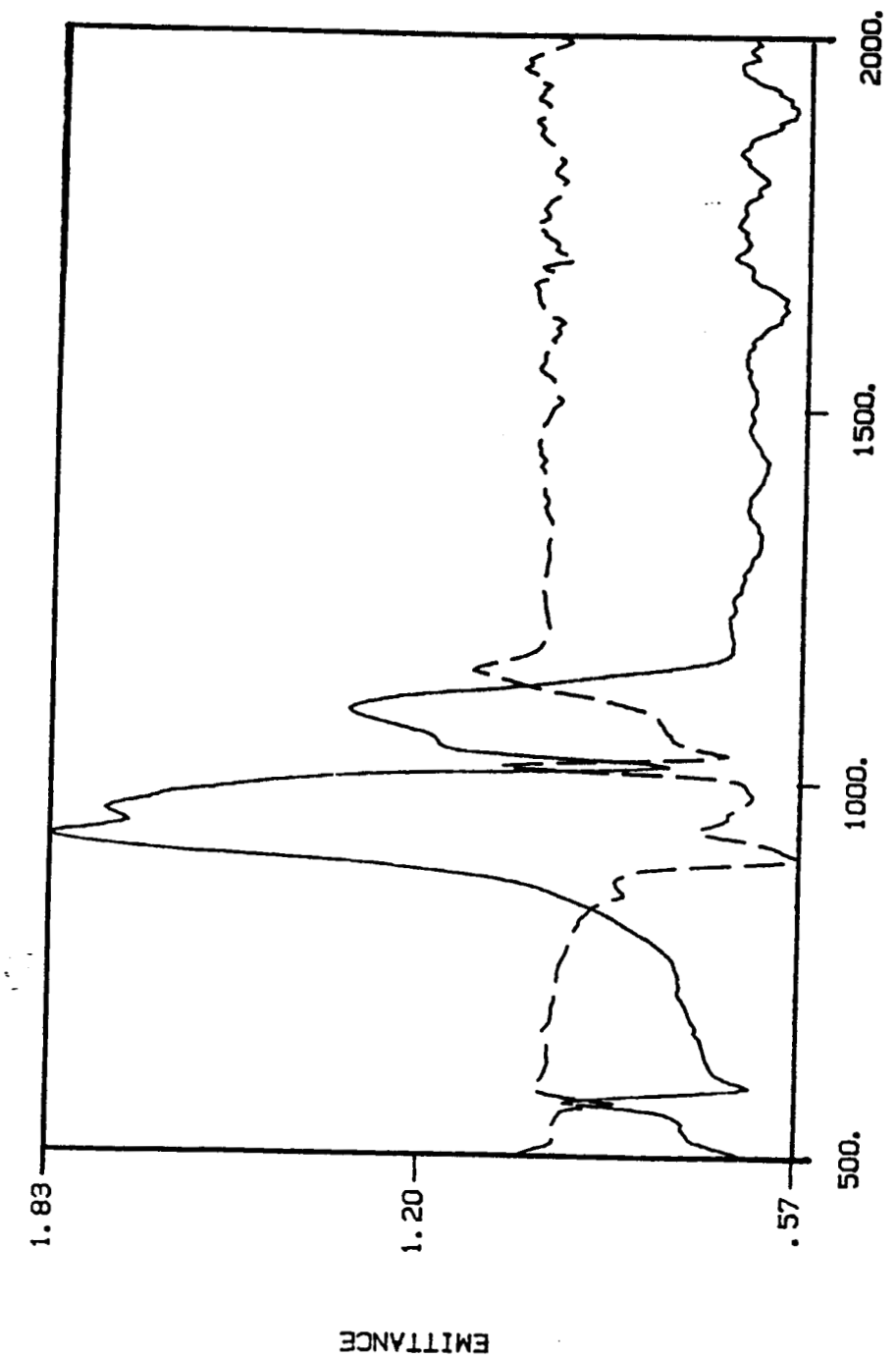

Figure 4.41 Ratioed Spectrum of Ball #4

Future work should be considered in which focused testing with one material and lubricant combination, but more varied temperatures, could be analyzed. Greater emphasis should be placed on past test analyses such as discussed here.

5.0 ANALYTICAL MODELLING

5.1 Traction Model Development

The purpose of the quantitative traction measurements conducted in Phase I and II is to provide the required information to predict the performance of bearings lubricated with various materials and solid lubricants.

A logical step toward achieving this is to incorporate a solid lubricated traction model based on actual test data in an advanced bearing analysis computer program. The computer program SHABERTH [9] which was developed previously at SKF Industries, was selected for this purpose. SHABERTH analyzes the thermomechanical performance of a mutiple number of bearings on a shaft.

A solid lubricant traction model (Figure 5.1) was installed in SHABERTH. It can be represented by the following equations:

$$\mu = \text{SLOPE} * \text{SRR} \tag{5.1}$$

$$\text{If } \mu > \mu_{MAX}, \ \mu = \mu_{MAX} \tag{5.2}$$

where

μ = traction coefficient

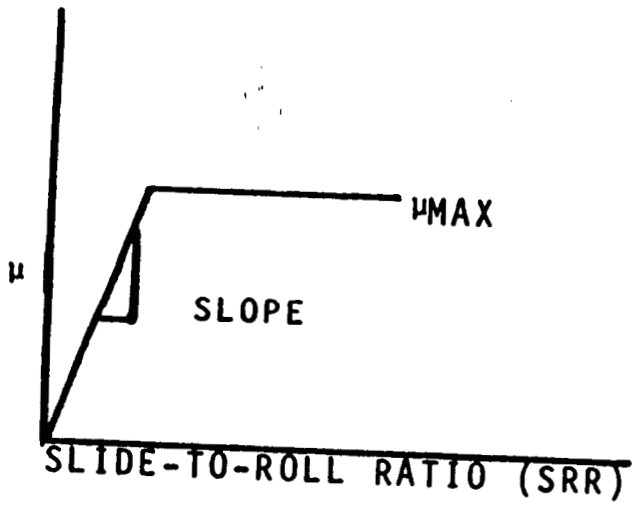

μ = (SLOPE) (SRR)

IF $\mu > \mu_{MAX}$, $\mu = \mu_{MAX}$

$SLOPE = C_1 P^{C_2} U^{C_3} T^{C_4}$

$\mu_{MAX} = D_1 P^{D_2} U^{D_3} T^{D_4}$

P = CONTACT PRESSURE (KSI)

U = ROLLING VELOCITY (IN/SEC)

T = TEMPERATURE (°F)

SRR = SLIDING VELOCITY/ ROLLING VELOCITY

Figure 5.1 Solid Lubrication Traction Analytical Model

SLOPE = slope of linear portion of traction curve

SRR = slide-to-roll ration = sliding velocity/rolling velocity

μ_{MAX} = maximum traction coefficient

Both the slope and the maximum traction coefficient are functions of pressure, rolling velocity and temperature as given by the following equations:

$$SLOPE = C_1 \, P^{C2} \, U^{C3} \, T^{C4} \tag{5.3}$$

$$\mu_{MAX} = D_1 \, P^{D2} \, U^{D3} \, T^{D4} \tag{5.4}$$

where

P = contact pressure

U = rolling velocity

T = temperature

The solid lubricated traction data of Phase I [3] were augmented by the results obtained and reported here in Phase II. The maximum or limiting tractions and traction curve slopes for the high temperature graphite tests were tabulated and placed in a data files. A regression analysis program, BMDP1R [10], was used to establish the values of the coefficients for the various material/lubricant combinations. The results of the regression analysis are shown summarized in Table 5.1. The model was

Table 5.1

Summary of Regression Analysis Results for Various Solid Lubricant/Material Combinations

Lubricant	C_1	C_2	C_3	C_4	D_1	D_2	D_3	D_4
P03AG/ M50 Disc	0.4278	0.326	1.087	0	0.009382	-0.021	0.521	0
P3310 M50 Disc	0.005343	0.944	0.639	0	0.0000172	0.910	0.770	0
P2003 M50 Disc	4.0878	0.505	-0.188	0	0.0009377	0.478	0.482	0
HAC2A/ Si_3N_4 Disc	0.09936	0.231	0.853	0	0.003942	-0.045	0.787	0
P2003/ Si_3N_4 Disc	223.855	-0.736	0.385	0	0.26106	-0.386	0.317	0
HAC2A/ M50 Disc	0.11452	0.693	0.329	0	0.0002993	1.004	0.150	0

installed in SHABERTH for both ball and cylindrical roller bearings.

5.2 Parametric Studies

To demonstrate the practical use of the newly updated SHABERTH traction models, a preliminary study of solid lubricated bearing heat generation was conducted. For comparison purposes, preliminary heat generations were computed for oil (SAE 15W-40) and solid lubricated (P3310) M50 steel bearings. A deep groove ball bearing (DGBB) and a cylindrical roller bearing (CRB) were compared under operating conditions typical of diesel engine mainshaft bearing applications. For a deep groove ball bearing where the ball/raceway curvature introduces a significant degree of microslip, the solid lubricated heat generation was found to be about 2.5 times the oil lubricated case. The distribution of heat generated (in watts) at the various contact locations is shown schematically in Figure 5.2. The number in parentheses indicate the heat generated with the solid lubricant (P3310).

A cylindrical roller bearing operates with much less microslip in the rolling element to raceway contacts. The preliminary analysis gives a lower heat generation for the solid lubricated CRB as shown in Figure 5.3. The major difference is the heat generated at the raceway contacts. The small amount of

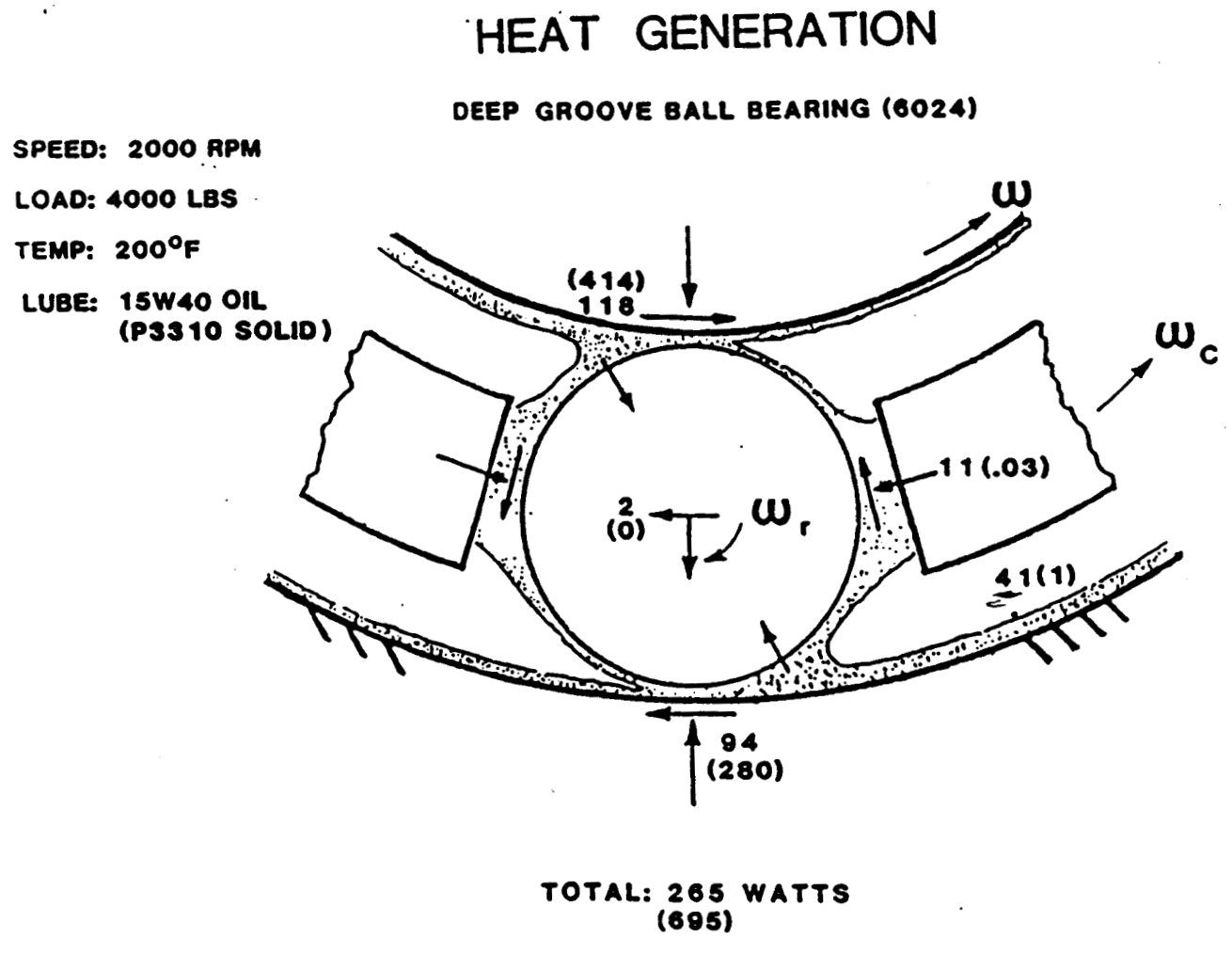

Figure 5.2 Solid and Liquid Lubrication Heat Generation for a Deep Groove Ball Bearing

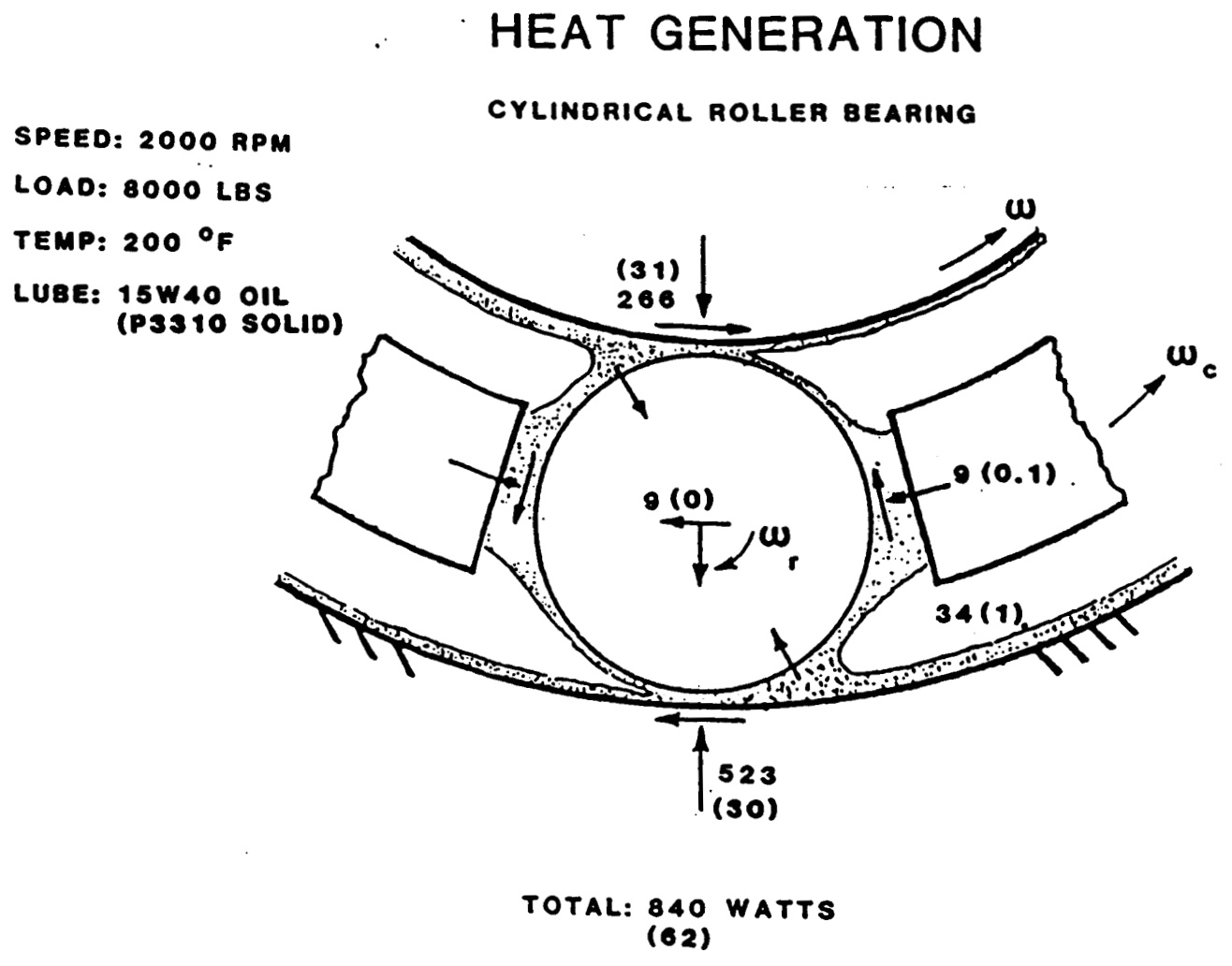

Figure 5.3 Solid and Liquid Lubrication Heat Generation for a Cylindrical Roller Bearing

microslip in the CRB allows the heat generation to be dominated by viscous inlet pumping of the oil outside the Hertzian contact. However, the degree to which a similar behavior may exist for solid lubricants is not known. This and other factors, such as roller/flange heat and cage/rolling element/land heat present unknowns to the study that require that these results be considered tentative at best.

Nevertheless, bearing in mind all the unknowns and assumptions, the possibility of a low friction, solid lubricated, cylindrical roller bearing remains hopeful.

6.0 CONCLUSIONS AND RECOMMENDATIONS

6.1 Conclusions

The rolling/sliding traction tests documented and presented in Section 4 of this report yielded the following conclusions:

1. The traction curves of solid lubricated contacts are characterized by a more rapid rise and a higher maximum traction level than the curves for oil lubricated contacts. Therefore, a bearing or contact geometry that inherently operates with micro/macroslip will be characterized by higher heat generation when lubricated with solids. This was demonstrated at the lower temperature tests of Phase I as well.

2. The graphite lubricants provided discontinuous performance as a function of temperature. All three lubricants tested performed poorly in terms of traction and wear protection at the 200°C (400°F) temperature range. This behavior is believed to be due to the evaporation of moisture in the graphite and the inability of the additives to function at that temperature.

3. Each of the graphite lubricants when tested on silicon nitride yielded lower traction levels and better wear protec-

tion at the 540°C (1000°F) temperature level, than at the 370°C (700°F) level.

4. The maximum traction measured for the graphite lubricated silicon nitride contacts showed to be sensitive to contact stress and rolling speed, with the former of the two dominating the behavior. Similar trends were noted at room temperature during Phase I.

5. The use of an electrodeposited thin dense chrome coating (Armoloy) on M50 steel did not enhance graphite lubricant burnishing, nor did it provide lower traction levels than graphite lubricated uncoated M50 steel.

6. The Armoloy coating when used in conjunction with silicon nitride test balls and graphite lubricants performed poorly. SEM examinations showed transfer of coating materials to the ball surface. Wear protection was minimal. This is in contrast to reports about the performance of Armoloy in running M50 steel bearings. It suggests that the silicon nitride/Armoloy tribological pairing is suspect.

7. The Titanium Nitride coated M50 steel disk when operated without lubricants of any type provided better wear protection than the Armoloy. Even though some Ti was found transferred to the ball and traction levels were higher than

expected, the wear was substantially less than other material combinations tested.

8. SEM examinations of the TiN coated disk did reveal that failure of the coating occurs at or along surface flaws and even grinding marks. This suggests that the success of these thin hard coatings is very dependent upon substrate surface preparation.

6.2 Design Criteria

The Phase I effort was summarized [3] by the documenting of several suggested design criteria which were formulated about the fact that solid lubrication in rolling bearings creates a heat dissipation problem. As stated in the Phase I report, solid lubricated rolling/sliding contacts generate larger amounts of heat than conventionally (oil) lubricated bearings. Dissipation of this heat is a major problem (due to the lack of a flowing medium) and must be dealt with at the bearing design level.

Several of the design criteria presented in the Phase I report are repeated and enhanced here with some additions. These criteria are:

1. Reduce Contact Stress - This can be achieved by using a larger number of rolling elements or a larger sized rolling element. This will lower the traction forces at the contact thereby lowering the generated heat. Lower contact stresses will also enhance the maintenance of a solid lubricant film.

2. Minimize Sliding in the Contact - Slip within the contacts of rolling bearings is a large contributor to the overall sliding present and hence a contributor to the heat generation. The amount of slip is a function of the conformity of the raceway to the rolling. Reducing the conformity, reduces

the slip. A cylindrical roller bearing, therefore, has a decided advantage built into its design. However, where the application warrants a ball bearing be used, a reduced conformity should be considered. Reducing the conformity will, however, increase the contact stress. The design effort should strike a balance between this criterion and criterion 1.

3. Heat Dissipation - The bearing and housing design must provide means of dissipating the heat generated at the contacts. Bearing geometry should be constructed in such a manner as to maximize surface area for cooling. The use of cooling air should be considered where possible. Materials with good thermal conductivity should be considered.

4. Wear Resistant Coatings and Materials - The use of wear resistant hard coats in selective areas will reduce the wear damage created by the lack of conventional lubrication. One critical area that might benefit from the use of wear resistant hard coats is the cage/land interface.

6.3 Recommendations For Future Analysis

The authors of this report are of the opinion that further work is needed in an effort to understand the inconsistencies

that were noted in the behavior of the solid lubricants tested. Extensive post test analysis along with careful experimentation is needed to understand the tribomechanisms that govern success or failure of a lubricant in a given tribosystem. The presence or absence of surface films is a key factor.

One post test examination that appears to hold promise to aid in this kind of study is Infrared (IR) Emission Spectroscopy. The detection of thin films, such as solid lubricant films, or oxides can be obtained by careful study of detailed IR-emission spectra.

The IR-emission studies presented in Section 4 of this report illustrated this potential. The authors feel that additional testing with a less broad matrix of conditions and materials but with increased emphasis on post-test analysis is needed. In this manner the understanding of the tribological laws governing the success or failure of a lubricant can be better achieved.

7.0 REFERENCES

1. "Heavy Duty Transportation Technology Development Plan," DOE/CE-0130, U.S. Department of Energy, Office of Transportation Systems, June 1985.

2. Wood, James C., "Heavy Duty Transport Technology Program Overview," Presented at the 23rd Automotive Technology Development Coordination Meeting," Detroit, MI, October 22, 1985.

3. Aggarwal, B. B., Yonushonis, T. M., and Bovenkerk, R. L., "Solid Lubrication Design Methodology," DOE/NASA/0323-1, NASA CR-174690, May 1984.

4. Singhal, S. C., "Oxidation and Corrosion - Erosion of Si_3N_4 and SiC," Ceramics for High Performance Applications, Vol. 2, edited by J. J. Burke, A. E. Gorum and R. N. Katz, Brook Hill Publishing Co., 1974.

5. Maurer, R. E., "Ceramic Bearing Materials in Hostile Environments," Final Report on Naval Air Systems Command Contract N00019-83-C-0227, Period July 1983 to April 1985, May 1985.

6. Yonushonis, T. M., "Solid Lubricated Silicon Nitride Bearings at High Speed and Temperature - Phase II," Naval Air Sytems Command Contract No. N00019-81-C-0473, SKF Report No. AT83D018, July 1983.

7. Maurer, R. E., Ninos, N. J. and Hahn, D. E., "Functional Testing of Armoloy, Noblizing and Electroless Nickel in Rolling Contact," SKF Industries, Inc., Report No. AL76M001, August 1976.

8. Maurer, R. E. and Pallini, R. A., "Development of New Materials for Turbopump Bearings," Final Report on NASA Contract NAS8-35341 for NASA Marshall Space Flight Center, February 1985.

9. Hadden, G. B. et al, "User's Manual for Computer Program AT81Y003 SHABERTH - Steady State and Transient Thermal Analysis of a Shaft Bearing System Including Ball, Cylindrical and Tapered Roller Bearings," SKF Report No. AT81D040, submitted to NASA Lewis Research Center under Contract No. NAS3-22690, May 1981.

10. Biomedical Computer Programs, Health Science Computing Facility, Department of Biomathematics, School of Medicine, UCLA, University of California Press, 1975.